DESIGNING A SLIDING MODE CONTROLLER FOR FIXED-WING UNMANNED AERIAL VEHICLE FOR MEDICAL SUPPLY MISSION

A Thesis

submitted to

Department of Electrical and Computer Engineering,

Addis Ababa Institute of Technology,

Addis Ababa University.

In partial fulfilment to the requirements for the degree of master of science in Electrical and Computer Engineering (Industrial Control Engineering)

by

Kedir Mustefa Aliye

November 2021

Advisors: Dr. Lebsework Negash

Dr. Dereje Shiferaw

Approval

This is to certify that the thesis prepared by ***Mr. Kedir Mustefa Aliye entitled "Designing A Sliding Mode Controller for Fixed-Wing Unmanned Aerial Vehicle for Medical Supply Mission"*** submitted as partial fulfillment for the Degree of Master of Science in Industrial Control Engineering fulfills the regulations of the university and meets the accepted standards for originality, content, and quality.

Signed by Examining Board:

Advisor: **Signature, Date:**

Dr. Lebsework Negash

Dr. Dereje Shiferaw

External Examiner: **Signature, Date:**

Internal Examiner: **Signature, Date:**

Chairperson: **Signature, Date:**

DGC Chairperson: **Signature, Date:**

College Dean/Associate Dean for GP: **Signature, Date:**

Declaration

I hereby declare that this thesis entitled ***"Designing A Sliding Mode Controller for Fixed-Wing Unmanned Aerial Vehicle for Medical Supply Mission"*** was prepared by me, with the guidance of my advisors. The work contained herein is my own except where explicitly stated otherwise in the text, and that this work has not been submitted, in whole or in part, for any other degree or professional qualification.

Author: **Signature, Date:**

Mr. Kedir Mustefa Aliye

Witnessed by:

Name of student advisors: **Signature, Date:**

Dr. Lebsework Negash

Dr. Dereje Shiferaw

Abstract

Over the past many years, the application of unmanned aerial vehicles (UAV) has increased. UAV's such as this has become an easy solution to tasks that are difficult and dangerous. Because of its highly non-linear and coupled nature, the control problem seems to be a challenge. As a contribution to this area, this thesis presents the modeling and control of a fixed-wing unmanned aerial vehicle for medical supply mission such as delivering blood, medicinal drugs and test kits to remote areas. The overall research work stars with conducting a literature survey to review thoroughly the works that has been done with regard to the subject matter to identify the gaps. Then after a careful mathematical modeling of the system using the Newton-Euler formalism was done. Furthermore, longitudinal and lateral-directional motions are addressed separately to minimize the coupled nature of the dynamics. The model was validated by considering two flight scenarios and in both scenario's, it meets the expected requirements. After model validation the next task performed was designing the controllers for regulation and reference tracking problems using the classical & super twisting sliding mode controller techniques. The simulation results shows that the classical sliding mode controller produces a faster response time, 1.75 seconds for roll angle, 2 seconds for pitch angle and 7 seconds for yaw angle but it suffers from an associated high frequency chattering problem in the control signal whereas the super twisting sliding mode controller eliminates the high frequency chattering problem in the control signal but takes 9 seconds to stabilize the system. The results show that despite a relatively large response time the elimination of the associated high frequency chattering problem in the control signal makes the super twisting sliding mode controller preferable.

Keywords: Fixed-wing UAV, Model-based design, Flight dynamics, classical SMC, Super twisting SMC, Longitudinal Motion, Lateral-Directional Motion.

Acknowledgment

First and foremost, praises and thanks are to ALLAH, the Almighty, for all the showers of blessings he has bestowed in my life.

I would like to express my deep and sincere gratitude to my advisors ***Dr. Lebsework Negash*** *Assistant Professor, School of Electrical and Computer Engineering, Addis Ababa Institute of Technology (AAiT), Addis Ababa University (AAU) and* ***Dr. Dereje Shiferaw*** *Assistant Professor, School of Electrical and Computer Engineering, Addis Ababa Institute of Technology (AAiT), Addis Ababa University (AAU)* for their mentorship, guidance, and support throughout this thesis.

Their dynamism, vision, sincerity and motivation has deeply inspired me, they had taught me the methodology to carry out the research and to present it as clearly as possible. It was a great privilege and honor to work and study under their guidance. I am extremely grateful for what they had offered me. I would also like to thank them for their friendship, empathy and great sense of humor.

I am also extremely grateful to my parents ***Mr. Mustefa Aliye*** and ***Mrs. Werkite Desalegn*** for their non-stopping love, motivation, prayer, caring and sacrifices for educating and preparing me for my future. I would also like to thank my siblings Mr. ***Nuredin and Mrs. Zebiba,*** for their strong support, motivation, and words of encouragement.

Special thanks go to my best friends for their unceasing support, motivation, guidance, and unforgettable memories.

Table of Contents

List of Symbols

UAV Mass ..... m
Sliding Surface ..... δ
Air Speed ..... V_a
Body X-Axis ..... X_b
Body Y-Axis ..... Y_b
Body Z-Axis ..... Z_b
Angle of Attack ..... α
Side Slip Angle ..... β
Aileron Deflection Angle ..... δa
Elevator Defelection Angle ..... δe
Rudder Deflection Angle ..... δr
Air Density ..... ρ
Dynamic Pressure ..... Q
Wing Mean Aerodynamic Chord c
Wing Span ..... b
Wing Surface Area ..... S
Coefficient of Drag Force ..... C_D
Coefficient of Lift Force ..... C_L
Coeficient of Side Force ..... C_Y
Coefficient of Rolling Moment ..... C_l
Coefficient of Pitching Moment ..... C_M
Coefficient of Yawing Moment ..... C_N
Force Along Body X-Axis ..... Fx
Force Along Body Y-Axis ..... F_Y
Force Along Body Z-Axis ..... F_Z
Moment Along Body X-Axis L
Moment Along Body Y-Axis ..... M
Moment Along Body Z-Axis ..... N
Roll Angle ..... ϕ
Pitch Angle ..... θ
Yaw Angle ..... ψ
Linear Velocity Along Body X-Axis ..... u
Linear Velocity Along Body Y-Axis v

Linear Velocity Along Body Z-Axis ..... w
Angular Velocity Along Body X-Axis ..... p
Angular Velocity Along Body Y-Axis ..... q
Angular Velocity Along Body Z-Axis..... r
Moment of Inertia Along Body X-Axis..... I_x
Moment of inertia Along Body Y-Axis..... I_y
Moment of Inertia Along Body Z-Axis ..... I_z
Product of Moment of Inertia Along Body X-Axis & Z-Axis..... I_{xz}

List of Acronyms

UAV ..... Unmaned Aerial Vehicle
FWUAV..... Fixed Wing Unmanned Aerial Vehicle
DOF..... Degree of Freedom
CG..... Center of Gravity
SMC..... Sliding Mode Control
HOSMC .....Higher Order Sliding Mode Control
STW-SMC .....Super Twisting Sliding Mode Control
2-SMC..... Second Order Sliding Mode Control
PD ..... Proportional-Derivative
PID ..... Proportional-Integral-Derivative
SISO..... Single Input Single Output
AVL .....Athena Vortex Lattice
PWM.....Pulse Width Modulation
SIGN .....Signim
SAT.....Saturation
TANH ..... Tanhyperpolic
FNN.....Fuzzy Neural Network
MFs ..... Membership Functions

List of Tables

List of Figures

Chapter One

1. Introduction

Unmanned aerial vehicle (UAV) refers to a flying machine without an on-board human pilot. These vehicles are increasingly popular platforms due to their ability to effectively carry out a wide range of applications from civilian and military domains[1]. In the coming decade, the number of potential applications is also expected to expand. These applications include environmental monitoring, autonomous delivery, spying, combating and warzone medical supply, data collection, and photography and video. The advantages of these systems are certainly attractive. They minimize risk to operators, provide on-demand capability, and allow increased flexibility for reaching denied areas [2].

In particular, the use of UAVs to provide improved medical care capability, including medical treatment supply and unmanned casualty evacuation had a growing interest. This thesis especially focuses on UAVs for blood delivery, a subset of the medical resource supply mission due to the fact that it has a unique constraint related to how it should be transported and saved and additionally has a finite shelf life. In short, blood should probably benefit from a pairing with a transport platform that approves for greater flexibility in its grant chain.[2].

In this regard, among the various types of UAVs, fixed wing UAVs are known for their remarkable advantages such as: longer flight autonomy, larger areas covered in less time, higher flight safety, etc.[3]. However, fixed wing UAV control system design is tremendously challenging because of dynamics complexity and system coupling. For these reasons, more UAV models has been developed to approximate the actual system whereof it is pretty beneficial to use robust control algorithms to deal with the stated problems [4].

In this regard a variable structure control algorithm generating sliding mode (SM) is a renowned control law. This method is reputed for its success to control dynamical systems, distinctly higher order sliding mode control (HOSMs) which guarantee a finite time convergence and decrease chattering which is the prime inconvenience of the SM controllers. In FWUAV control, most of the works that use HOSM focus on the Second Order Sliding Mode (SOSM). Among them, the super twisting (STW) algorithm is presumed for its robustness and finite time convergence.

Besides the benefits of HOSM, the STW implementation doesn't request the definition of the sliding variable time derivative [4].

1.1. Research Motivation

This research is stirred by the challenge to design, model, control and test a small-scale fixed wing unmanned aerial vehicle, with proven flight capability. The idea was first initiated when I saw a video in YouTube about a company called Zipline. Zipline is an American medical product delivery company headquartered in South San Francisco, California that designs, manufactures, and operates delivery drones. The company runs distribution hubs in Rwanda and the US.

Like Ethiopia, Rwanda is among the poorest countries in the world and much of its regions are connected by bumpy & dirty roads in the mountains, that get washed out in the rainy seasons that made it incredibly difficult for regional hospitals to procure blood using a vehicle in an emergency, leaving doctors unable to perform many lifesaving operations. So, the zipline company was came up with an idea of drone delivery and they able to deliver blood to hospitals up to 80 km distance. These things really fascinate me and motivates me to ask myself about the small things that I can contribute to show to these who are responsible the fact that we can do it here. Well as a control engineer the first thing that comes to my mind is modelling and designing a controller.

1.2. Problem Statement

In order to tackle the flight control problem, several approaches have been proposed. For instance, a method based on linear approximations, a linearization in an equilibrium point has been proposed for trajectory tracking[4]. However, this methodology lacks of robustness as the exact cancellation of nonlinearities is not ensured. Several nonlinear control techniques have been proposed to flight control. For instance, an adaptive backstepping scheme based on invariant manifolds, [5] has been designed to track angle of attack, sideslip angle and roll angle. Nonetheless, this control is designed based on a linearized aerodynamic model. On the other hand, Active Disturbances Rejection Control (ADRC) approach offers a robust controller that does not require an exact model [6]. However, the need for Extended state observers to overcome problems that arise from external disturbances makes it unfavorable.

In this research paper, a sliding mode control scheme which is known for its robustness is designed and applied to fixed wing UAV for regulation and reference tracking problem. This technique allows to design robust control laws that are insensitive to uncertainties [7]. Regarding the stability properties of the closed-loop system, the above methods can only ensure asymptotic stability properties. However, using the sliding mode techniques the robustness and insensitivity to uncertainties can be guaranteed, and convergence in finite time is ensured. Thanks to its properties of robustness against uncertainties in the model and external disturbances, the high order sliding mode approach is an interesting alternative to overcome such problems.

1.3. Objective of the Research

1.3.1. General Objective

The general objective of this thesis paper is to design sliding mode controller for attitude control of a fixed-wing UAV.

1.3.2. Specific Objective

The specific objective of this thesis paper is:

- ✓ Obtain the mathematical model of Fixed Wing UAV dynamics
- ✓ Design classical SMC for attitude control of a Fixed Wing UAV dynamics
- ✓ Design higher order SMC for attitude control of a Fixed Wing UAV dynamics
- ✓ Implementing the controller on MATLAB/Simulink

1.4. Contributions of the Research

It is evident that Ethiopia is transforming from agricultural to industrialization. The main ingredients in industrialization are the application of science and technology. Among different technological products, UAVs become a vital tool to cope up with emerging population growth, human needs, risk minimization, poverty reduction activities, accuracy, and versatility in different sectors. UAVs can be applied in agriculture, health, military, geological survey, transportation,

security, meteorology, and entertainment sectors which significantly helps provide a state-of-the-art service to the above sector.

In particular, the use of UAVs to provide improved medical care capability, including medical treatment supply and unmanned casualty evacuation had a growing interest [2]. This paper particularly focusses on UAVs for blood delivery, a subset of the medical resource supply mission, because it has special constraints regarding how it needs to be transported and stored and additionally has a finite shelf life. In short, blood should doubtlessly benefited from a pairing with a transport platform that approves for greater flexibility in its grant chain [2].

1.5. Scope and Limitations

The scope of this research thesis is from deriving mathematical modeling of the fixed wing UAV dynamics all the way through designing SMC for Attitude control up to simulation of the final system using MATLAB/Simulink software and it does not include practical implementation of the controller.

1.6. Methodology

To meet the specified objectives, the research activities are done in four core procedures. The first procedure was conducting a literature survey to review thoroughly the works that has been done with regard to the subject matter. Since we are following a model-based design approach a careful mathematical modeling of the system using the Newton-Euler formalism was the next procedure that has been accomplished. Once we got the established model the next task performed was designing the controllers using the classical & super twisting techniques. Finally, the controllers are implemented on the model and a detail analysis of the result has been done.

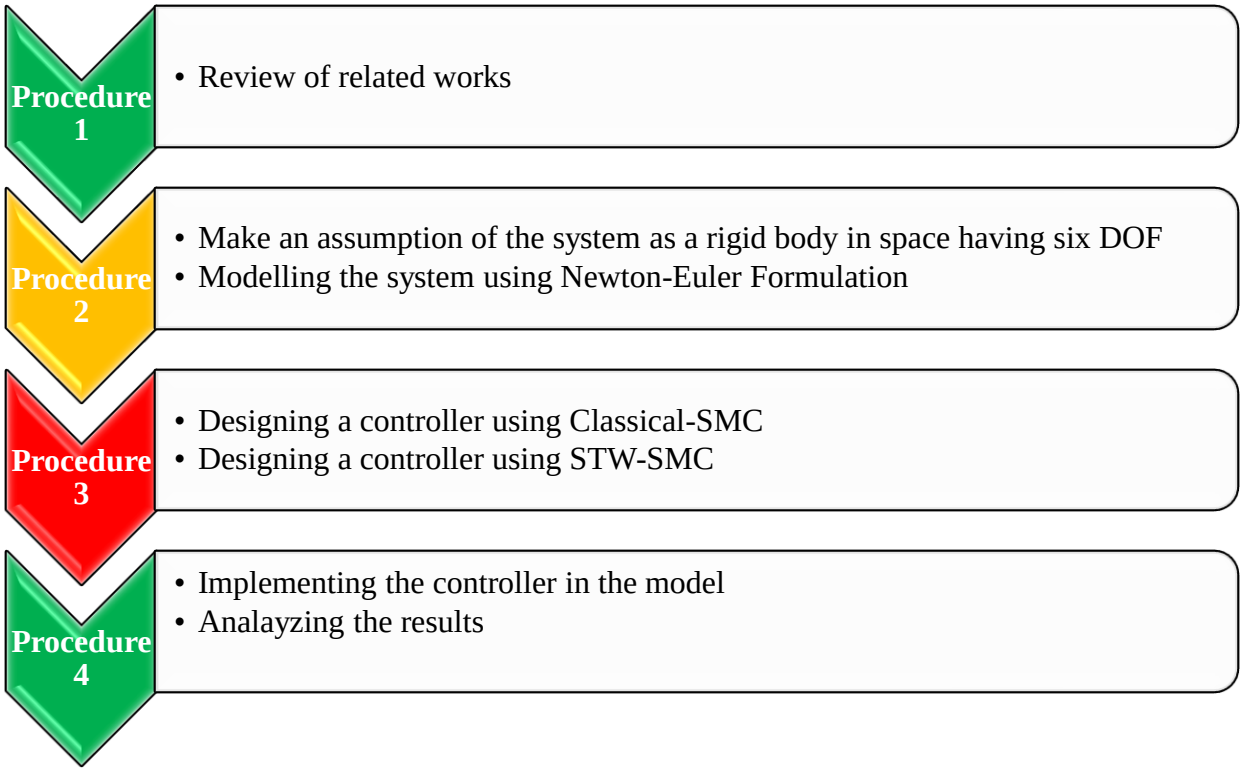

1.7. Organization of the Thesis

This paper is organized as follows: In chapter two a literature survey of different modeling techniques and control methods for this system is addressed. Chapter three presents mathematical modeling with the particular aerodynamic analysis of the fixed wing UAV. In chapter four control design for two complementary flight modes is explained and a classical and super twisting sliding mode controllers are designed for the model. A closed loop simulation result for regulation and reference tracking problem for both controllers was presented and analyzed in chapter five. And finally, conclusion, recommendation and future work was presented in chapter six.

Chapter Two

2. Literature Review

Today, UAVs bring unquestioned list of capabilities and increasing array of critical tasks for military and civil applications. Because of its key features, UAVs are useful for survey, far flung delivery, aid assessment, observing and planning rescue activities in risky areas, surveillance, surrounding monitoring, battlefield monitoring, etc., making it an alluring technological know-how in the close to future. Recently, there has been a great interest in the development of advanced flight control systems for UAVs to adjust the flight path dynamically with the information on the surroundings. These topics have been intensively covered by the robotics community since the late 1970s. Based on these efforts, various algorithms and implementations are currently available. The aim is to make a system perform in a chosen way and at a preferred performance [8].

In [10] the dynamic modelling of unmanned aerial vehicles was introduced through an example of Sky-Sailor airplane. It uses the Newton-Euler approach to come up with a 6 DOF equation that describes dynamics and kinematics of the FWUAV. However, the paper doesn't consider the wind reference frame which is a crucial frame to express the aerodynamic forces and moments with respect to the FWUAV in the modeling process.

In[8] a linear control method mainly proportional-derivative (PD) and proportional-integral-derivative (PID) has been used. In this paper, a flight path PID controller for a fixed-wing 3-DOF UAV is implemented. The control block consists of three PID loops: an airspeed controller, a turn and turn-rate block, and an altitude controller. The system was simulated based on 6-DOF fixed-wing equations of motions. This model had lateral and longitudinal instabilities that had been corrected with the flight controller using nested PID loops. Simulations were conducted to test the performance of the system. The controller successfully followed the desired path even under small wind disturbance. Although the method worked well through various simulations, further improvement will make the system more practical, like it would be a good challenge to introduce adaptive techniques to tune controller parameters in real time.

In [11] a full 6-DOF non-linear UAV dynamic model is demonstrated using the Newton-Euler approach and then an adaptive PID control is designed based on parameter optimization together

with fuzzy inference system for controlling the altitude of UAV. To show the effectiveness of the proposed adaptive PID control, it is compared with both genetically-tuned PID control and fuzzy logic control. The simulation results for the three different controllers based on the full nonlinear model are analyzed from performance and robustness points of view.

In [12] , an SMC theory-based learning algorithm has been introduced for the control of a fixed-wing UAV in the presence of wind. The adaptation laws for the parameters of the fuzzy neural network (FNN) are proposed and their learning stability conditions are investigated for a structure with two inputs, each being modeled by gaussian member functions (GMFs). The projected control system consists of a P-controller and an FNN that may learn the converse dynamics of the system model online instead of a necessity for an accurate predefined main dynamic model of the plant. It is observed that the proposed method is not only robust but also ease for implementation.

With regard to the various types of sliding mode control schemes in [13] attitude and airspeed observer based control for a fixed wing unmanned aerial vehicle have been designed for tracking of desired trajectories. The extended observer is used to estimate the necessary information about state vector and external disturbances. The adaptive SOSM control law provides finite time convergence to desired trajectories and robustness under external disturbances.

In [14], the author tries to compare and analyze by simulation the use of a non-linear STW-SMC technique with a linear PID control to stabilize the UAV's attitude and height, to prove that in some cases only a linear control technique is enough to stabilize the UAV and also prove that the amount of energy to control the UAV is similar in both techniques. So, the majority of computational resources can be assigned to object detection and collision avoidance tasks, for vehicles under 5 kilograms.

[15] presents a comparative study between back-stepping and SMC. Once the modelling has been done using the Newton-Euler formulation, a back-stepping, a HOSM, a back-stepping in conjunction with SM, a back-stepping with HOSM controller design techniques was used to control the FWUAV. The simulation result shows that the independent use of back-stepping controller produces a high torque and the HOSMC has the well-known chattering effect but the mixed use of the two control techniques produces a satisfactory performance.

Chapter Three

3. Mathematical Modelling

Dynamic modeling is a vital step in the development and control of any dynamic system. In fact, the model lets the engineer to analyze the system, its likelihoods and its demeanor depending on a number of conditions. In this section, a complete dynamic model of FWUAV is established using the Newton-Euler formulation.

3.1. Reference Frames and Coordinate Systems

In order to accurately describe a body motion, it is required to define (i) the forces and moments acting on the body and thus resulting in the body motion and (ii) the coordinate system that can be used as a reference for the motion states definition. It is vital to be aware that there are two types of forces acting on a body in arbitrary motion. First, the inertial forces and moments that depend on the velocities and accelerations relative to an inertial reference frame; the classical Newtonian dynamics equations hold only in the inertial frame. The second group consists of the aerodynamic forces and moments resulting from interaction of the body with the surrounding airflow and therefore relative to the air. Since the airflow might not be stationary, it is therefore convenient to describe the resulting aerodynamics in the coordinate frames connected to the body and to the surrounding air. The resulting motion can be conveniently described in terms of the position, velocity, acceleration, and attitude coordinates which comprise the states of the moving body. Some of these states, in turn, need to be defined with respect to a reference frame of choice which is defined by the specifics of the UAV application. Thus, the information carried by various reference frames is what facilitates the complete and convenient definition of the free body motion.[16] Therefore, this section starts with a definition of a reference frame , a coordinate system and the description of the coordinate system rotation.

Definition: - Reference frame (or sometimes called frame of reference) is a rigid body or a set of rigidly connected points that can be used to define or establish velocity, acceleration or motion in general. It is used to specify the relationship between a moving observer and the phenomenon or phenomena under observation. Whereas a Coordinate System is a measurement system usually

attached to a reference frame. It uses one or more numbers, or coordinates, to uniquely determine the position of a point or other elements on a space. Reference frames and coordinate systems often used in flight mechanics are presented in the following table.

Table 3.1: Reference frames and coordinate systems often used in flight mechanics

No	Reference Frame	Coordinate System Often Attached	Description of the Coordinate System
1	Inertial Reference Frame (F_I)	Inertial Coordinate System	✓ Assumed to be fixed with respect to distant stars. ✓ It is the ultimate frame where the Newtonian physics is valid. ✓ Origin – It can be anywhere on earth however as the earth moves the inertial frame has to stay fixed.
2	Earth-Fixed Reference Frame (F_E)	Earth Fixed Coordinate System	✓ Origin - FWUAV center of gravity. ✓ X_E axis - Points toward North Pole. ✓ Z_E axis - Points toward the center of the earth. ✓ Y_E axis - perpendicular to the X_E, Z_E-plane, positive determined by the right-hand rule.
3	Body-Fixed Reference Frame (F_B)	Body Fixed Coordinate System	✓ Origin - FWUAV center of gravity. ✓ X_B axis - positive out the nose of the FWUAV in the plane of symmetry of the FWUAV. ✓ Z_B axis - perpendicular to the X_B axis, in the plane of symmetry of the FWUAV, positive below the FWUAV.

			✓ Y_B axis - perpendicular to the X_B, Z_B-plane, positive determined by the right-hand rule.
4	Vehicle-Carried Reference Frame (F_V)	Vehicle Carried Coordinate System	✓ Origin - FWUAV center of gravity. ✓ X_V axis - Points toward North. ✓ Z_V axis -Points toward the local gravity vector (Down). ✓ Y_V axis - perpendicular to the X_B, Z_B-plane, positive determined by the right-hand rule.
5	Wind-Fixed Reference Frame (F_W)	Wind-Fixed Coordinate System	✓ Origin - FWUAV center of gravity. ✓ X_W axis - Points toward the local air-velocity vector (V_∞). ✓ Z_W axis - perpendicular to the X_W axis, in the plane of symmetry of the FWUAV, positive below the FWUAV. ✓ Y_W axis - perpendicular to the X_W, Z_W-plane, positive determined by the right-hand rule.

3.2. Rigid Body Equations of Motion

The derivation of the motion equations for a rigid body (FWUAV) moving freely in the 3D space, using the newton's laws, leads to 6 scalar equations, three translational and three rotational. In the following section we present a compact, linear algebra-based expression that reduce the written complexity without losing any property.

In order to simplify the overall modeling of the FWUAV, the following assumptions are taken without losing any generality. The FWUAV is assumed to be a rigid body in space and symmetric on the X-Z plane, the CG of the FWUAV coincides with the origin of the body-fixed coordinate System, the FWUAV has a constant mass and the earth is assumed to be an inertial frame of reference.

3.3. Kinematics

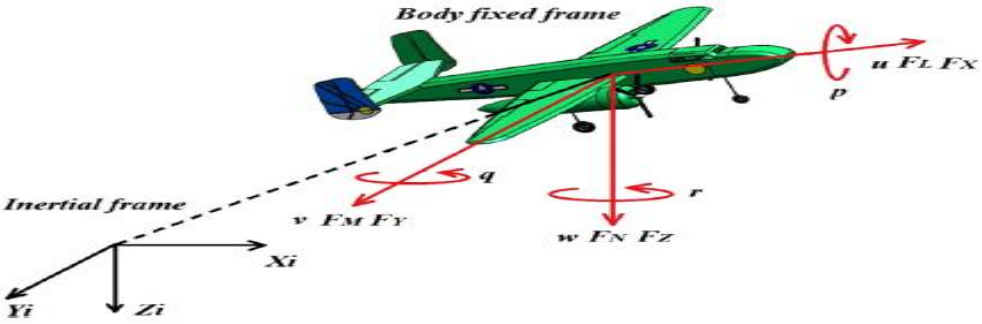

Figure 3.1: Referential Frame Configuration

3.3.1. Description of the FWUAV

Figure 3.2: North American B-25 Mitchell

The particular model of the FWUAV to be used along this work is an approximate 1:10 scaled model of the North American B-25 Mitchell, shown in figure 3.2 above, whose main parameters are also shown in Table 3.1 below. The B-25 Mitchell is a warzone aircraft (bomber) brought in 1941 and named after a pioneer of U.S. military aviation Major General William "Billy" Mitchell. The B-25 was used in almost every occasion of World War II, and after the war ended, many continued in service, operating throughout 4 decades.

The differences due to control surfaces between the scaled model and a manned version are: Unlike the North American B-25 Mitchell the modelled FWUAV is equipped with a single engine, the scaled FWUAV does not have flaps, but it does have the same ailerons, rudder and elevator and the maximum speed of the prototype is 85 meter per second. Then the prototype behaves mostly as the real one, although it is more sensible to the environment (wind currents and turbulence).

Table 3.2: FWUAV Specification

Parameter	Manned Version	Scaled Version	Units
Over all mass	12,270	8	Kg
Wing Span	20.4216	2.05	m
Wing Surface Area	56.67	0.55	m^2
Mean Aerodynamic Chord	2.823	0.28	m
Length	16.154	1.6	m
Cruising Speed	102.82	Vary	m/sec
Top Speed	127.41	85	m/sec
Inertia Moment (I_{xx})	-	0.5526	$Kg.m^2$
Inertia Moment (Iyy)	-	0.6335	$Kg.m^2$
Inertia Moment (Izz)	-	1.0783	$Kg.m^2$
Inertia Moment ($I_{xz} = I_{zx}$)	-	0.0015	$Kg.m^2$

3.3.2. FWUAV State Vector

The variables describing the state of the system are

Table 3.3: FWUAV State vector

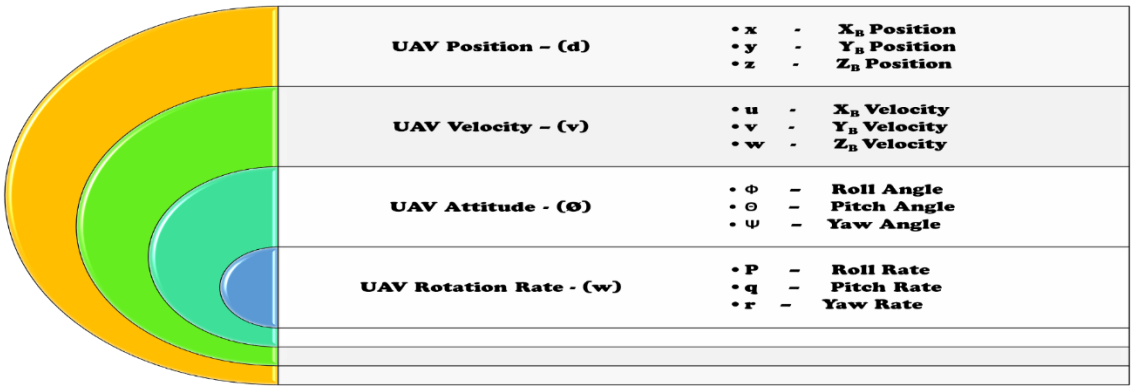

3.3.3. Rotation Parametrization

Referring to the above figure the position of any point *p* in the FWUAV is constant if is measured from F_B but it is not when measured from F_I. Although both frames are reference frames that express vector quantities (positions, velocities, accelerations and so on) in cartesian coordinates, it is evident that they do not have the same inertial properties (see [9]). The relationship between these frames is given by a Rotation Matrix (R) which produce the change of frame expression of any vector V by the equation $V^{FI} = R\ V^{FB}$, where the superscript represents the base frame from which the components of the vector are expressed.

In this document, we use Euler Angle Rotations to describe the orientation of our FWUAVs. It is extensively used in aerospace engineering where they are a mathematical representation of three successive rotations about different possible axes which are Rotation of φ around x: roll ($-\pi<\varphi<\pi$), Rotation of θ around y: pitch ($-\pi/2<\theta<\pi/2$) and Rotation of ψ around z: yaw ($-\pi<\psi<\pi$).

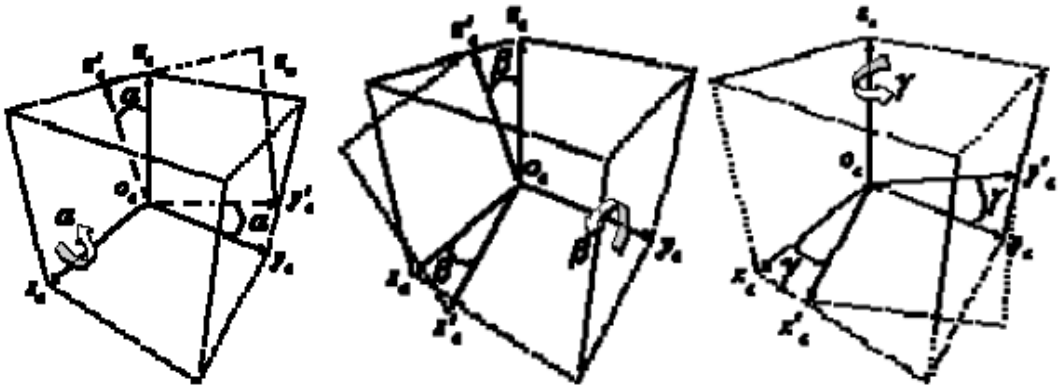

Figure 3.3: Rotation Parametrization

$$R(x, \alpha) = \begin{bmatrix} 1 & 0 & 0 \\ 0 & \cos(\alpha) & -\sin(\alpha) \\ 0 & \sin(\alpha) & \cos(\alpha) \end{bmatrix} \qquad R(y, \beta) = \begin{bmatrix} \cos(\beta) & 0 & \sin(\beta) \\ 0 & 1 & 0 \\ -\sin(\beta) & 0 & \cos(\beta) \end{bmatrix}$$

$$R(z, \gamma) = \begin{bmatrix} \cos(\gamma) & -\sin(\gamma) & 0 \\ \sin(\gamma) & \cos(\gamma) & 0 \\ 0 & 0 & 1 \end{bmatrix}$$

The complete rotation matrix, called Rotation Matrix or *Direct Cosine Matrix* is then:

$R(\phi, \theta, \psi) = R(x, \alpha)\, R(y, \beta)\, R(z, \gamma)$

$$R(\phi, \theta, \psi) = \begin{bmatrix} 1 & 0 & 0 \\ 0 & \cos(\alpha) & -\sin(\alpha) \\ 0 & \sin(\alpha) & \cos(\alpha) \end{bmatrix} \begin{bmatrix} \cos(\beta) & 0 & \sin(\beta) \\ 0 & 1 & 0 \\ -\sin(\beta) & 0 & \cos(\beta) \end{bmatrix} \begin{bmatrix} \cos(\gamma) & -\sin(\gamma) & 0 \\ \sin(\gamma) & \cos(\gamma) & 0 \\ 0 & 0 & 1 \end{bmatrix}$$

$$R(\phi, \theta, \psi) = \begin{bmatrix} C\psi C\theta & C\psi S\theta S\phi - S\psi S\phi & C\psi S\theta C\phi + S\psi S\phi \\ S\psi C\theta & S\psi S\theta S\phi + C\psi C\phi & S\psi S\theta C\phi \\ -S\theta & C\theta S\phi & C\theta C\phi \end{bmatrix} \text{---------- (eq.3.1)}$$

Where ϕ, θ, ψ are the three Euler angles and Cx stands for cos(x), Sx stands for sin(x) function in their parallel arguments.

Note: The Rotation matrix $R \varepsilon SO_3$ is an orthonormal 3X3 square matrix (of the Special Orthogonal matrices of order 3) with unit determinant $|R| = 1$ and the important property: $R^{-1} = R^T$.

So, the position of the FWUAV is given by the relation

$$\begin{bmatrix} \dot{X} \\ \dot{Y} \\ \dot{Z} \end{bmatrix} = R(\phi, \theta, \psi) \begin{bmatrix} U \\ V \\ W \end{bmatrix}$$

$$\begin{bmatrix} \dot{X} \\ \dot{Y} \\ \dot{Z} \end{bmatrix} = \begin{bmatrix} C\psi C\theta & C\psi S\theta S\phi - S\psi S\phi & C\psi S\theta C\phi + S\psi S\phi \\ S\psi C\theta & S\psi S\theta S\phi + C\psi C\phi & S\psi S\theta C\phi \\ -S\theta & C\theta S\phi & C\theta C\phi \end{bmatrix} \begin{bmatrix} U \\ V \\ W \end{bmatrix} \text{---------- (eq.3.2)}$$

3.3.4. Angular Rates

The time variation of the Euler angles $(\dot{\phi}, \dot{\theta}, \dot{\psi})^{-1}$ is a discontinuous function. Thus, it is different from body angular rates $(p, q, r)^{-1}$ which are physically measured with gyroscopes for instance.

Here the time derivative of the direction cosine matrices (DCM) is used to define the dynamics of the Euler angles.

$$\dot{R} = [\, W^{FI} \, x]\, R$$

where the matrix term $[W^{FI}\ x]$ stands for the matrix expression of the vector cross product and is defined as

$$[W^{FI}\ x] \approx \begin{bmatrix} 0 & -wz & wx \\ wz & 0 & wy \\ wy & wx & 0 \end{bmatrix}$$

A vector expression for the angular velocity can be computed as $w^{FI} = \frac{1}{2}(r_1 \times \dot{r1} + r2 \times \dot{r2} + r3 \times \dot{r3})$ where vectors r_i are the column vectors of matrix R (see for more details [9]). From last expression in can be deduced that the inertial expression of the angular velocity can be computed as

$$W = R_r \dot{\emptyset}$$

$$\begin{bmatrix} p \\ q \\ r \end{bmatrix} = R_r \begin{bmatrix} \dot{\phi} \\ \dot{\theta} \\ \dot{\psi} \end{bmatrix}, \text{ Were}$$

$$R_r = \begin{bmatrix} 1 & 0 & -\sin(\theta) \\ 0 & \cos(\phi) & \sin(\phi)\cos(\theta) \\ 0 & \sin(\phi) & \cos(\phi)\cos(\theta) \end{bmatrix} \text{---------- (eq.3.3)}$$

$$\begin{bmatrix} \dot{\phi} \\ \dot{\theta} \\ \dot{\psi} \end{bmatrix} = (R_r)^{-1} \begin{bmatrix} p \\ q \\ r \end{bmatrix}, \text{ Were}$$

$$(R_r)^{-1} = \begin{bmatrix} 1 & \sin(\phi)\tan(\theta) & \cos(\phi)\tan(\theta) \\ 0 & \cos(\phi) & -\sin(\phi) \\ 0 & \frac{\sin(\phi)}{\cos(\theta)} & \frac{\cos(\phi)}{\cos(\theta)} \end{bmatrix}$$

However, the above representation suffers from a singularity ($\theta = \pm \pi/2$) also known as the "gimbal lock". In practice, this limitation does not affect the FWUAV in normal flight mode.

So, the orientation of the FWUAV is given by the relation

$$\begin{bmatrix} \dot{\phi} \\ \dot{\theta} \\ \dot{\psi} \end{bmatrix} = (R_r)^{-1} \begin{bmatrix} p \\ q \\ r \end{bmatrix}$$

$$\begin{bmatrix} \dot{\phi} \\ \dot{\theta} \\ \dot{\psi} \end{bmatrix} = \begin{bmatrix} 1 & \sin(\phi)\tan(\theta) & \cos(\phi)\tan(\theta) \\ 0 & \cos(\phi) & -\sin(\phi) \\ 0 & \frac{\sin(\phi)}{\cos(\theta)} & \frac{\cos(\phi)}{\cos(\theta)} \end{bmatrix} \begin{bmatrix} p \\ q \\ r \end{bmatrix} \text{---------- (eq.3.4)}$$

3.4. Dynamics

"The four forces acting on an aircraft in straight, level and unaccelerated flight are Thrust, Drag, Lift and Weight [17] ." They are defined as follows:

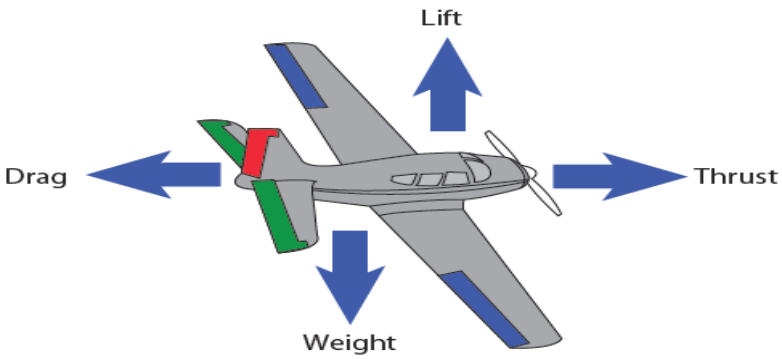

Figure 3.4: Forces Acting on an FWUAV (Source: NASA, 2010)

3.4.1. Propulsion Force and Moments

Definition: - "Thrust is the onward force produced by the engine. It overcomes the force of drag. As a universal rule, it acts parallel to the longitudinal axis" [17]. The engine for the FWUAV has to be placed at a location where all the moment created by the thrust around the CG is zero.

$$F_T = \begin{bmatrix} Tx\,(Va, \delta a) \\ 0 \\ 0 \end{bmatrix}$$

3.4.2. Gravitational Force and Moments

Definition: - “Weight is the combined load of the aircraft itself, the crew, the fuel, and the cargo or baggage. Weight is a force that pulls the aircraft downward because of the force of gravity. It opposes lift and acts vertically downward through the aircraft’s center of gravity (CG)” [17]. In the inertial frame, its representation is as

$$(F_g)^{IF} = \begin{bmatrix} 0 \\ 0 \\ mg \end{bmatrix}$$

$$(F_g)^{BF} = R^{-1} (F_g)^{IF}$$

$$(F_g)^{BF} = R^{-1} \begin{bmatrix} 0 \\ 0 \\ mg \end{bmatrix}$$

$$(F_g)^{BF} = \begin{bmatrix} C\psi C\theta & S\psi C\theta & -S\theta \\ C\psi S\theta S\phi - S\psi S\phi & S\psi S\theta S\phi + C\psi C\phi & C\theta S\phi \\ C\psi S\theta C\phi + S\psi S\phi & S\psi S\theta C\phi & C\theta C\phi \end{bmatrix} \begin{bmatrix} 0 \\ 0 \\ mg \end{bmatrix}$$

$$(F_g)^{BF} = mg \begin{bmatrix} -S\theta \\ S\phi C\theta \\ C\phi C\theta \end{bmatrix} \text{---------- (eq.3.5)}$$

On the basis of the assumption, the CG of the FWUAV coincides with the origin of the body-fixed coordinate System, the moment due to this force will be zero.

3.4.3. Aerodynamic Force and Moments

Definition: - “An aerodynamic force is a force exerted on a body by the air (or other gas) in which the body is immersed and it is due to the relative motion of the body and the gas” [18].

Definition: - “Lift is a force that is produced by the dynamic effect of the air acting on the airfoil, and acts perpendicular to the flight path through the center of lift (CL) and perpendicular to the lateral axis. In level flight, lift opposes the downward force of weight” [17].

Definition: - “Drag is a rearward, retarding force caused by disruption of airflow by the wing, rotor, fuselage, and other protruding objects. As a general rule, drag opposes thrust and acts rearward parallel to the relative wind” [17].

Definition: - “Airfoil is shaped surface, such as an airplane wing, tail, or propeller blade, that produces lift and drag when moved through the air. An airfoil produces a lifting force that acts at right angles to the airstream and a dragging force that acts in the same direction as the airstream” [19]. A typical airfoil and its properties are shown in figure 3.4, and are also described below.

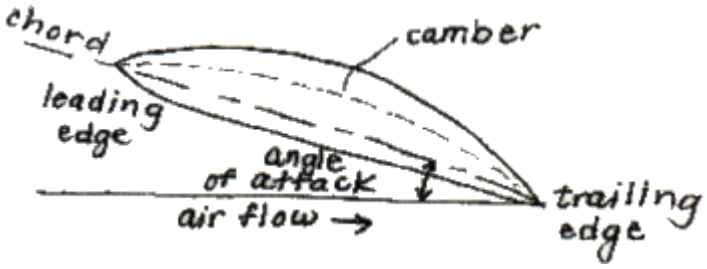

Figure 3.5: Forces Acting on an FWUAV

Chord:	A line from leading edge to trailing edge of the wing.
Camber line:	A line that indicates the halfway between chord and upper wing surface.
Angle of attack:	An Angle between the chord & direction of airflow.

The wings provide a lift force with the aid of developing a situation where the pressure on the upper part of the wing is lesser than the pressure beneath the wing. Since the pressure beneath the wing is higher than the pressure above the wing, there is a net upward force. To produce this pressure difference, the surface of the wing must satisfy one or each of the following conditions. The wing surface must be [20] : -

1. Cambered (curved); and/or
2. Inclined relative to the airflow direction.

3.4.3.1. Determination of the Aerodynamic Forces and Moments

The total Aerodynamic force on the body is due to the pressure (P) and the shear stress (τ) distribution integrated over the total exposed surface area. [21]

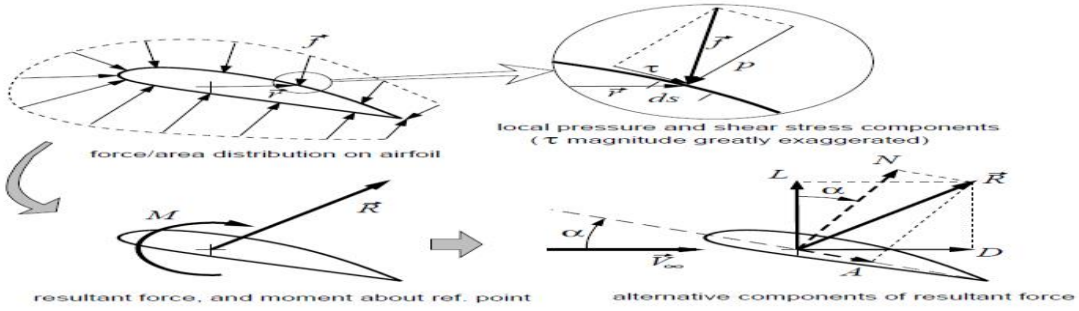

Figure 3. 6: Aerodynamic forces & Moments Acting on a wing

The figure above greatly exaggerates the magnitude of the τ stress component just to make it visible. In regular aerodynamic conditions, the pressure p (or even the relative pressure $p - p_\infty$) is normally larger than τ by way of at least two orders of magnitude, and so, f is almost perpendicular to the surface. But the small τ often meaningfully contributes to drag, so it cannot be abandoned completely. The stress distribution f, integrated over the surface produces a resultant force R, and also a moment M about some selected moment-reference point. In 2-D cases, the sign convention for M is positive nose up, as shown in the figure 3.5. The net force R has perpendicular components along any selected axes. These axes are random, but two particular selections are utmost important in practice.[16]

1. Freestream Axes: The R components are the drag D and the lift L, parallel and perpendicular to V_∞.
2. Body Axes: The R components are the axial force A and normal force N, parallel and perpendicular to the airfoil chord line.

If one of the components is computed, the other component can then be found by an easy axis transformation using the angle of attack α. Specifically, L and D are bought from N and A as follows [16].

$$L = N \cos \alpha - A \sin \alpha$$

$$D = N \sin \alpha + A \cos \alpha$$

However, this expression just shows the dependence of aerodynamic forces and moments on angle of attack α, but in reality, they are affected by several factors including Air Density (ρ), Relative Air Speed Magnitude (V_∞), Wing Surface Area (S), Wing Span (b), Mean Aerodynamic Chard (c) etc.

$$f, M = f(\rho, V_\infty, S, b, c)$$

$$f, M = \frac{1}{2}\rho\, V\infty^2\, S\, C\, (*)$$

$$f, M = QSC\,(*), \text{ were } Q = \frac{1}{2}\rho\, V\infty^2$$

Therefore, the FWUAV aerodynamics forces and moments can be calculated using aerodynamic coefficients as follows

$$f = [F_x, F_y, F_z]^T \quad \varepsilon \quad R^3$$

$$f = \begin{bmatrix} Fx \\ Fy \\ Fz \end{bmatrix} = \begin{bmatrix} Tx \\ 0 \\ 0 \end{bmatrix} + QS\,[\hat{C}\,(\alpha, \beta)]^{-1} \begin{bmatrix} -CD(*) \\ CY(*) \\ -CL(*) \end{bmatrix} \text{---------- (eq.3.6)}$$

$$M = [\tau_L, \tau_M, \tau_N]^T \quad \varepsilon \quad R^3$$

$$M = \begin{bmatrix} \tau L \\ \tau M \\ \tau N \end{bmatrix} = QS \begin{bmatrix} bCl(*) \\ cCm(*) \\ bCn(*) \end{bmatrix}$$

Were

$$\hat{C}\,(\alpha, \beta) = \begin{bmatrix} C\alpha C\beta & S\beta & S\alpha C\beta \\ -C\alpha S\beta & C\beta & -S\alpha S\beta \\ -S\alpha & 0 & C\alpha \end{bmatrix}$$

- C stands for cosine and S stands for sine

$\hat{C}\,(\alpha, \beta)$ is a rotation matrix that maps a body fixed frame coordinate to a virtual wind frame coordinates defined along the relative velocity of the aircraft.

Table 3.4: Coefficients of Aerodynamic Forces and Moments [23]

Parameter	Name
$\alpha = \text{Arctan}\left(\frac{w}{u}\right)$	Angle of attack
$\beta = \text{Arcsine}\left(\frac{v}{Va}\right)$	Side slip angle
$Va^2 = u^2+v^2+w^2$	Relative airspeed magnitude
$Q = \frac{1}{2}\rho Va^2$	Dynamic Pressure
ρ	Air density
S	Wing surface area
b	Wing span
c	Mean aerodynamic chord
$CL = C_{Lo} + C_{L\alpha}\alpha + C_{L\delta f}\delta f + C_{L\delta e}\delta e + \frac{c}{2V}(C_L\dot{\alpha}\dot{\alpha} + C_{Lq}q) + C_{LM}M$	Lift force coefficient
$CD = C_{Do} + C_{D\alpha}\alpha + C_{D\delta f}\delta f + C_{D\delta a}\delta a + C_{D\delta e}\delta e + C_{D\delta r}\delta r + C_{LM}M$	Drag force coefficient
$CY = C_{y\beta}\beta + \frac{b}{2V}(C_{yp}p + C_{yr}r) + Cy_{\delta a}\delta a + Cy_{\delta r}\delta r$	Side force Coefficient
$Cl = C_{l\beta}\beta + \frac{b}{2V}(C_{lp}p + C_{lr}r) + C_{l\delta a}\delta a + C_{l\delta r}\delta r$	Roll Moment Coefficient
$Cm = C_{mo} + C_{m\alpha}\alpha + C_{m\delta f}\delta f + C_{m\delta e}\delta e + \frac{c}{2V}(C_{m\alpha}\dot{\alpha} + C_{mq}q) + C_{LM}M$	Pitch Moment Coefficient
$Cn = C_{n\beta}\beta + \frac{b}{2V}(C_{np}p + C_{nr}r) + C_{n\delta a}\delta a + C_{n\delta r}\delta r$	Yaw Moment Coefficient

The non-dimensional aerodynamic coefficients for both lateral and longitudinal forces and moments are dependent on the sideslip angle (β), angle of attack (α), the body angular rates (p, q, r), and the control surfaces (δa, δe, δr) [23]. Typical values for these coefficients can obtained either experimentally through a wind tunnel experiment or with the help of a software such as AVL. For the motive of this thesis an extensive literature investigation was executed to attain the appropriate aerodynamic coefficients for the wing type selected in addition with the AVL software.

Table 3.5: Typical values Coefficients of Aerodynamic Forces and Moments[23]

Coefficient	Value	Coefficient	Value
$C_{L\alpha}$	5.19230	$C_{D\delta e}$	0.026848
C_{Lo}	0.45454	$C_{n\delta a}$	0.014258
C_{Lq}	11.2138	$C_{n\delta r}$	0.068250
C_{Do}	0.01190	$C_{l\delta a}$	0.206880
$C_{D\alpha}$	0.27227	$C_{l\delta r}$	0.012136
C_{Dq}	0.48183	$C_{Y\delta a}$	0.015862
C_{mq}	-17.9711	$C_{Y\delta r}$	-0.155020
$C_{m\alpha}$	-3.10370	$C_{m\delta e}$	-1.64590
$C_{n\beta}$	-0.03077	$C_{l\delta e}$	0.569740
C_{nr}	-0.20076	C_{lp}	-0.50180
C_{np}	-0.01529	$C_{y\beta}$	1.76490
$C_{l\beta}$	0.15875	C_{yr}	-1.85580
C_{lr}	0.02036	C_{yp}	0.028185

3.4.4. FWUAV Equation of Motion

In this section we lay the basic groundwork for the development of a complete 6 DOF equations of motion starting with some basic Assumptions

Assumption 1: - FWUAV is assumed to be a rigid body

In a rigid body the distance between any specified points in the body are fixed, so that this assumption eliminates consideration of the forces acting between individual elements of mass. Consequently, the FWUAV motion can be described completely by translation of the center of mass and by a rotation about this point.[24]

Assumption 2: - The earth is assumed to be fixed in space.

The inertial frame of reference defined by this assumption, i.e., one that is fixed or moves at constant velocity relative to the earth, permits a description of vehicle motion which is accurate for relatively short-term guidance and control analysis purposes. It does have practical limitations when very long-term navigation or extra-atmospheric operations are of interest[24]. With the above two assumptions as a basis, we have a reference frame in which newton's law are valid and a rigid body to which these laws may be applied. Consider that the FWUAV has a linear momentum vector, P, and angular momentum vector, H, each measured in the inertial coordinate frame. By newton's second law the time rate of change of linear momentum equals the sum of all externally applied forces and the rate of change of angular momentum equals the sum of all externally applied torques.[24]

$$\frac{dp}{dt} = F \quad \text{and} \quad \frac{dH}{dt} = M$$

$$\frac{dP}{dt} = F$$

$$m\frac{dV}{dt} = F$$

$$m\frac{dV}{dt} = F_{aero} + mg$$

Using Coriolis equation

$$\frac{d}{dt}V^{IF} = \frac{d}{dt}V^{BF} + (W^{BF} \text{ x } V^{BF})$$

Then

$$F_{aero} + mg = m\frac{d}{dt}V$$

$$F_{aero} + mg = m\left(\frac{d}{dt}V^{BF} + (W^{BF} \text{ x } V^{BF})\right)$$

Solving for $\frac{d}{dt}V^{BF}$

$$\frac{d}{dt}V^{BF} = \frac{1}{m}F^{BF}_{aero} + g^{BF} - (W^{BF} \text{ x } V^{BF})$$

Were

$$F^{BF}_{aero} = f = [F_x, F_{y,} F_z]^T \quad \varepsilon \quad R^3$$

$g^{BF} = [-g\sin(\theta),\ g\sin(\phi)\cos(\theta),\ g\cos(\phi)\cos(\theta)]^T$

$W^{BF} = [p,\ q,\ r]^T$

$V^{BF} = [u,\ v,\ w]^T$

$$\begin{bmatrix}\dot{u}\\ \dot{v}\\ \dot{w}\end{bmatrix} = \frac{1}{m}\begin{bmatrix}Fx\\ Fy\\ Fz\end{bmatrix} + \begin{bmatrix}-g\sin(\theta)\\ g\sin(\phi)\cos(\theta)\\ g\cos(\phi)\cos(\theta)\end{bmatrix} - \begin{bmatrix}p\\ q\\ r\end{bmatrix} x \begin{bmatrix}u\\ v\\ w\end{bmatrix}$$ ----------(eq.3.7)

$$\frac{dH}{dt} = M$$

Using Coriolis equation

$$\frac{d}{dt}H^{IF} = \frac{d}{dt}H^{BF} + (W^{BF} \text{ x } H^{BF})$$

Then

$$\frac{dH}{dt} = M$$

$$\frac{d}{dt}H^{BF} + (W^{BF} \text{ x } H^{BF}) = M$$

But $H^{BF} = I^{BF}W^{BF}$, hence $\frac{d}{dt}H^{BF} = I^{BF}\frac{d}{dt}W^{BF}$

Note that: in the body axis the inertial tensor doesn't change

$$\Sigma M = \frac{d}{dt}H^{BF} + (W^{BF} \text{ x } H^{BF})$$

$$I^{BF}\frac{d}{dt}W^{BF} + (W^{BF} \text{ x } (I^{BF}W^{BF})) = M^{BF}$$

Solving for $\frac{d}{dt}W^{BF}$

$$\frac{d}{dt}W^{BF} = (I^{BF})^{-1}\ (M^{BF} - W^{BF}\ X\ (I^{BF}W^{BF}))$$

Were

$$I^{BF} = \begin{bmatrix}Ixx & 0 & -Ixz\\ 0 & Iyy & 0\\ -Izx & 0 & Izz\end{bmatrix}$$ (with x-z plane of symmetry)

$$(I^{BF})^{-1} = \begin{bmatrix} \frac{Izz}{IxxIzz-IxzIzx} & 0 & \frac{Ixz}{IxxIzz-IxzIzx} \\ 0 & \frac{1}{Iyy} & 0 \\ \frac{Izx}{IxxIzz-IxzIzx} & 0 & \frac{Ixx}{IxxIzz-IxzIzx} \end{bmatrix}$$

$M^{BF} = [\tau_L, \tau_M, \tau_N]^T \quad \varepsilon \quad R^3$

$W^{BF} = [p, q, r]^T$

$$I^{BF}W^{BF} = \begin{bmatrix} Ixx & 0 & -Ixz \\ 0 & Iyy & 0 \\ -Izx & 0 & Izz \end{bmatrix} \begin{bmatrix} p \\ q \\ r \end{bmatrix} = \begin{bmatrix} Ixx\ p - Ixz\ r \\ Iyy\ q \\ Izx\ p - Izz\ r \end{bmatrix}$$

Therefore

$$\frac{d}{dt}W^{BF} = (I^{BF})^{-1}\ (M^{BF} - W^{BF}\ X\ (I^{BF}W^{BF}))$$

$$\begin{bmatrix} \dot{p} \\ \dot{q} \\ \dot{r} \end{bmatrix} = \begin{bmatrix} \frac{Izz}{IxxIzz-IxzIzx} & 0 & \frac{Ixz}{IxxIzz-IxzIzx} \\ 0 & \frac{1}{Iyy} & 0 \\ \frac{Izx}{IxxIzz-IxzIzx} & 0 & \frac{Ixx}{IxxIzz-IxzIzx} \end{bmatrix} \{ \begin{bmatrix} \tau x \\ \tau y \\ \tau z \end{bmatrix} \begin{bmatrix} p \\ q \\ r \end{bmatrix} x \begin{bmatrix} Ixx\ p - Ixz\ r \\ Iyy\ q \\ Izx\ p - Izz\ r \end{bmatrix} \} \text{-------- (eq.3.8)}$$

Finally, by using a Newton-Euler formulation a full 6-DOF FWUAV dynamic model is given by

$$\dot{d} = R(Ø)\ V \text{ ---------- (eq.3.9)}$$

$$\dot{Ø} = Rr^{-1}(Ø)\ W \text{ ---------- (eq.3.10)}$$

$$\dot{V}^{BF} = \frac{1}{m} F^{BF}_{aero} + g^{BF} - (W^{BF} \text{ x } V^{BF}) \text{ ---------- (eq.3.11)}$$

$$\dot{W}^{BF} = (I^{BF})^{-1}\ (M^{BF} - W^{BF}\ X\ (I^{BF}W^{BF})) \text{ ---------- (eq.3.12)}$$

3.5. Simplified Motion Modes

The overall movement of the FWUAV (in fact any aircraft) can be divided in to two complementary motion modes that allows a simpler representation on which control techniques would be applied easily. These are the longitudinal motion mode and lateral - directional motion mode.

3.5.1. Longitudinal Motion Mode

At the point when a symmetric aircraft is either in steady level flight or climbing or plunging in the upward plane, longitudinal and lateral- directional movements are uncoupled. The most significant longitudinal dynamic effects can be described by just four equations addressing perturbations in the translational and vertical velocity, pitch angle and angular rates [4]. To get the expression of this mode, we introduced the following assumptions to the full model [23].

Assumption 1: The roll and yaw angles are zero, i.e., $\phi = \psi = 0$, the lateral angle β does not exist and the angular velocities $p = r = 0$.

Assumption 2: The position along X_B is changing at a constant rate, i.e., $\dot{x} = 0$ and altitude is changing at a constant rate., i.e., $\dot{z} = 0$. Therefore, the equation set representing the longitudinal motion mode of an airplane can be simplified to

$$\dot{u} = \frac{Fx}{m} - qw - g\sin(\theta) \quad \text{---------- (eq.3.13)}$$

$$\dot{w} = \frac{Fz}{m} + qu + g\cos(\theta) \quad \text{---------- (eq.3.14)}$$

$$\dot{q} = \frac{\tau M}{Iyy} \quad \text{----------(eq.3.15)}$$

$$\dot{\theta} = q \quad \text{----------(eq.3.16)}$$

3.5.2. Lateral-Directional Motion Mode

This mode represents the remaining three degrees of freedom equations: sideslip displacement (y-direction), the roll and the yaw angle. Small yawing and rolling motions that occur in steady, level flight can account for lateral-directional dynamics only so that longitudinal motions can be neglected. To get the expression of this mode, again the following assumptions to the full model is introduced.

Assumption 3: If longitudinal motion is controlled and steady, then the pitch rate is zero, i.e., q = 0, translational velocity can be considered constant, i.e., $\dot{U} = 0$, the pitch angle can be considered constant, i.e., $\dot{\theta} = 0$ and horizontal and vertical dynamics can be neglected, i.e., $\dot{X} = \dot{W} = 0$. Therefore, the equation set representing the lateral motion of an airplane can be simplified to

$$\dot{v} = \frac{Fy}{m} - pw - ru + g\sin(\phi)\cos(\theta) \text{ ---------- (eq.3.17)}$$

$$\dot{p} = \frac{Izz\,\tau L + Ixz\,\tau N}{Ixx\,Izz - Ixz\,Izx} \text{ ---------- (eq.3.18)}$$

$$\dot{r} = \frac{Izx\,\tau L + Ixx\,\tau N}{Ixx\,Izz - Ixz\,Izx} \text{ ---------- (eq.3.19)}$$

$$\dot{\psi} = r \text{ ----------(eq.3.20)}$$

$$\dot{\phi} = p \text{ ---------- (eq.3.21)}$$

3.6. Controlling the Motion of Flight

In order for an aircraft to reach its destination, the forces of flight have to be precisely manipulated. To do this, the aircraft has control surfaces (see figure 3.6.) which can direct airflow in a very specific ways [25].

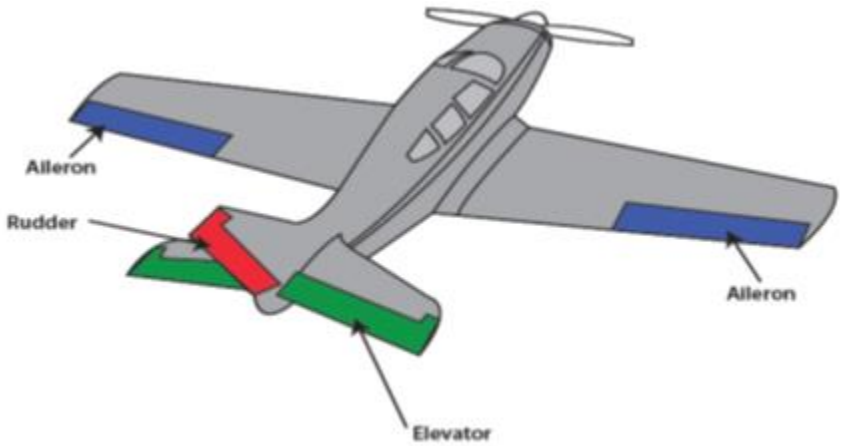

Figure 3.7: Flight Control Surfaces (Source: NASA, 2010)

Definition: - “Elevator | Pitch - As the name implies, the elevator helps ‘elevate’ the aircraft. It is usually located on the tail of the aircraft and serves two purposes. The first is to provide stability by producing a downward force on the tail. Airplanes are traditionally nose-heavy and this downward force is required to compensate for that. The second is to direct the nose of the aircraft either upwards or downwards, known as pitch, in order to make the airplane climb and descend” (see figure 3.7) [25].

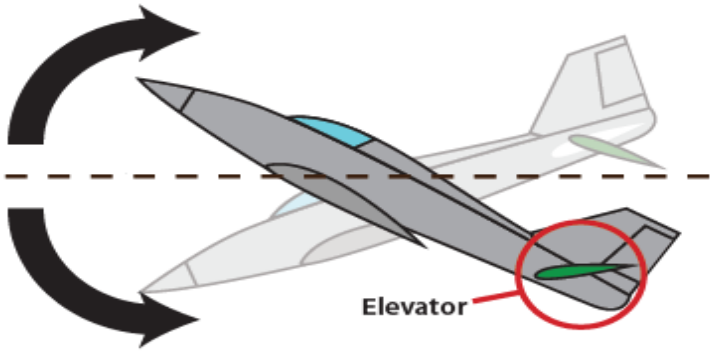

Figure 3.8: Elevator and Pitch Movement (Source: NASA, 2010)

Definition: - “Ailerons | Roll - The ailerons are located at the rear of the wing, one on each side. They work opposite to each other, so when one is raised, the other is lowered. Their job is to increase the lift on one wing, while reducing the lift on the other. By doing this, they roll the aircraft sideways, which allows the aircraft to turn. This is the primary method of steering a fixed-wing aircraft” (see figure 3.8) [25].

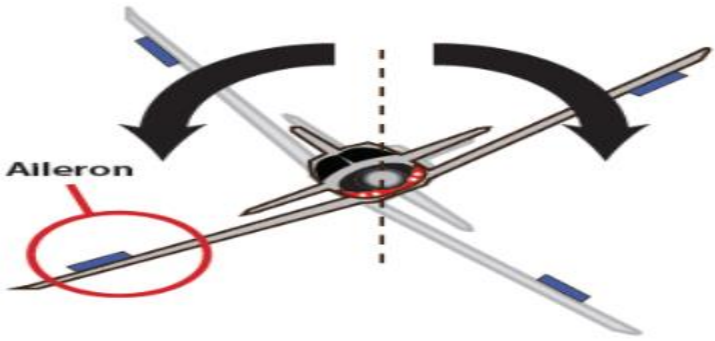

Figure 3.9: Aileron and Roll Movement (Source: NASA, 2010)

Definition: - “Rudder | Yaw - The rudder is located on the tail of the aircraft. It works identically to a rudder on a boat, steering the nose of the aircraft left and right. Unlike the boat however, it is not the primary method of steering. Its main purpose is to counteract the drag caused by the

lowered aileron during a turn. This adverse yaw, as it is known, causes the nose of the airplane to point away, or outwards, from the direction of the turn. The rudder helps to correct this by pushing the nose in the correct direction, maintaining what is known as coordinated flight" (see figure 3.9) [25]

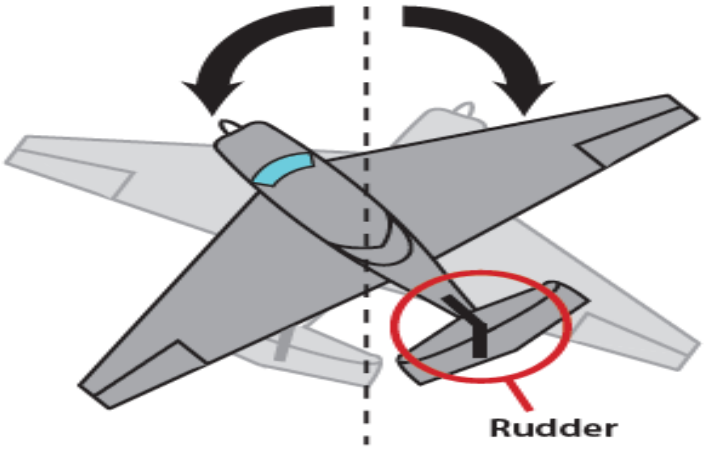

Figure 3.10: Rudder and Yaw Movement (Source: NASA, 2010)

3.7. The Axes of Flight

Every axis of flight is an imaginary line around which an aircraft can turn. Think of an airplane revolving around an axis as a wheel rotates round an axle. Irrespective of the kind of an aircraft, there are three axes up on which it can move: left-ward and right-ward, onwards and rearward, up and down. In aviation however, their technical names are the lateral axis, longitudinal axis and vertical axis.[25]

Definition: - "The Longitudinal Axis (Roll) -The longitudinal axis runs from the nose of the aircraft to the tail. This is the axis around which the aircraft rolls" (see figure 3.10) [25].

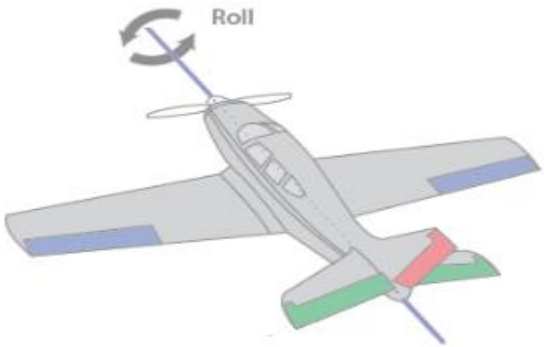

Figure 3.11: The Longitudinal Axis (Source: NASA, 2010)

Definition: - "The Lateral Axis (Pitch) - The lateral axis runs from wing tip to wing tip. The aircraft pitches around this axis" (see figure 3.11) [25].

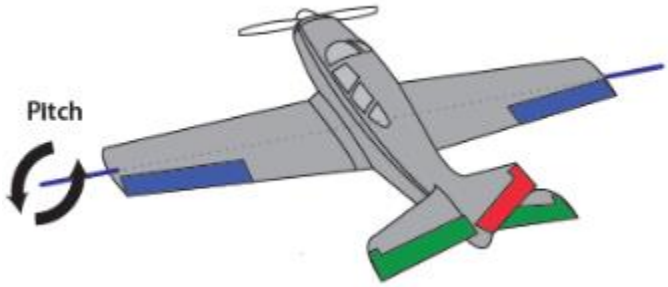

Figure 3.12: The Lateral Axis (Source: NASA, 2010)

Definition: - "The Vertical Axis (Yaw) - The vertical axis is slightly different to the others, running vertically through the center of the aircraft. The aircraft yaws around this axis" (see figure 3.12) [25].

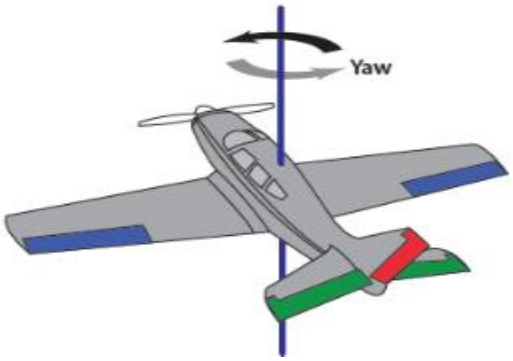

Figure 3.13: The Vertical Axis (Source: NASA, 2010)

3.8. Open Loop Simulation

Model validation is done using the MATLAB Simulink software.

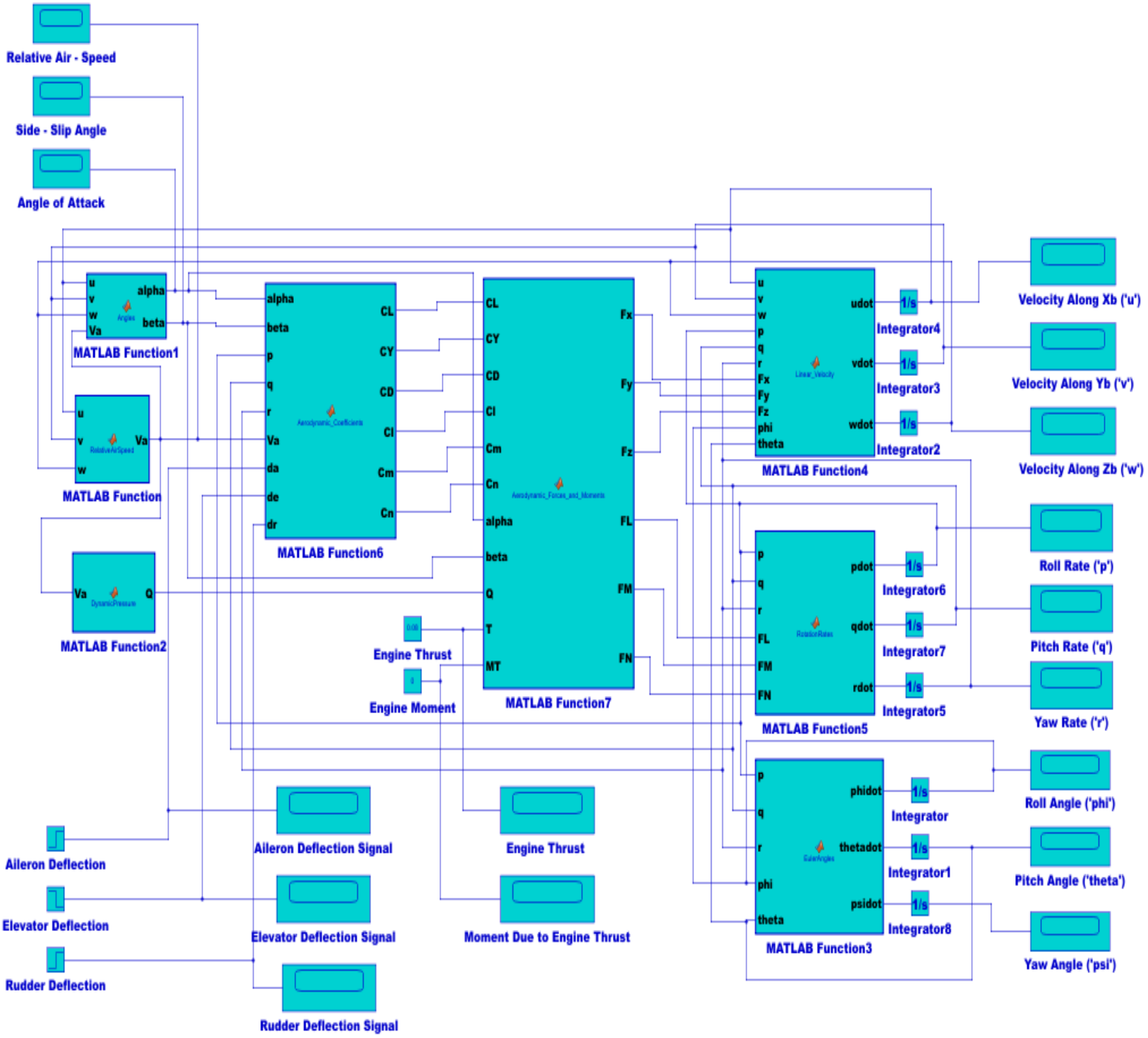

Figure 3.14: Open Loop Simulation Block Diagram

3.8.1. Scenario-1 (Solo Flight - I)

A constant -5.17-degree (-0.1 radians) elevator kick was introduced with no deflection on the aileron and rudder while keeping the trust force at 0.08N and initial forward velocity 85m/sec for a duration of 360 seconds.

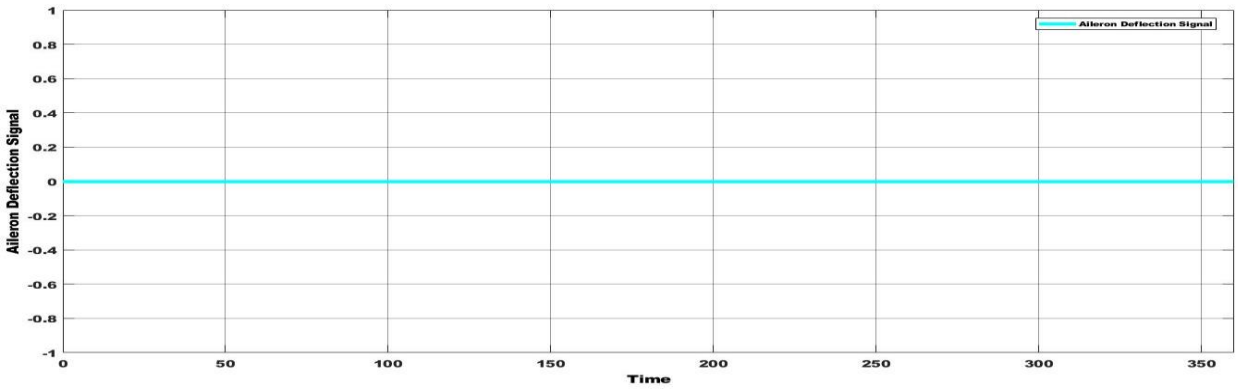

Figure 3.15: Aileron Deflection Signal

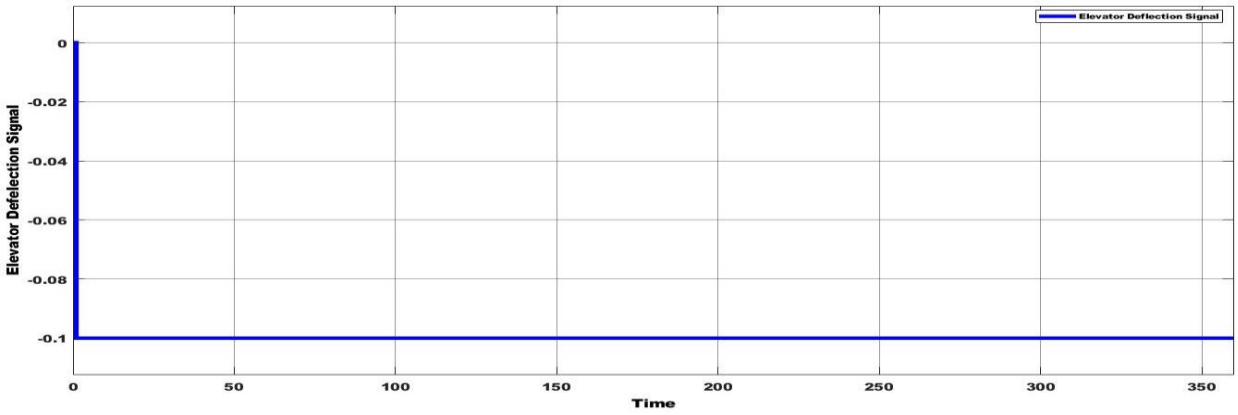

Figure 3.16: Elevator Deflection Signal

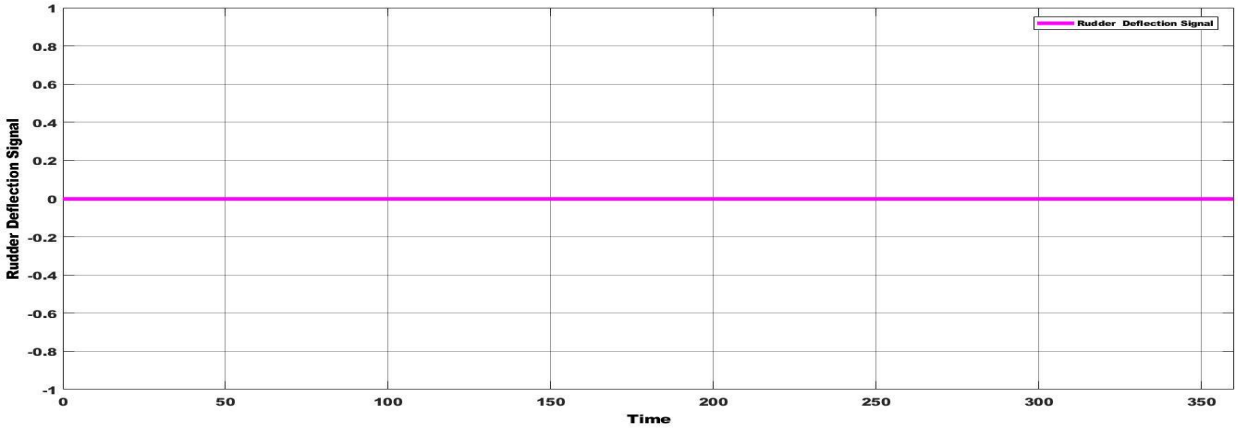

Figure 3.17: Rudder Deflection Signal

The response was presented as follows.

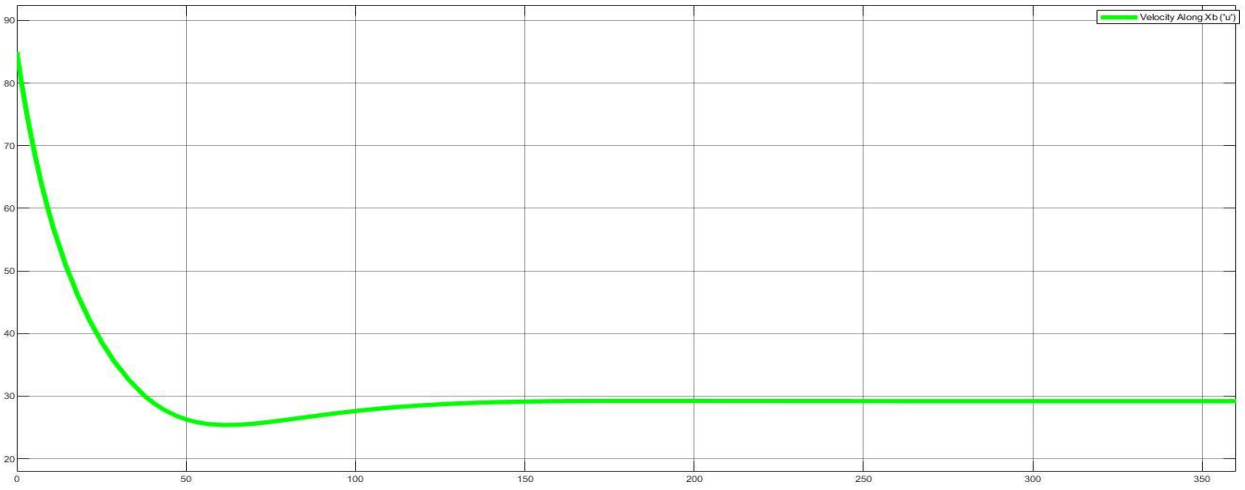

Figure 3.18: Velocity Along X_B ("u")

Figure 3.19: Velocity Along Y_B ("v")

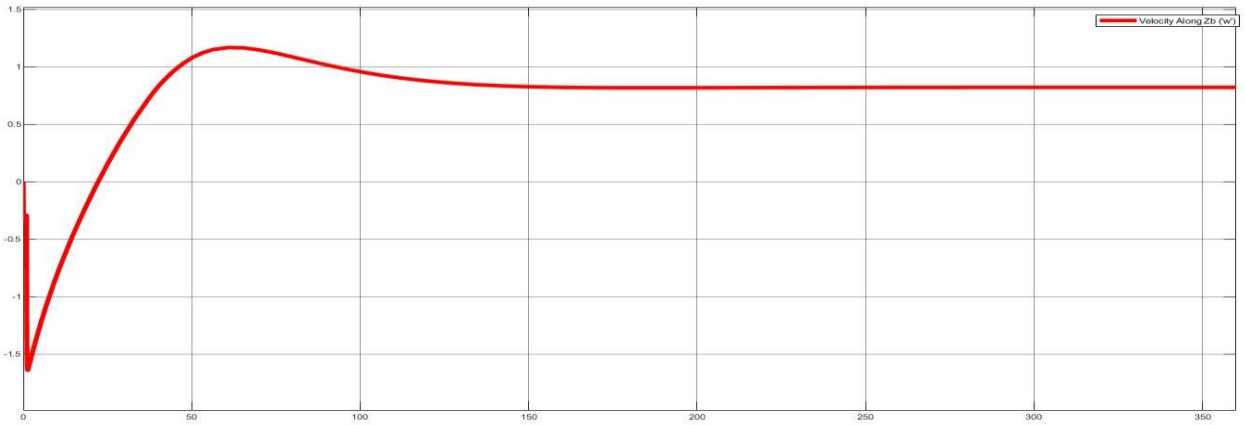

Figure 3.20: Velocity Along Z_B ("w")

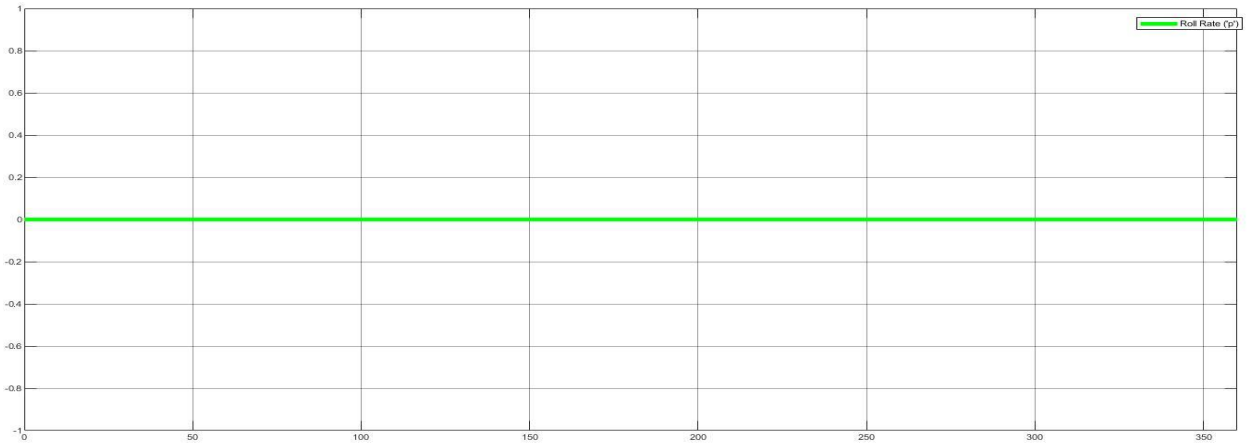

Figure 3.21: Roll Rate (“p”)

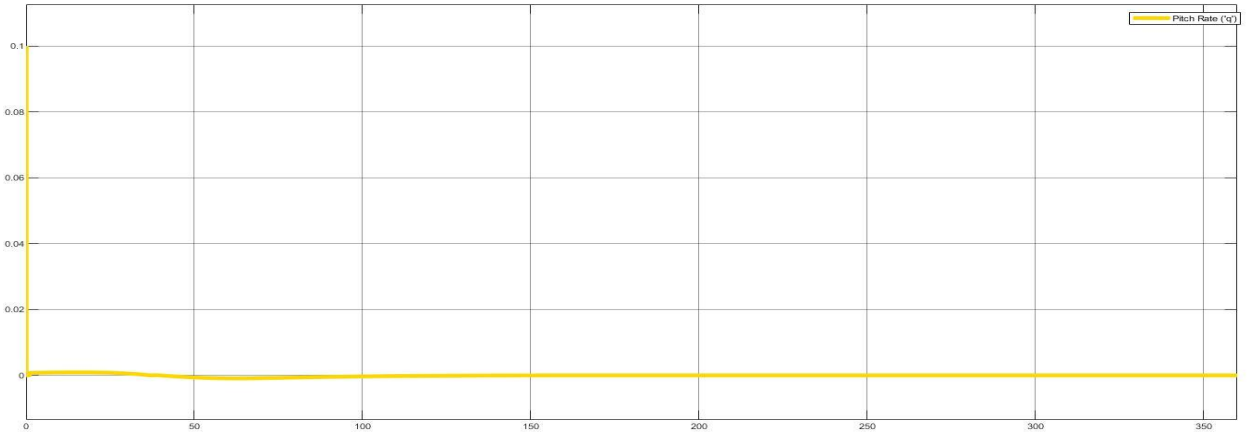

Figure 3.22: Pitch Rate (“q”)

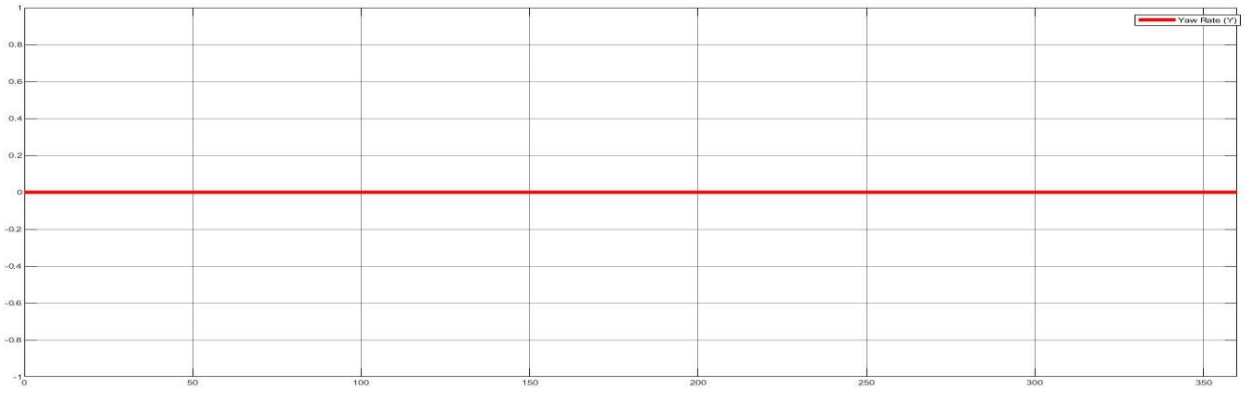

Figure 3.23: Yaw Rate (“r”)

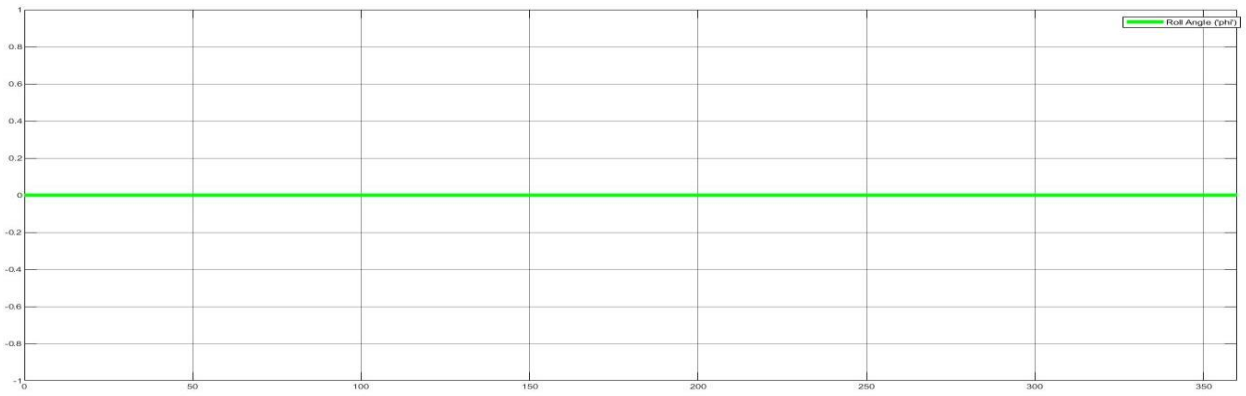

Figure 3.24: Roll Angle (“Phi”)

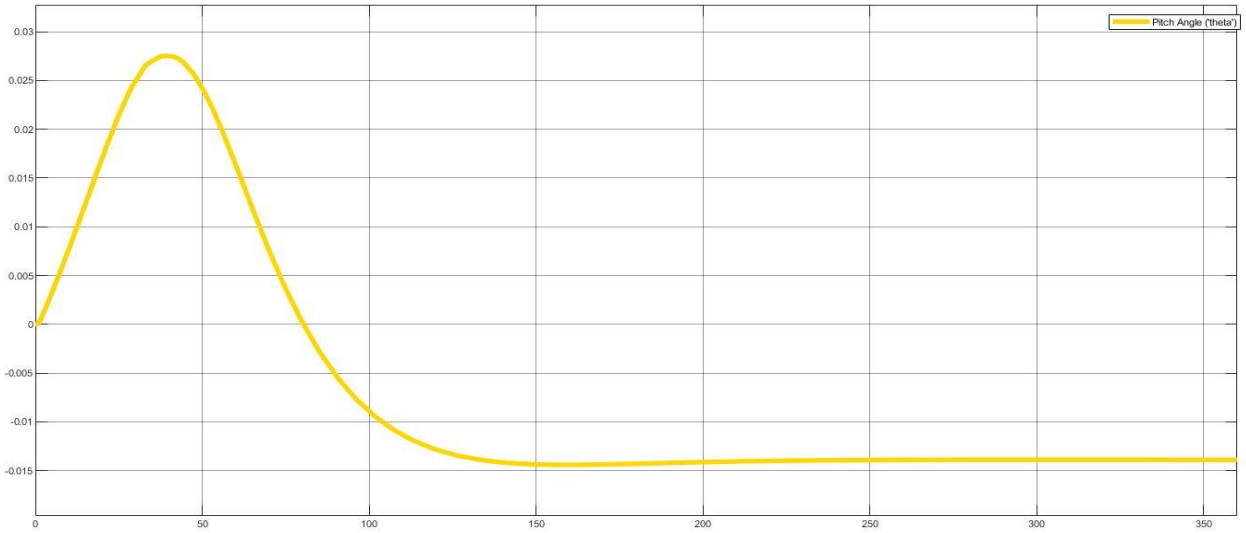

Figure 3.25: Pitch Angle (“Theta”)

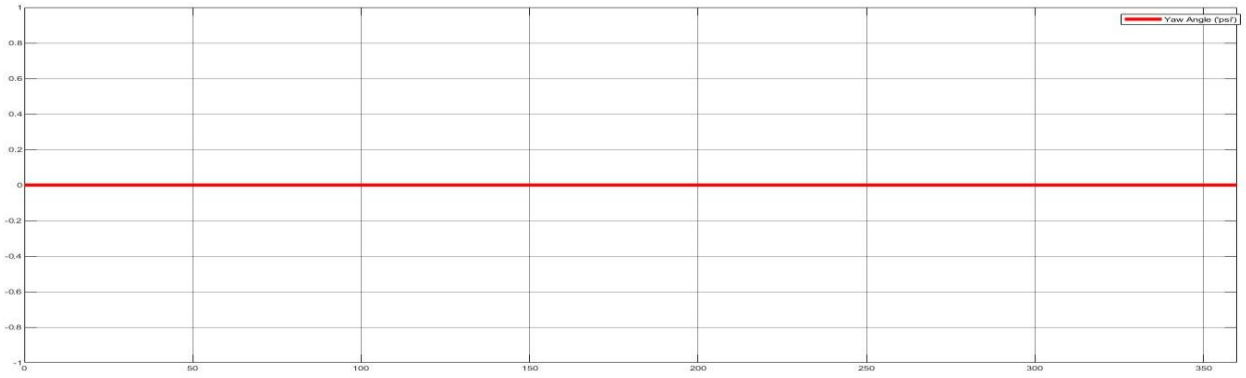

Figure 3.26: Yaw Angle (“Psi”)

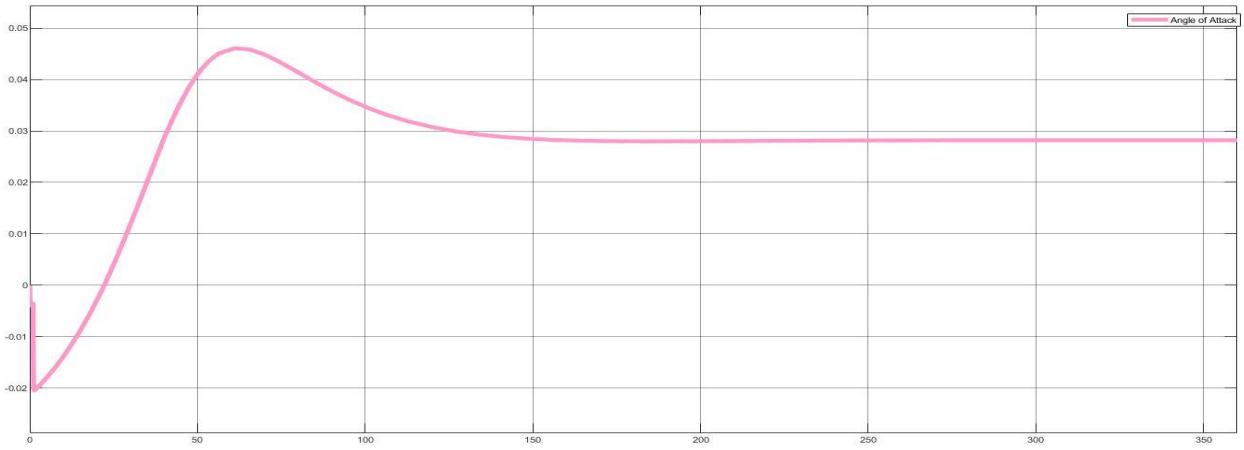

Figure 3.27: Angle of Attack ("Alpha")

3.8.1.1. Remarks on the Response

As can be seen from figure 3.17 the FWUAV started at 85m/sec initial forward velocity then actually it lost some speed and reach it peak drop at around 60 seconds and eventually stabilizes at speed of 29 m/sec. This response has some undesirable characteristics like settling at different velocity than initially perturbed with large settling time around 100 seconds and some overshoot. Again, it started with zero vertical velocity experience some oscillations and finally stabilizes at around 0.7 m/sec with a settling time of around 150 seconds (figure 3.19).

There is no motion in the lateral-directional axis, i.e., no side way velocity, zero roll & yaw rate and of course no rolling and yawing which kind of make sense, since we started only with elevator kick. The model brings an acceptable peak angle of attack which is less than 3 degrees (less than 0.05 radians) resulted in stalling free solo flight.

3.8.2. Scenario-2 (Solo Flight - II)

A constant -5.17-degree (-0.1 radians) elevator kick was introduced with no deflection on the rudder and no deflection on aileron for 30 seconds, then the aileron is pulsed for 2 seconds at +5.17 degree then bring it back to zero while keeping the trust force at 0.08N and initial forward velocity 85m/sec for a duration of 360 seconds.

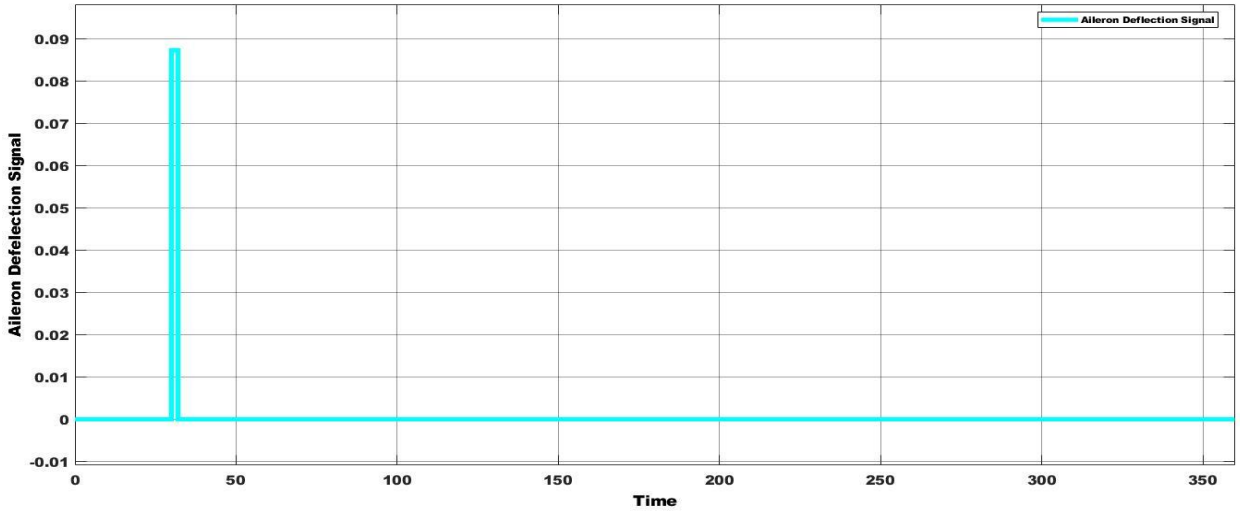

Figure 3.28: Aileron Deflection Signal

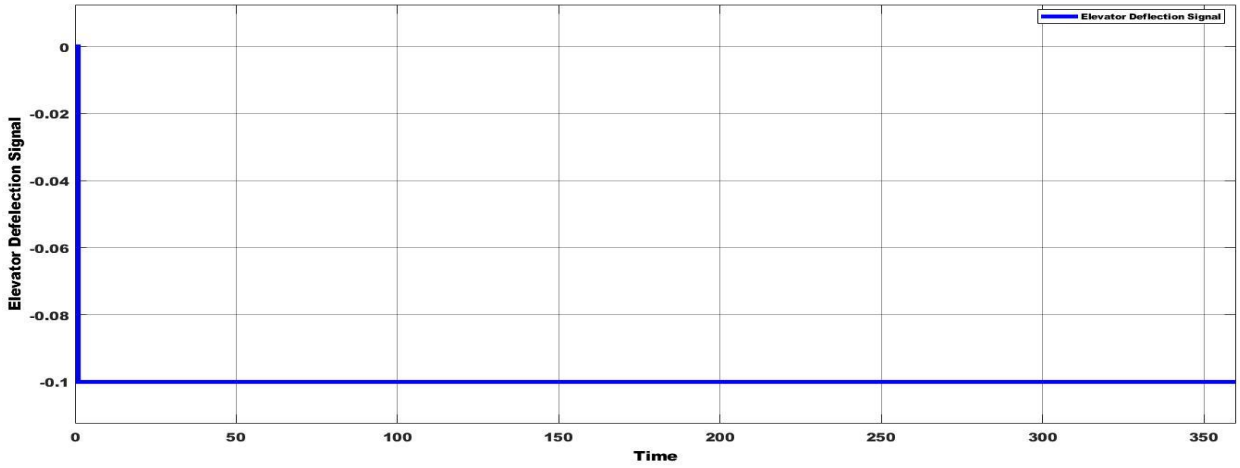

Figure 3.29: Elevator Deflection Signal

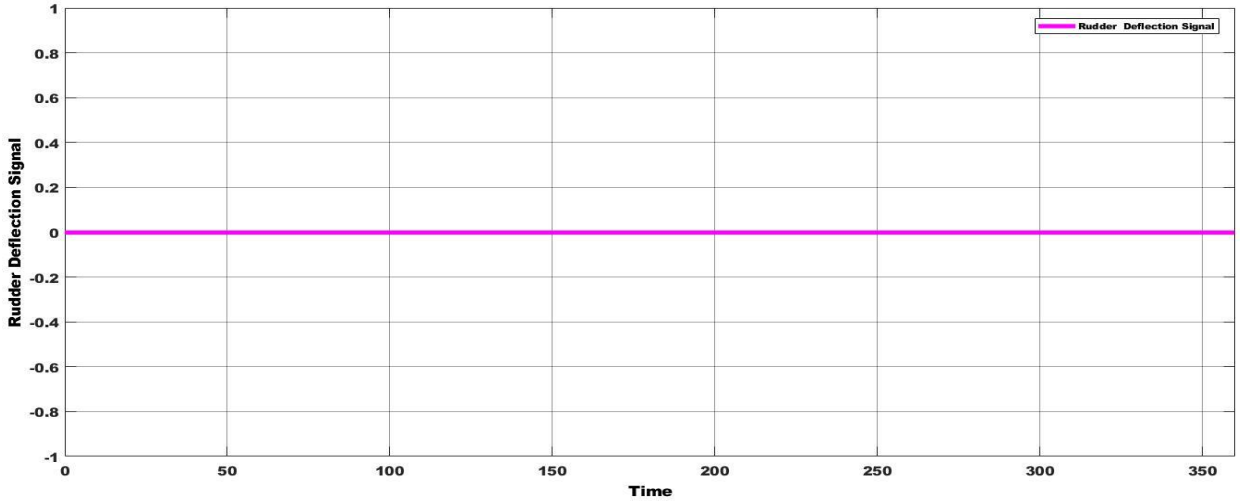

Figure 3.30: Rudder Deflection Signal

The response was presented as follows.

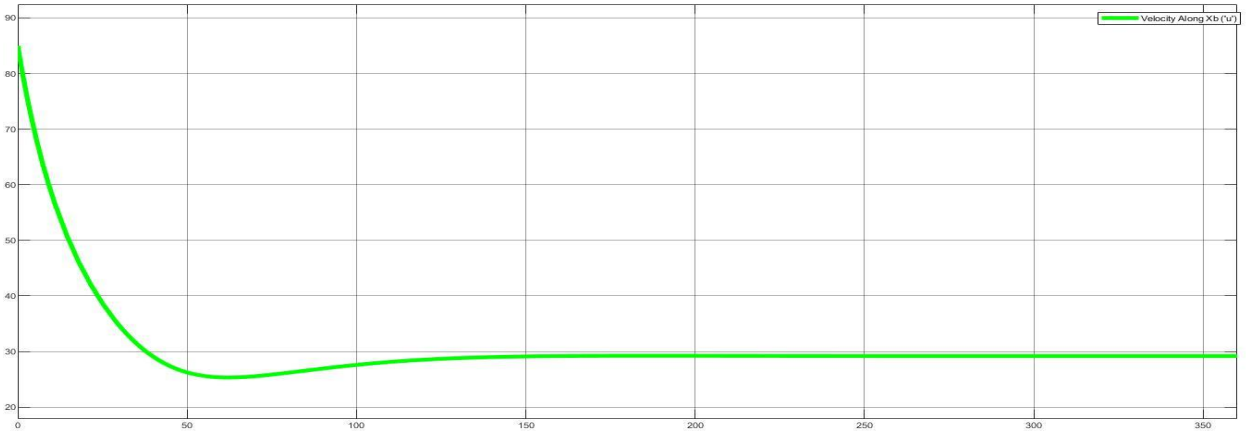

Figure 3.31: Velocity Along X_B (“u”)

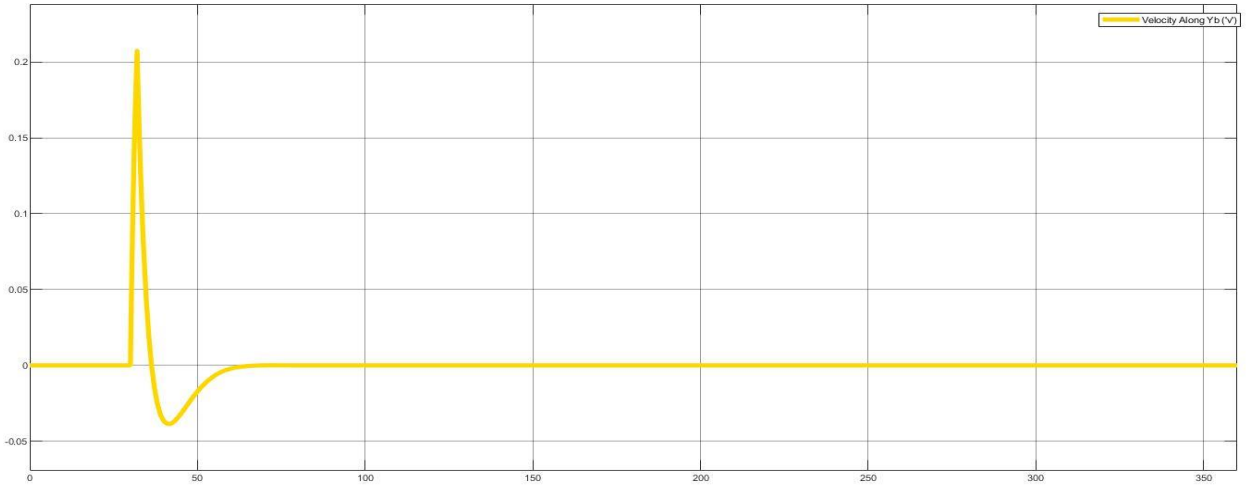

Figure 3.32: Velocity Along Y_B (“v”)

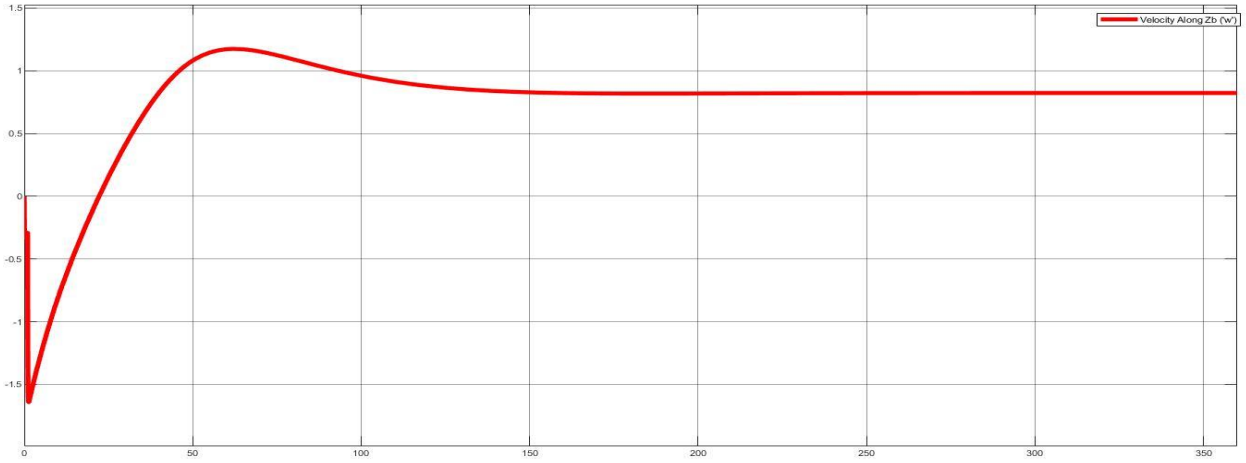

Figure 3.33: Velocity Along Z_B (“w”)

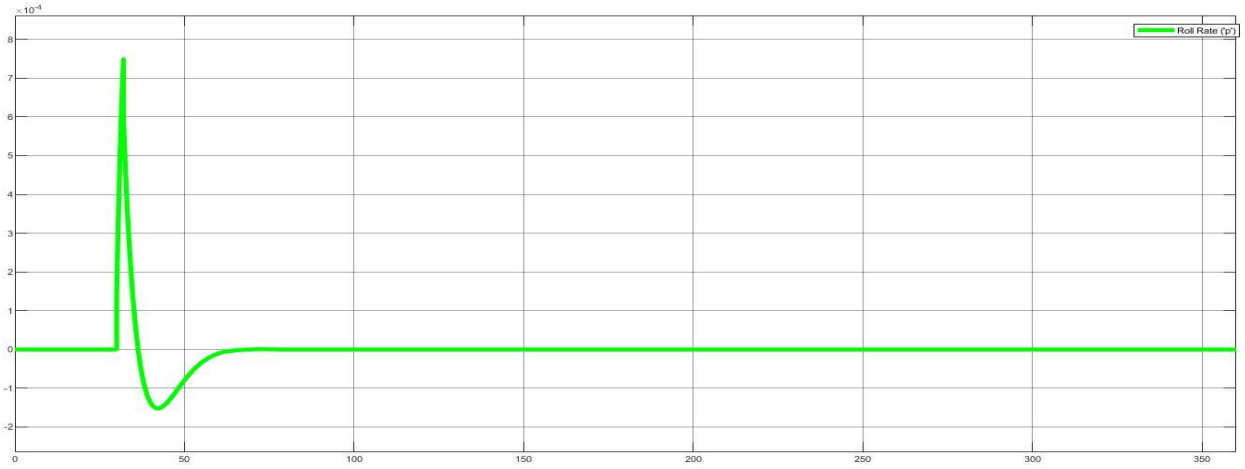

Figure 3.34: Roll Rate (“p”)

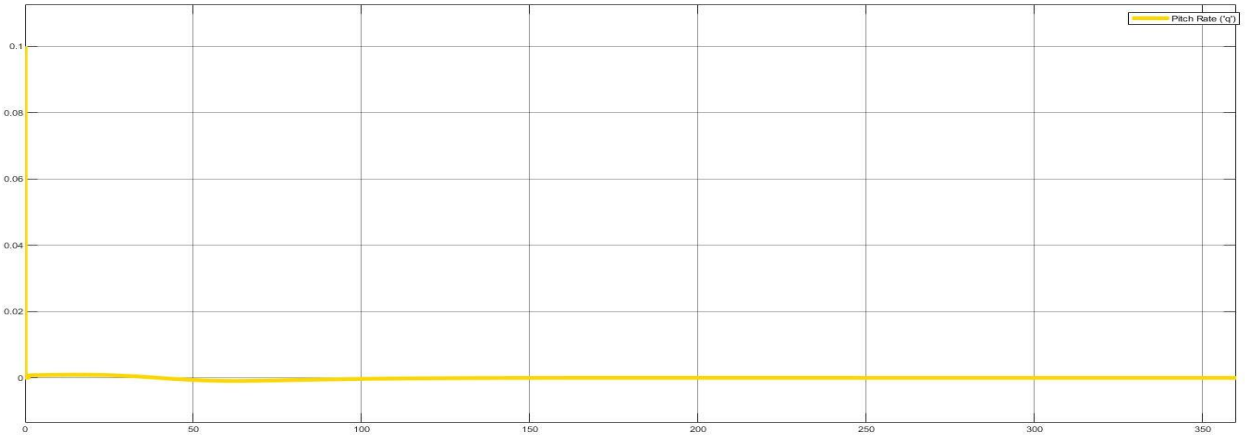

Figure 3.35: Pitch Rate (“q”)

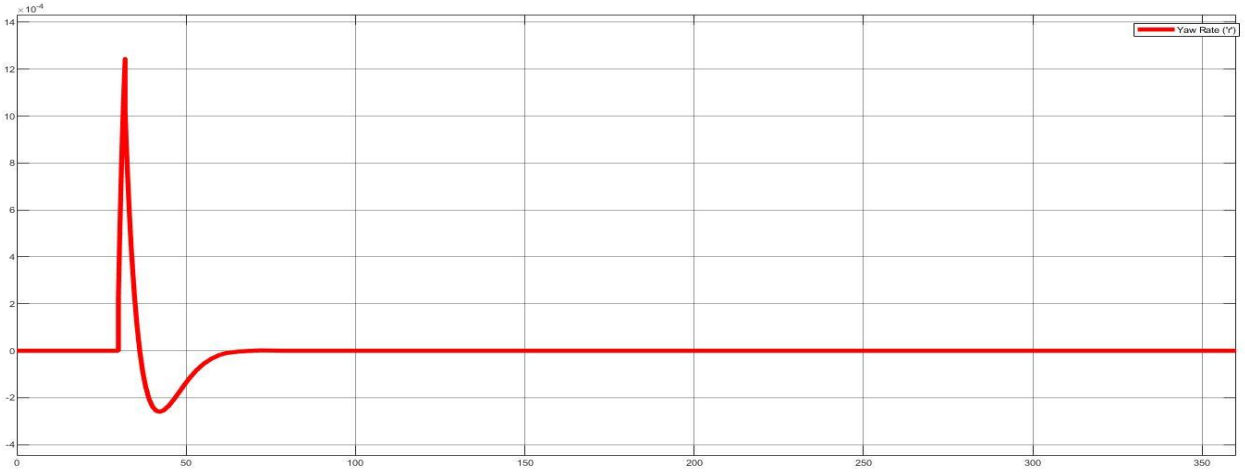

Figure 3.36: Yaw Rate (“r”)

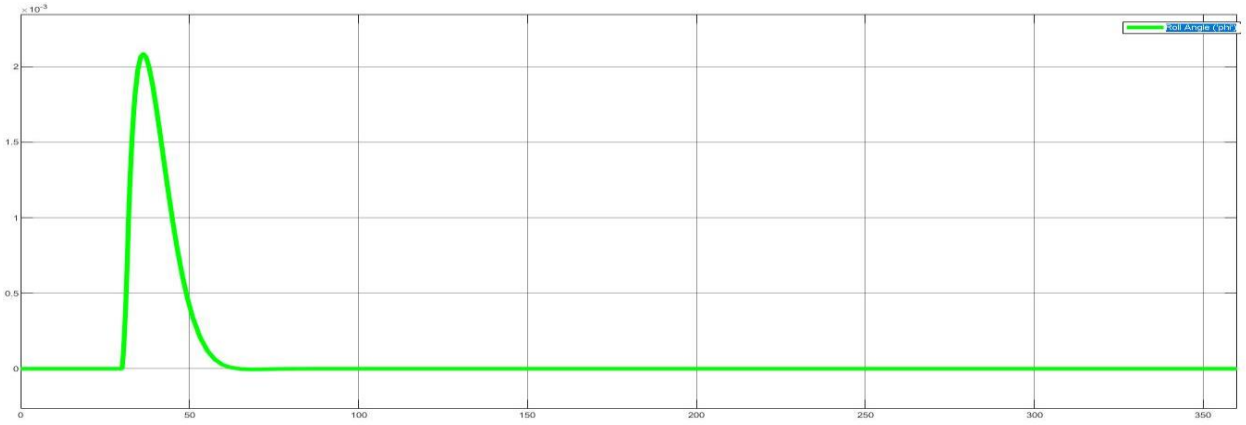

Figure 3.37: Roll Angle (“Phi”)

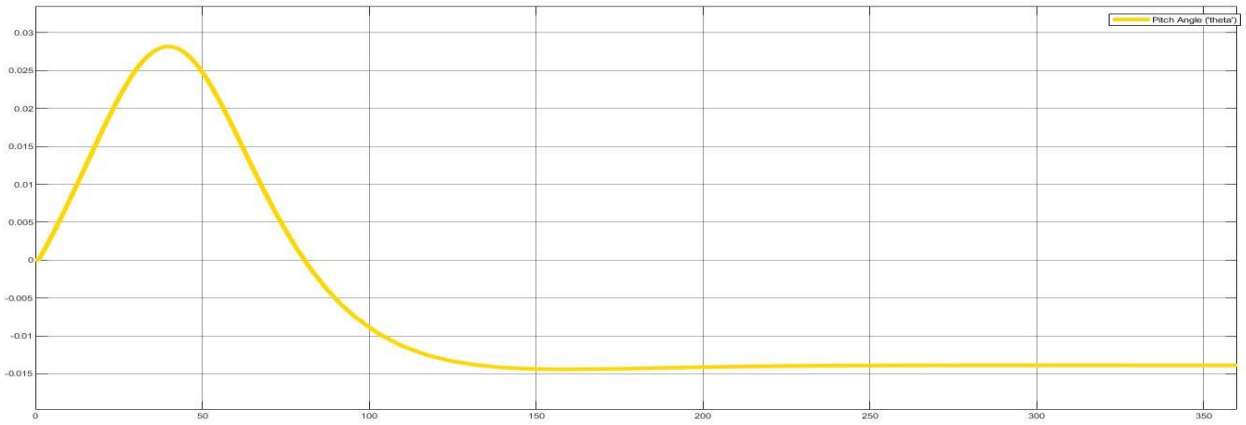

Figure 3.38: Pitch Angle (“Theta”)

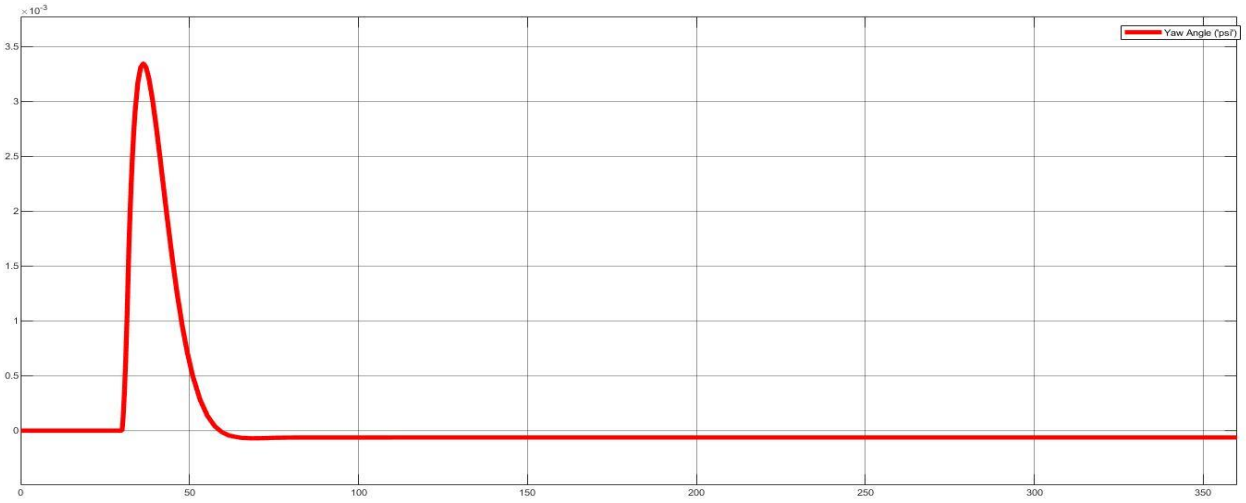

Figure 3.39: Yaw Angle (“Psi”)

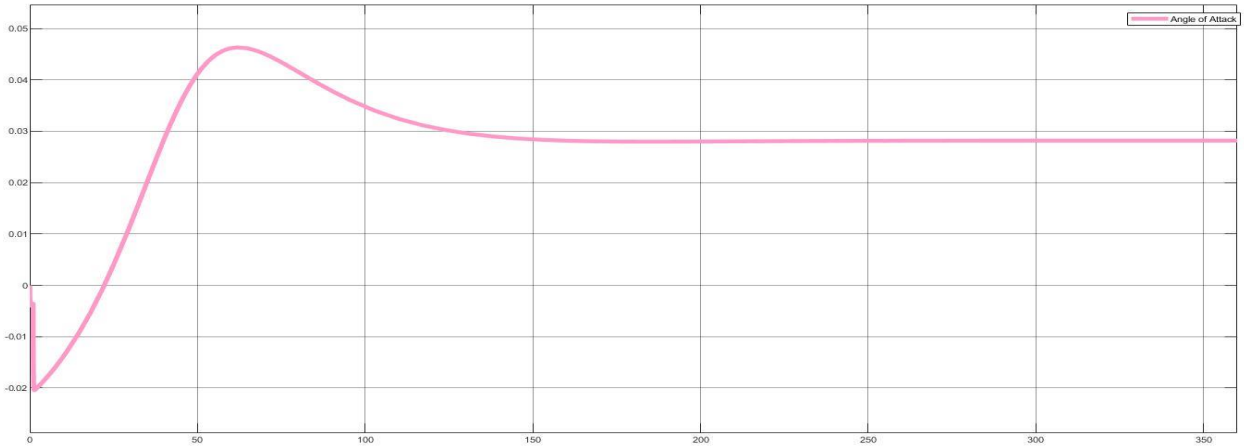

Figure 3.40: Angle of Attack (“Alpha”)

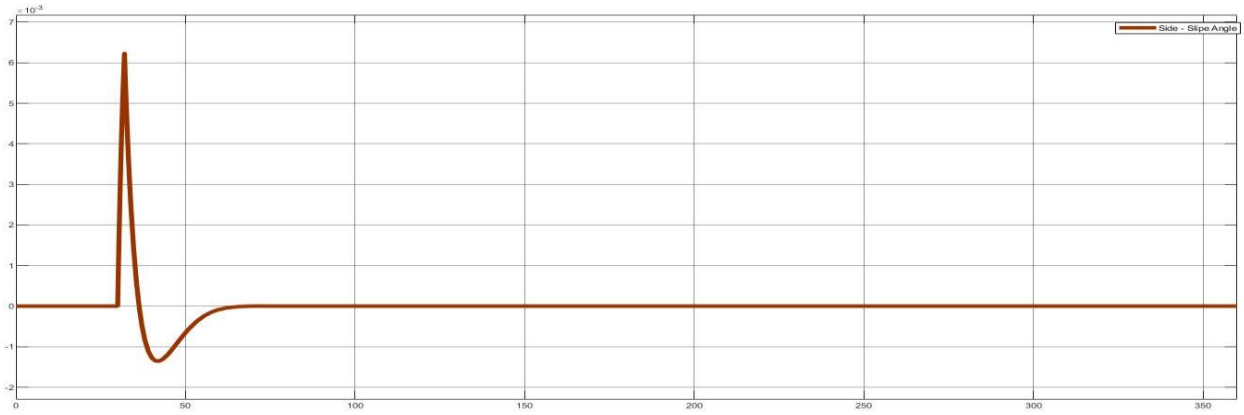

Figure 3.41: Side Slip Angle (“Beta”)

3.8.2.1. Remarks on the Response

Now there is no lateral-direction motion for 30seconds and as the aileron was kicked it starts inducing some short-lived lateral-directional motion and after few seconds the system starts stabilizing. As expected, the **FWUAV** is now no longer heading to north since **Psi** has a non-zero value. From the two solo flights, it is very clear to see that the system is unstable hence a controller design that can reduce or possibly eliminate the undesired response occurring in the system is needed.

Chapter Four

4. Control System Design

4.1. Overview of Sliding Mode Control

Sliding mode control (SMC) is a nonlinear control approach featuring outstanding properties of accuracy, robustness, and easy tuning and implementation. Its fundamental concept is to steer the system states onto a unique favored or user defined surface in the state space, which is called sliding or switching surface. Once the sliding surface is reached, sliding mode control maintains the states on the closest neighborhood of the sliding surface for all subsequent time. Hence the sliding mode control is a two-part controller design. The first section includes the design of a sliding surface so that the sliding action satisfies design specifications. The second phase is involved with the selection of a control law that will make the switching surface desirable to the system state.[26].

SMC is a popular technique among control engineering practitioners due to the fact that, it introduces robustness to unknown external disturbances, uncertain parameter variations of the plant and unmodeled dynamics that belong to the control sub-space. Another main advantage of sliding mode control is that the dynamic behavior of the system may be tailored by the particular choice of the sliding function [26].

4.2. Description

Consider the nonlinear SISO system

$$\dot{X} = f(x, t) + g(x, t)\, U \quad \text{---------- (eq.4.1)}$$

$$Y = h(x, t) \quad \text{---------- (eq.4.2)}$$

where Y and U denote the scalar output and input variable, $X \varepsilon R^n$ and denotes the state vector. The aim of the control is to make the output variable Y to track a desired profile Y_{DES}, that is, it is required that the output error variable $e = Y - Y_{DES}$ tends to some small vicinity of zero after a transient of acceptable duration [26]. As mentioned, SMC synthesis entails two phases,

Phase 1: - “Sliding Surface Design”

Phase 2: - “Control Input Design”

The first phase is the definition of a certain scalar function of the system state, says

$$\sigma(x): R^{n} \rightarrow R$$

Often, the sliding surface depends on the tracking error e_y together with a certain number of its derivatives.

$$\sigma = \sigma (e, \dot{e}, \ldots\ldots..., e^{(k)}) \text{ ---------- (eq.4.3)}$$

The function σ should be selected in such a way that its vanishing, σ = 0, gives rise to a “stable” differential equation of any solution $e_y(t)$ of which will tend to zero eventually [26]. The most typical choice for the sliding manifold is a linear combination of the following type.

$$\sigma = c_0 e + \dot{e} \text{ ---------- (eq.4.4)}$$

$$\sigma = c_0 e + c_1 \dot{e} + \ddot{e} \text{ ---------- (eq.4.5)}$$

$$\sigma = \sum_{i=0}^{k-1} e^{(k)} c_i + e^{(k)} \text{ ---------- (eq.4.6)}$$

The number of derivatives to be included (the “k” coefficient in (Eq.4.6)) should be k = r - 1, where r is the input output relative degree of (Eq.4.1)-(Eq.4.2) [26].

With properly selected c_i coefficients, if one steers the σ variable to zero, exponential vanishing of the error and its derivatives is obtained. If this behavior holds, then the control task is to deliver the finite time convergence of σ, “neglecting” any other characteristics. From a geometrical consideration, the equation σ = 0 describes a surface in the error space, that is called “switching surface”. All the trajectories of the controlled system are enforced onto the switching surface, along which the system characteristics meets the design specifications [26]. A common form of expression for the switching surface is the following, which depends on just a solo scalar constraint, p.

$$\sigma = \left(\frac{d}{dt} + p\right)^k e \text{ ---------- (eq.4.7)}$$

for k = 1, $\sigma = pe + \dot{e}$

for k = 2, $\sigma = p^2e + 2p\dot{e} + \ddot{e}$

The choice of the positive parameter p is almost arbitrary, and define the unique pole of the resulting "reduced dynamics" of the system when in sliding [26]. The integer parameter k is on the contrary somewhat crucial, it must be equal to r-1, with r being the relative degree between U and Y. This means that the relative degree of the σ variable is one [26].

The second stage (PHASE 2) is finding a control action that steers the system trajectories onto the sliding surface, i.e., the control is able to steer the σ variable to zero in finite time [26]. There are several approaches based on the sliding mode control approach [26]: -

- ❖ Classical (or First-order) sliding mode control
- ❖ High-order sliding mode control

4.2.1. Classical Sliding Mode Control

The control is discontinuous across the manifold σ = 0 [26].

$$U = -k \, \text{sign}(\sigma)$$

that is

$$U = \begin{cases} k, & \text{for } \sigma < 0 \\ -k, & \text{for } \sigma > 0 \end{cases}$$

k is a sufficiently large positive constant.

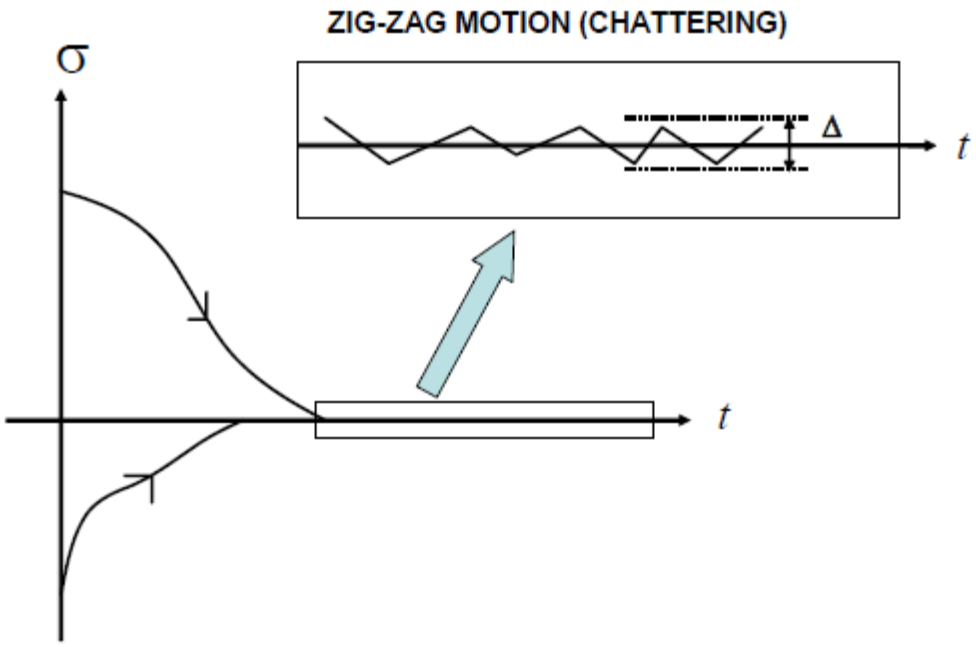

Figure 3: Typical evolution of the σ variable starting from different initial conditions

In steady state the control variable U will commute at very high (theoretically infinite) frequency between the values and U = k and U = −k [26]. (See figure 4.2)

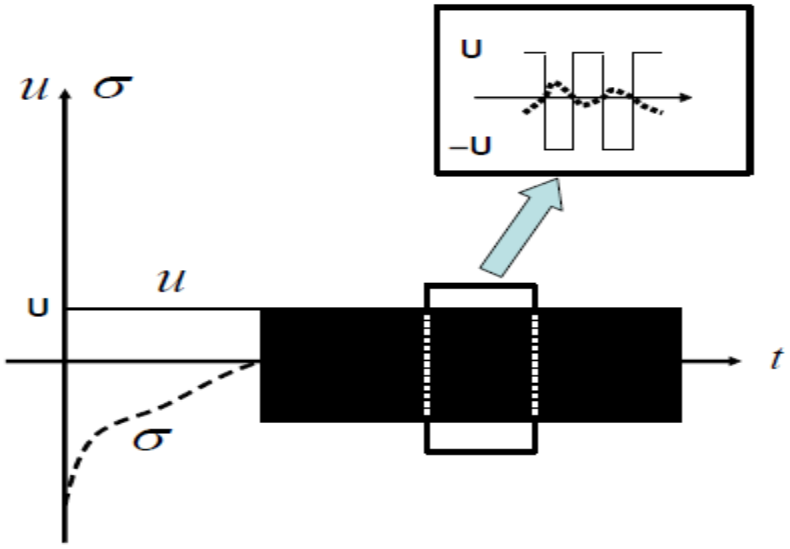

Figure 4: Common evolution of the control signal U (--- represents σ)

In order to solve the "chattering phenomenon" smoothed estimate implementations of sliding mode control techniques have been recommended where "Signum" term is replaced by a continuous smooth estimation function as follows[26]:-

Saturation function $U = -k \text{ sat } (\sigma, \varepsilon) \equiv -k \frac{\sigma}{\sigma+\varepsilon}$, $\varepsilon > 0, \varepsilon \approx 0$

Tan hyperbolic function $U = -k \tanh(\sigma/\varepsilon)$, $\varepsilon > 0, \varepsilon \approx 0$

Unfortunately, this technique is effective only when hard uncertainties are not present and when the control action that offset them can be set to zero in the sliding mode [26].

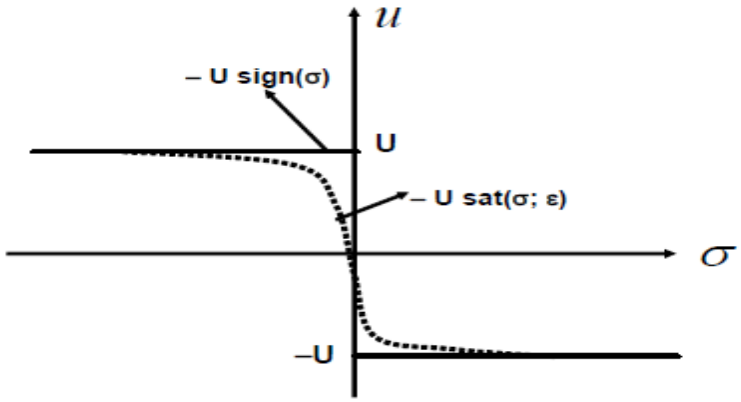

Figure 5: Smooth approximations of SMC

Some problems are attenuated using the above-described smooth approximations at the price of a loss of robustness. However, HOSM control algorithms, specifically SOSM control are a powerful substitute that entirely solves the chattering issue without bargaining the robustness characteristics as well [26].

4.2.2. High-Order Sliding Mode Control

Let us consider a dynamic system with an output function S of class $\mathbf{C}^{r-1}$ closed by a dynamic discontinuous feedback or a constant as in [27]. Then, the calculated time derivatives S, $\dot{S}$, ., $\mathbf{S}^{r-1}$, are continuous functions of the system state, where the set $S = \dot{S} =, \ldots, \mathbf{S}^{r-1} = 0$ is non-empty and consists locally of Filippov trajectories. The motion on the set above mentioned is said to exist in *r*-sliding mode or r^{th} order sliding mode. The r^{th} derivative $\mathbf{S}^r$ is considered to be discontinuous or

non-existent. Therefore, the HOSM removes the relative-degree restriction and can almost eliminate the chattering problem. There are several algorithms to realize HOSM. In particular, the SOSM controllers are used to zero the outputs with relative degree two or to avoid chattering while zeroing outputs with relative degree one. Among SOSM algorithms one can find the sub-optimal controller, Quasi-Continuous Controller, the terminal sliding mode controller, the twisting controller and the super-twisting controller.

In particular, the twisting algorithm forces the sliding variable S of relative degree two in to the 2-sliding set, requiring knowledge of $\dot{S}$. The super-twisting algorithm does not require $\dot{S}$, but the sliding variable has relative degree one. Therefore, the super-twisting algorithm is nowadays preferable over the classical siding mode, since it eliminates the chattering phenomenon.

4.2.2.1. The super twisting Algorithm

Consider the dynamical system of relative degree 1 and suppose that

$$\dot{\delta} = h(t, x) + g(t, x)\, U \quad \text{---------- (eq.4.8)}$$

Furthermore, assume that for some positive constants C, K_M, K_m, U_M and q such that $|\dot{h}| + U_M\,|\dot{g}| < C$, $\left|\frac{h}{g}\right| < qU_M$, $0 < K_m < g(t, x) < K_M$ and $0 < q < 1$ then the control signal becomes

$$U = -K1\ \sqrt{\boldsymbol{\delta}}\ \text{sign}(\delta) + v \quad \text{---------- (eq.4.9)}$$

Were $\dot{\mathbf{v}}$ $\begin{cases} = & -U, \text{ for } |\mathbf{U}| > UM \\ & -k2\ \text{sign}(\delta) \text{ for } |\mathbf{U}| < UM \end{cases}$

Theorem

with $K_m K_2 > C$ and K_1 sufficiently large, the above controller guarantees the appearance of a 2-sliding mode $\delta = \dot{\delta} = 0$ in the system, which attracts the trajectories in finite time. The control u enters in finite time the segment $[-U_M, U_M]$ and stays there. It never leaves the segment, if the initial value is inside at the beginning. Then the controller given above is called the super-twisting controller. A sufficient (very crude!) condition for validity of the theorem is

$$K_1 > \frac{\left(\sqrt{\frac{2}{km\ k2-c}}\right)(Km\ K2+C)\ Km\ (1+q)}{km^2\ (1+q)}$$

4.4. Regulation Control of FWUAV using Classical SMC

4.4.1. Designing the Pitch Controller

The pitch controller is designed to stabilize the longitudinal dynamics of the aircraft. To do so the aerodynamic pitch moment coefficient given below is used under the following conditions.

$$CM = C_{mo} + C_{m\alpha}\alpha + C_{m\delta f}\delta f + C_{m\delta e}\delta e + \frac{c}{2Va}(C_{m\alpha}\dot{\alpha} + C_{mq}q) + C_{LM}M \text{ ---------- (eq.4.10)}$$

To simplify the design the following design considerations have been taken. Flap, which is auxiliary control surface is neglected i.e., $C_{m\delta f}\delta f = 0$, Mach influence is neglected i.e., $C_{LM}M = 0$, symmetric wing structure is considered i.e., $C_{mo} = 0$ and symmetric and truss fuselage structure is considered i.e., $C_{m\alpha}\dot{\alpha} = 0$. Then the simplified pitch moment coefficient becomes

$$CM = C_{m\alpha}\alpha + C_{m\delta e}\delta e + \frac{c}{2Va} C_{mq}q$$

And the simplified dynamic equation for pitch movement becomes

$$\dot{\theta} = q$$
$$\dot{q} = \frac{\tau M}{Iyy}, \text{ were}$$

$$\tau M = QScCM = QSc\left[C_{m\alpha}\alpha + \frac{c}{2Va} C_{mq}q + C_{m\delta e}\delta e\right]$$

$$\dot{\theta} = q$$
$$\dot{q} = \frac{QScCM}{Iyy} = \frac{QSc}{Iyy}\left[C_{m\alpha}\alpha + \frac{c}{2Va} C_{mq}q + C_{m\delta e}\delta e\right]$$

Let

$$X1 = \theta$$

$$X2 = q = \dot{\theta}$$

The state-space representation becomes

$$\dot{x1} = x2$$
$$\dot{x2} = \frac{QSc}{Iyy}\left[C_{m\alpha}\alpha + \frac{c}{2Va} C_{mq}x2 + C_{m\delta e}\delta e\right], \text{ Were } \delta e \text{ is the control}$$

choosing a linear sliding surface of the form

$$\delta = cx_1 + x_2;\ c>0$$
Selecting C=3
$$\delta = 3x_1 + x_2$$
$$\dot{\delta} = 3\dot{x1} + \dot{x2}$$
$$\dot{\delta} = 3x2 - \frac{QSc}{Iyy}\left[C_{m\alpha}\alpha + \frac{c}{2Va} C_{mq}\, x2 + C_{m\delta e}\delta e\right]$$

The equivalent control becomes

$$0 = 3x2 + \frac{QSc}{Iyy}[C_{m\alpha}\alpha + \frac{c}{2Va} C_{mq}\, x2 + C_{m\delta e}\delta e]$$

$$\frac{QSc}{Iyy}[C_{m\delta e}\delta e] = -\, 3x_2 - \frac{QSc}{Iyy}[C_{m\alpha}\alpha + \frac{c}{2Va} C_{mq}\, x_2]$$

$$U_{eq}(t) = [\delta e] = (\frac{Iyy}{QSc})(\frac{1}{Cm\delta e}) *- 3x_2 - \frac{1}{Cm\delta e}[C_{m\alpha}\alpha + \frac{c}{2Va} C_{mq}x_2] \text{ ---------- (eq.4.11)}$$

The corrective control

$$U_{cr}(t) = k_2 * sign(\delta_2) \text{ ---------- (eq.4.12)}$$

The total control

$$U(t) = U_{eq}(t) + U_{cr}(t) \text{ ---------- (eq.4.13)}$$

4.4.2. Designing the Roll Controller

The roll controller is designed to stabilize the lateral-directional dynamics of the aircraft. To do so the aerodynamic roll moment coefficient given below is used under the following conditions.

$$Cl = C_{l\beta}\beta + \frac{b}{2Va}(C_{lp}p + C_{lr}r) + C_{l\delta a}\delta a + C_{l\delta r}\delta r \text{ ---------- eq.4.14}$$

To simplify the design the following design simplification has been taken. Lateral speed is very small compared to front displacement i.e., $\beta = 0$, Angular velocity in the other direction of rotation is zero i.e., $r = 0$ and the rudder is in neutral position i.e., $\delta r = 0$. Then the simplified roll moment coefficient becomes

$$Cl = \frac{b}{2Va}(C_{lp}p) + C_{l\delta a}\delta a$$

And the simplified dynamic equation for roll movement becomes

$$\dot{\phi} = p$$

$$\dot{p} = \frac{Izz\tau L}{IxxIzz - IxzIzx}$$, were $\tau L = QSbCl = \frac{Izz}{\Gamma'}(QSbCl)$ and $\Gamma' = IxxIzz - IxzIzx$

Let

$$X3 = \phi$$

$$X4 = p = \dot{\phi}$$

The state-space representation becomes

$\dot{x3} = x4$

$\dot{x4} = \frac{Izz}{\Gamma}(QSb)[\frac{b}{2Va}(C_{lp}x4) + C_{l\delta a}\delta a]$, Were δa is the control

choosing a linear sliding surface of the form

$\delta = cx_3 + x_4;\ c>0$

Selecting C=3

$\delta = 3x_3 + x_4$

$\dot{\delta} = 3\dot{x3} + \dot{x4}$

$\dot{\delta} = 3x_4 + \frac{Izz}{\Gamma}(QSb)[\frac{b}{2Va}(C_{lp}x_4) + C_{l\delta a}\delta a]$

The equivalent control becomes

$\dot{\delta} = 3x_4 + \frac{Izz}{\Gamma}(QSb)[\frac{b}{2Va}(C_{lp}x_4) + C_{l\delta a}\delta a]$

$0 = 3x_4 + \frac{Izz}{\Gamma}(QSb)[\frac{b}{2Va}(C_{lp}x_4) + C_{l\delta a}\delta a]$

$\frac{Izz}{\Gamma}(QSb)[C_{l\delta a}\delta a] = -3x_4 - \frac{Izz}{\Gamma}(QSb)[\frac{b}{2Va}(C_{lp}\ x_4)]$

$U_{eq}(t) = [\delta a] = -(\frac{\Gamma}{Izz})(\frac{1}{QSb})(\frac{1}{Cl\delta a})* 3x_4 - (\frac{1}{Cl\delta a})[\frac{b}{2Va}(C_{lp}x_4)]$ ---------- (eq.4.15)

The corrective control becomes

$U_{cr}(t) = k_1 * sign(\delta_1)$ ---------- (eq.4.16)

The total control becomes

$U(t) = U_{eq}(t) + U_{cr}(t)$ ---------- (eq.4.17)

4.4.3. Designing the Yaw Controller

Finally, to get the heading control the Yaw controller is designed. To do so the aerodynamic Yaw moment coefficient given below is used under the following conditions.

$Cn = C_{n\beta}\beta + \frac{b}{2Va}(C_{np}p + C_{nr}r) + C_{n\delta a}\delta a + C_{n\delta r}\delta r$ ----------(eq.4.18)

To simplify the design the following design simplification has been taken. Angular velocity in the other direction of rotation is zero i.e., $p = 0$ and the aileron is in neutral position i.e., $\delta a = 0$.

Then the simplified yaw moment coefficient becomes

$$Cn = C_{n\beta}\beta + \frac{b}{2Va}(C_{nr}r) + C_{n\delta r}\delta r$$

And the simplified dynamic equation for yaw movement becomes

$$\dot{\psi} = r$$

$$\dot{r} = \frac{Ixx\tau N}{IxxIzz - IxzIzx}$$, were $\tau N = QSbCn = \frac{Ixx}{\Gamma'}(QSbCn)$, $\Gamma' = IxxIzz - IxzIzx$

Let

$$X5 = \psi$$

$$X6 = r = \dot{\psi}$$

The state-space representation becomes

$$\dot{x5} = x6$$

$$\dot{x6} = \frac{Ixx}{\Gamma'}(QSb)\left[C_{n\beta}\beta + \frac{b}{2V}(C_{nr}r) + C_{n\delta r}\delta r\right]$$, Were δr is the control

choosing a linear sliding surface of the form

$$\delta = cx_5 + x_{6;}\ c>0$$

Selecting C=3

$$\delta = 3x_5 + x_6$$

$$\dot{\delta} = 3\dot{x5} + \dot{x6}$$

$$\dot{\delta} = 3x_6 + \frac{Ixx}{\Gamma'}(QSb)\left[C_{n\beta}\beta + \frac{b}{2Va}(C_{nr}x_6) + C_{n\delta r}\delta r\right]$$

The equivalent control becomes

$$\dot{\delta} = 3x_6 + \frac{Ixx}{\Gamma'}(QSb)\left[C_{n\beta}\beta + \frac{b}{2Va}(C_{nr}x_6) + C_{n\delta r}\delta r\right]$$

$$0 = 3x_6 + \frac{Ixx}{\Gamma'}(QSb)\left[C_{n\beta}\beta + \frac{b}{2Va}(C_{nr}x_6) + C_{n\delta r}\delta r\right]$$

$$U_{eq}(t) = [\delta r] = -\left(\frac{\Gamma'}{Ixx}\right)\left(\frac{1}{QSb}\right)\left(\frac{1}{Cn\delta r}\right) * 3x_6 - \left(\frac{1}{Cn\delta r}\right)\left[C_{n\beta}\beta + \frac{b}{2Va}(C_{nr}x_6)\right]$$ ---------- (eq.4.19)

The corrective control becomes

$$U_{cr}(t) = k_3 * sign(\delta_3)$$ ---------- (eq.4.20)

The total control

$$U(t) = U_{eq}(t) + U_{cr}(t)$$ ---------- (eq.4.21)

4.5. Regulation Control of FWUAV using Super-twisting Algorithm

4.5.1. Designing the Pitch Controller

The pitch controller is designed to stabilize the longitudinal dynamics of the aircraft. To do so the aerodynamic pitch moment coefficient given below is used under the following conditions.

$$CM = C_{mo} + C_{m\alpha}\alpha + C_{m\delta f}\delta f + C_{m\delta e}\delta e + \frac{c}{2Va}(C_{m\alpha}\dot{\alpha} + C_{mq}q) + C_{LM}M \text{ ---------- (eq.4.22)}$$

To simplify the design the following design considerations have been taken. Flap, which is auxiliary control surface is neglected i.e., $C_{m\delta f}\delta f = 0$, Mach influence is neglected i.e., $C_{LM}M = 0$, symmetric wing structure is considered i.e., $C_{mo} = 0$ and symmetric and truss fuselage structure is considered i.e., $C_{m\alpha}\dot{\alpha} = 0$. Then the simplified pitch moment coefficient becomes

$$CM = C_{m\alpha}\alpha + C_{m\delta e}\delta e + \frac{c}{2Va} C_{mq}q$$

And the simplified dynamic equation for pitch movement becomes

$$\dot{\theta} = q$$
$$\dot{q} = \frac{\tau M}{Iyy}, \text{ were } \tau M = QScCM = QSc\left[C_{m\alpha}\alpha + \frac{c}{2Va} C_{mq}q + C_{m\delta e}\delta e\right]$$
$$\dot{\theta} = q$$
$$\dot{q} = \frac{QScCM}{Iyy} = \frac{QSc}{Iyy}\left[C_{m\alpha}\alpha + \frac{c}{2Va} C_{mq}q + C_{m\delta e}\delta e\right]$$

Let

$$X1 = \theta$$

$$X2 = q = \dot{\theta}$$

The state-space representation becomes

$$\dot{x1} = x2$$
$$\dot{x2} = \left(\frac{QSc}{Iyy}\right)C_{m\alpha}\alpha + \left(\frac{QSc}{Iyy}\right)\left(\frac{c}{2Va}\right) C_{mq}x_2 + \left(\frac{QSc}{Iyy}\right)C_{m\delta e}\delta e, \text{ were } \delta e \text{ is the control}$$

Choosing a linear sliding surface of the form

$$\delta = cx_1 + x_{2;}\ c>0$$
Selecting C=3
$$\delta = 3x_1 + x_2$$
$$\dot{\delta} = 3\dot{x1} + \dot{x2}$$
$$\dot{\delta} = 3x_2 + \left(\frac{QSc}{Iyy}\right)C_{m\alpha}\alpha + \left(\frac{QSc}{Iyy}\right)\left(\frac{c}{2Va}\right) C_{mq}x_2 + \left(\frac{QSc}{Iyy}\right)C_{m\delta e}\delta e$$

Here

$h(t, x) = 3x_2 + (\frac{QSc}{Iyy})C_{m\alpha}\alpha + (\frac{QSc}{Iyy})(\frac{c}{2Va})C_{mq}x_2$

$g(t, x) = (\frac{QSc}{Iyy})C_{m\delta e}$

$U = \delta e$

Assuming that for some *positive constants* C, K_M, K_m, U_M and q that $|\dot{h}| + U_M |\dot{g}| < C$, $\left|\frac{h}{g}\right| < qU_M$, $0 < K_m < g(t, x) < K_M$ and $0 < q < 1$ then the control signal becomes

$U = \delta e = -K_1\sqrt{|\delta|}\,\text{sign}(\delta) + v$ ---------- (eq.4.23)

Were $\dot{v}$ $\begin{cases} = -\delta e, \text{ for } |\delta e| > U_M \\ -k_2\,\text{sign}(\delta) \text{ for } |\delta e| < U_M \end{cases}$

With $K_1 > \frac{\left(\sqrt{\frac{2}{Km\,K2-C}}\right)(Km\,K2+C)Km\,(1+q)}{Km^2(1-q)}$

4.6. Tracking Control of FWUAV using Super-twisting Algorithm

4.6.1. Designing the Pitch Controller

The pitch controller is designed to stabilize the longitudinal dynamics of the aircraft. To do so the aerodynamic pitch moment coefficient given below is used under the following conditions.

$CM = C_{mo} + C_{m\alpha}\alpha + C_{m\delta f}\delta f + C_{m\delta e}\delta e + \frac{c}{2Va}(C_{m\alpha}\dot{\alpha} + C_{mq}q) + C_{LM}M$ ---------- (eq.4.24)

To simplify the design the following design considerations have been taken. Flap, which is auxiliary control surface is neglected i.e., $C_{m\delta f}\delta f = 0$, Mach influence is neglected i.e., $C_{LM}M = 0$, symmetric wing structure is considered i.e., $C_{mo} = 0$ and symmetric and truss fuselage structure is considered i.e., $C_{m\alpha}\dot{\alpha} = 0$. Then the simplified pitch moment coefficient becomes

$CM = C_{m\alpha}\alpha + C_{m\delta e}\delta e + \frac{c}{2Va}C_{mq}q$

And the simplified dynamic equation for pitch movement becomes

$\dot{\theta} = q$

$\dot{q} = \frac{\tau M}{Iyy}$, were $\tau M = QScCM = QSc\,[C_{m\alpha}\alpha + \frac{c}{2Va}C_{mq}q + C_{m\delta e}\delta e]$

$\dot{\theta} = q$

$\dot{q} = \frac{QScCM}{Iyy} = \frac{QSc}{Iyy}[C_{m\alpha}\alpha + \frac{c}{2Va}C_{mq}q + C_{m\delta e}\delta e]$

Let

$X1 = \theta$

$X2 = q = \dot{\theta}$

The state-space representation becomes

$\dot{x1} = x2$

$\dot{x2} = (\frac{QSc}{Iyy})C_{m\alpha}\alpha + (\frac{QSc}{Iyy})(\frac{c}{2Va})C_{mq}x_2 + (\frac{QSc}{Iyy})C_{m\delta e}\delta e$, were δe is the control

Choosing a linear sliding surface of the form

$\delta = ce + \dot{e}; c>0$

Selecting C=3

$\delta = 3e + \dot{e}$, were

$e = (x_1)^d - x_1$

$\dot{e} = (\dot{x1})^d - \dot{x1}$

$\ddot{e} = (\ddot{x1})^d - \ddot{x1}$

$\dot{\delta} = 3\dot{e} + \ddot{e}$

$\dot{\delta} = 3((\dot{x1})^d - \dot{x1}) + (\ddot{x1})^d - \ddot{x1}$

$\dot{\delta} = 3(\dot{x1})^d - 3\dot{x1} + (\ddot{x1})^d - \ddot{x1}$

$\dot{\delta} = (\ddot{x1})^d + 3(\dot{x1})^d - 3\dot{x1} - \ddot{x1}$

$\dot{\delta} = (\ddot{x1})^d + 3(\dot{x1})^d - 3x2 - \frac{QSc}{Iyy}[C_{m\alpha}\alpha + \frac{c}{2Va}C_{mq}\,x2 + C_{m\delta e}\delta e]$

Here

$h(t, x) = (\ddot{x1})^d + 3(\dot{x1})^d - 3x_2 + (\frac{QSc}{Iyy})C_{m\alpha}\alpha + (\frac{QSc}{Iyy})(\frac{c}{2Va})C_{mq}x_2$

$g(t, x) = (\frac{QSc}{Iyy})C_{m\delta e}$

$U = \delta e$

Assuming that for some *positive constants* C, K_M, K_m, U_M and q such that $|\dot{h}| + U_M|\dot{g}| < C$, $|\frac{h}{g}| < qU_M$, $0 < K_m < g(t, x) < K_M$ and $0 < q < 1$ then the control signal becomes

$U = \delta e = -K_1\sqrt{|\delta|}\,\text{sign}(\delta) + v$ ---------- (eq.4.25)

Were $\dot{v} = \begin{cases} -\delta e, \text{ for } |\delta e| > U_M \\ -k_2\,\text{sign}(\delta) \text{ for } |\delta e| < U_M \end{cases}$

With $K_1 > \frac{\left(\sqrt{\frac{2}{Km\,K2-C}}\right)(Km\,K2+C)Km\,(1+q)}{Km^2(1-q)}$

Table 4.1: Parameters for regulation problem in classical SMC

States	Gain (K)
ϕ	$K_1 = -15$
θ	$K_2 = 20$
ψ	$K_3 = -50$

Table 4.2: Parameters for regulation problem in ST-SMC

States	K_1	K_2
θ	0.5	0.03

Table 4.3: Parameters for tracking problem in ST-SMC

States	K_1	K_2
θ	10	0.3

Table 4.4: Initial conditions for regulation problem in classical SMC

States	Initial Conditions
ϕ	0.2 rad/sec
θ	0.2 rad/sec
ψ	0.1 rad/sec

Table 4.5: Initial conditions for regulation problem in ST-SMC

States	Initial Conditions
θ	0.2 rad/sec

Table 4.6: Frequency for best tracking in ST-SMC

States	Frequency best tracking
θ	30 Hz

Chapter Five

5. Simulation and Result Analysis

5.1. Simulation

In this section, the validity and stabilization of the proposed sliding mode controllers are verified and analyzed using the MATLAB/Simulink software.

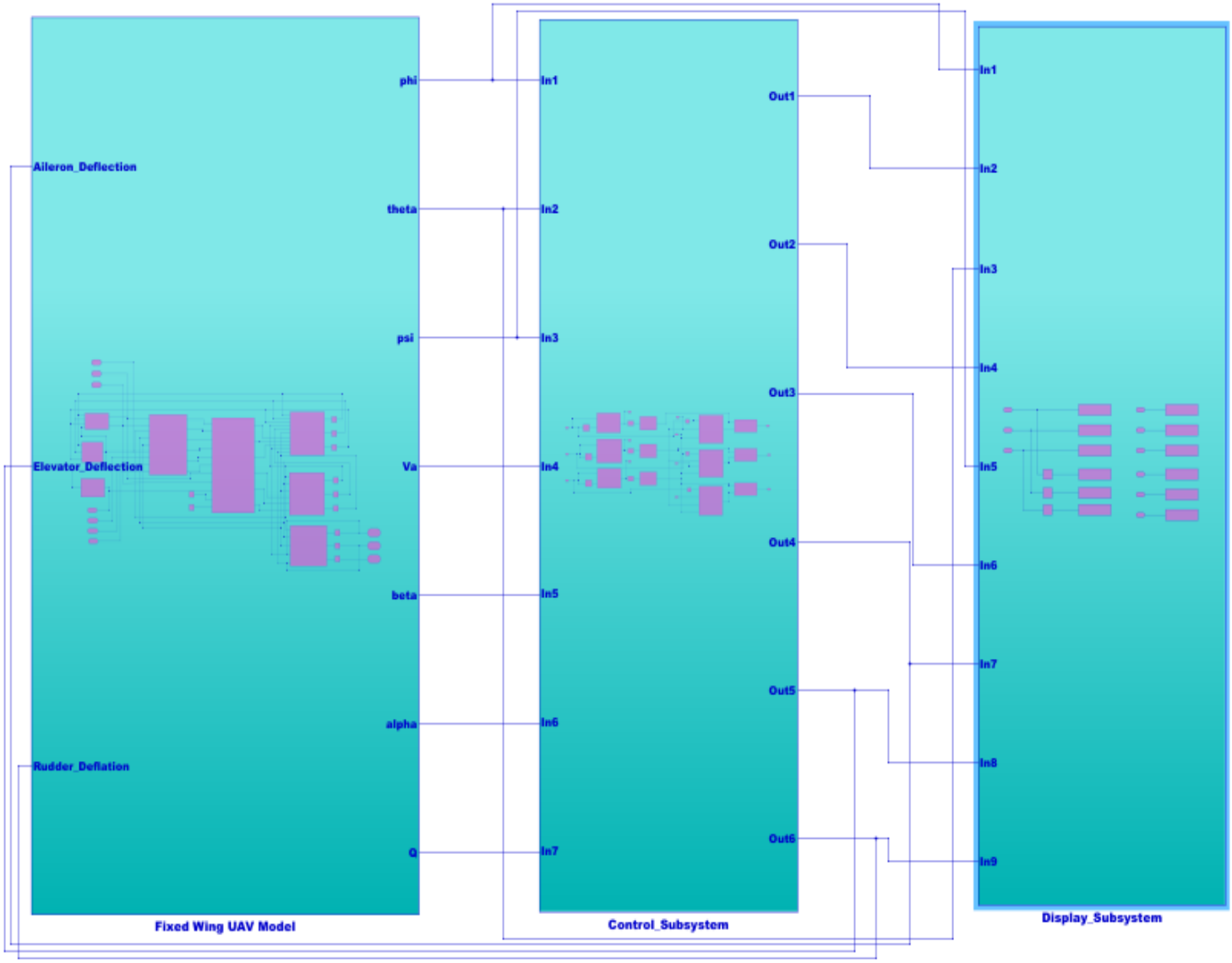

Figure 5.1: Simulink block diagram for regulation control of FWUAV using classical SMC

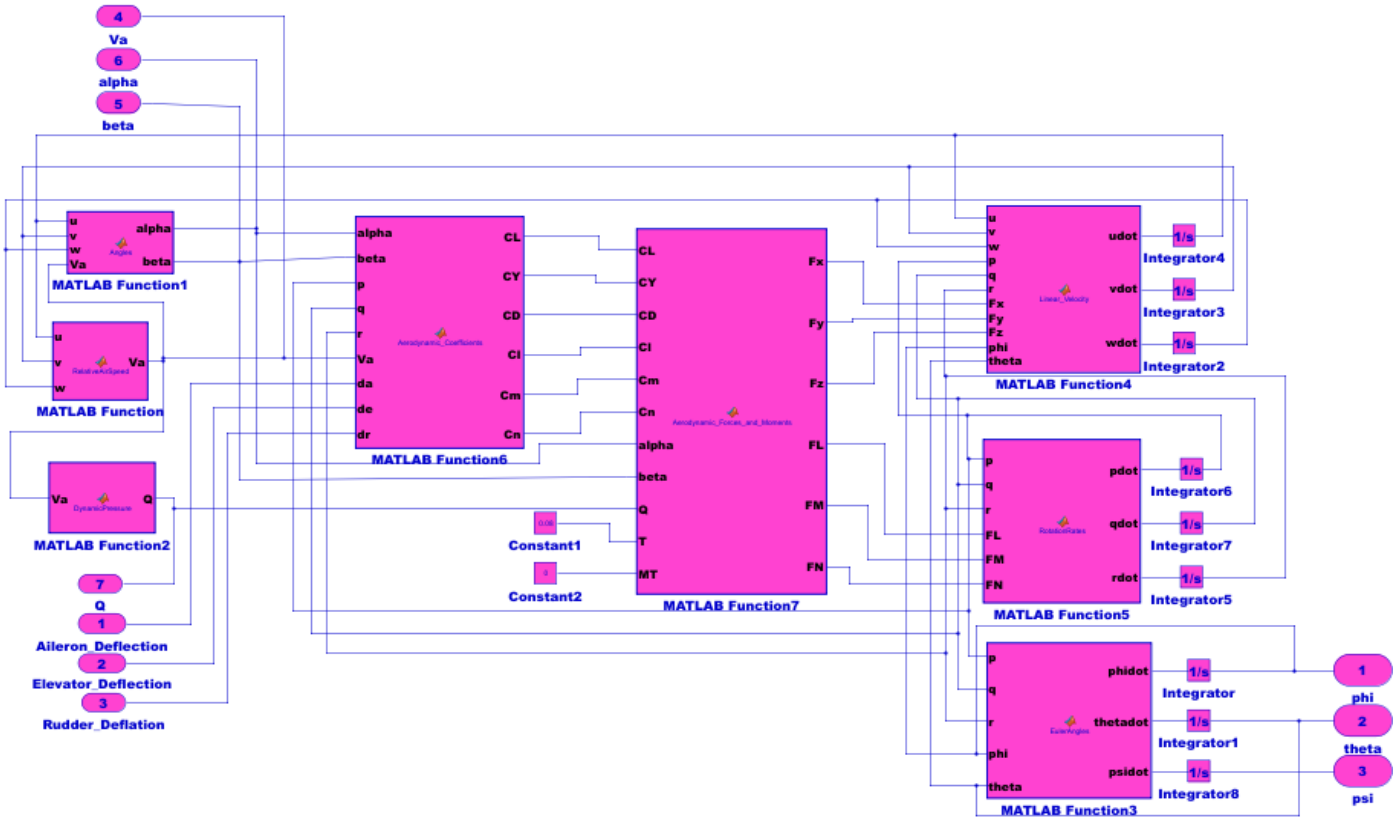

Figure 5.2: The inside of FWUAV model subsystem of figure 5.1

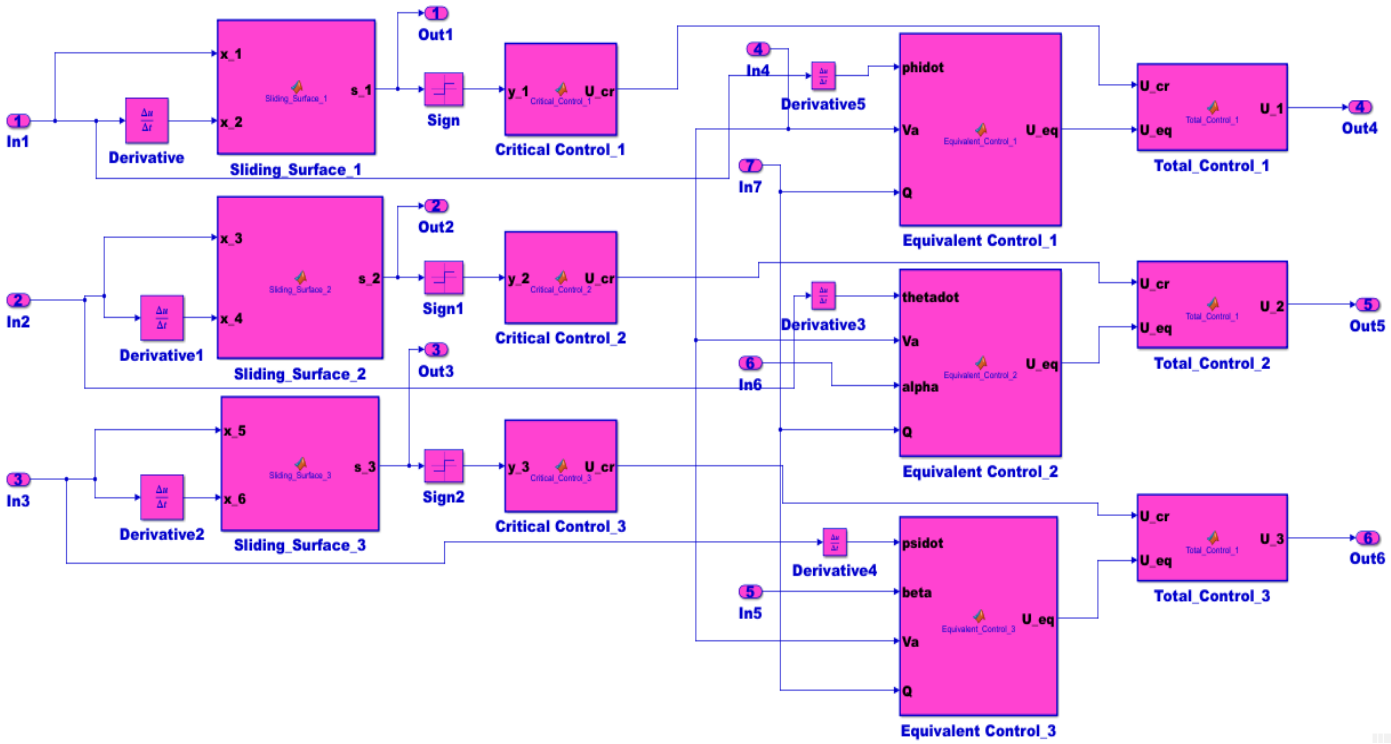

Figure 5.3: The inside of control subsystem of figure 5.1

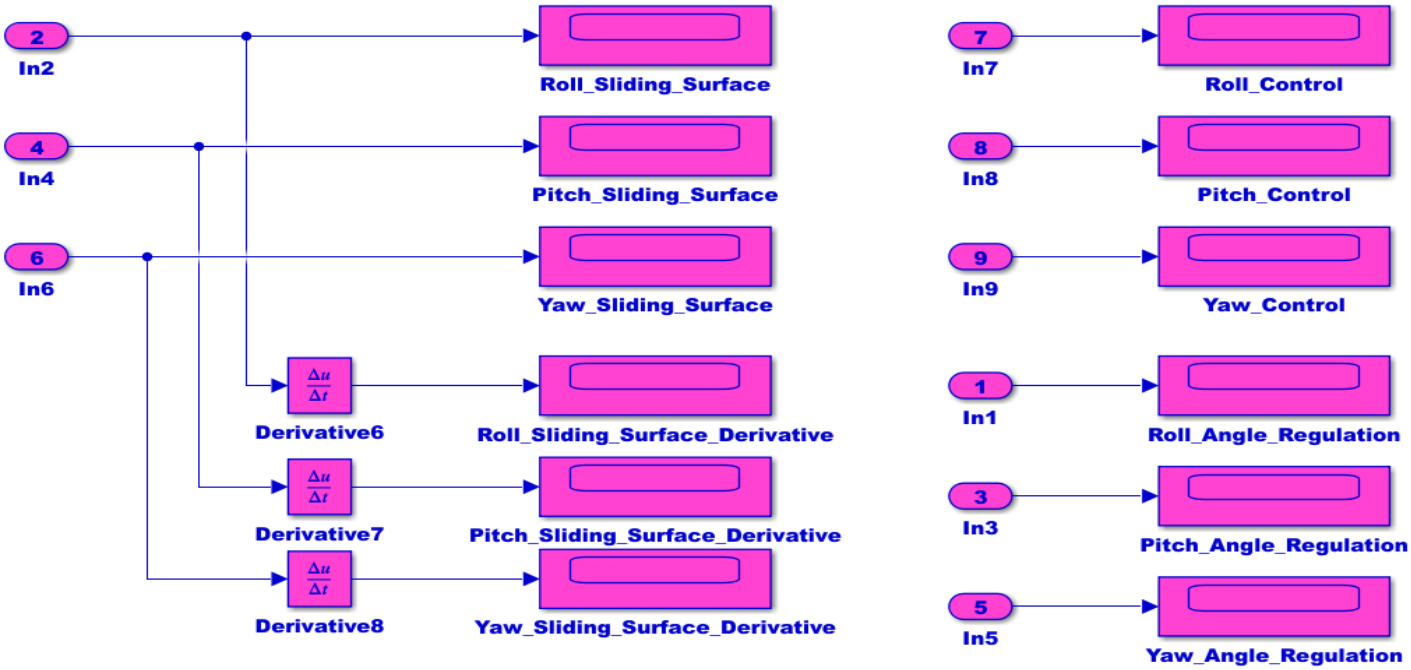

Figure 5.4: The inside of display subsystem of figure 5.1

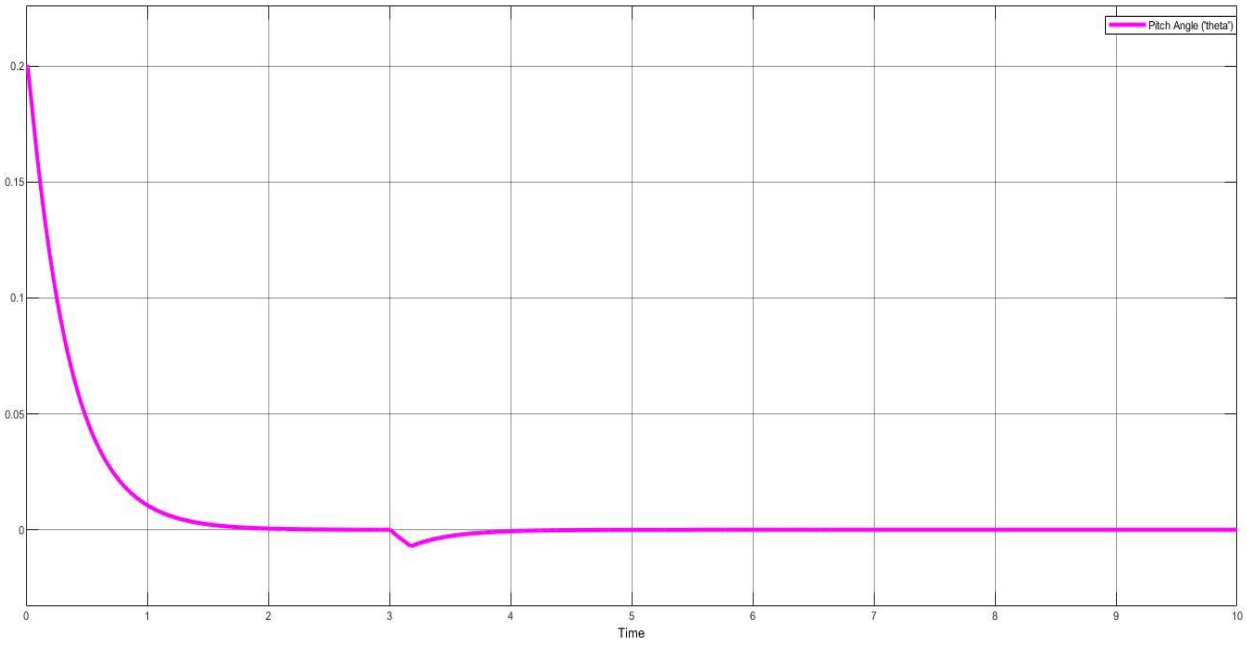

Figure 5.5: Pitch angle regulation

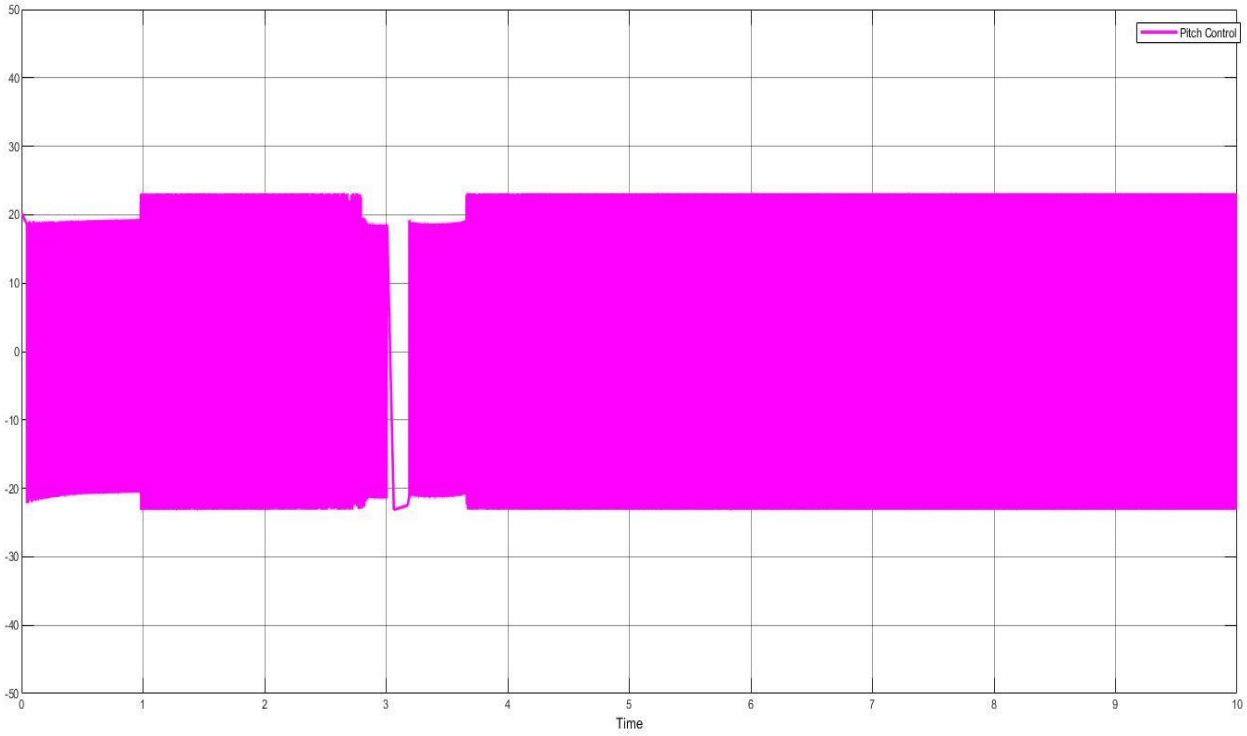

Figure 5.6: Control energy for pitch angle regulation

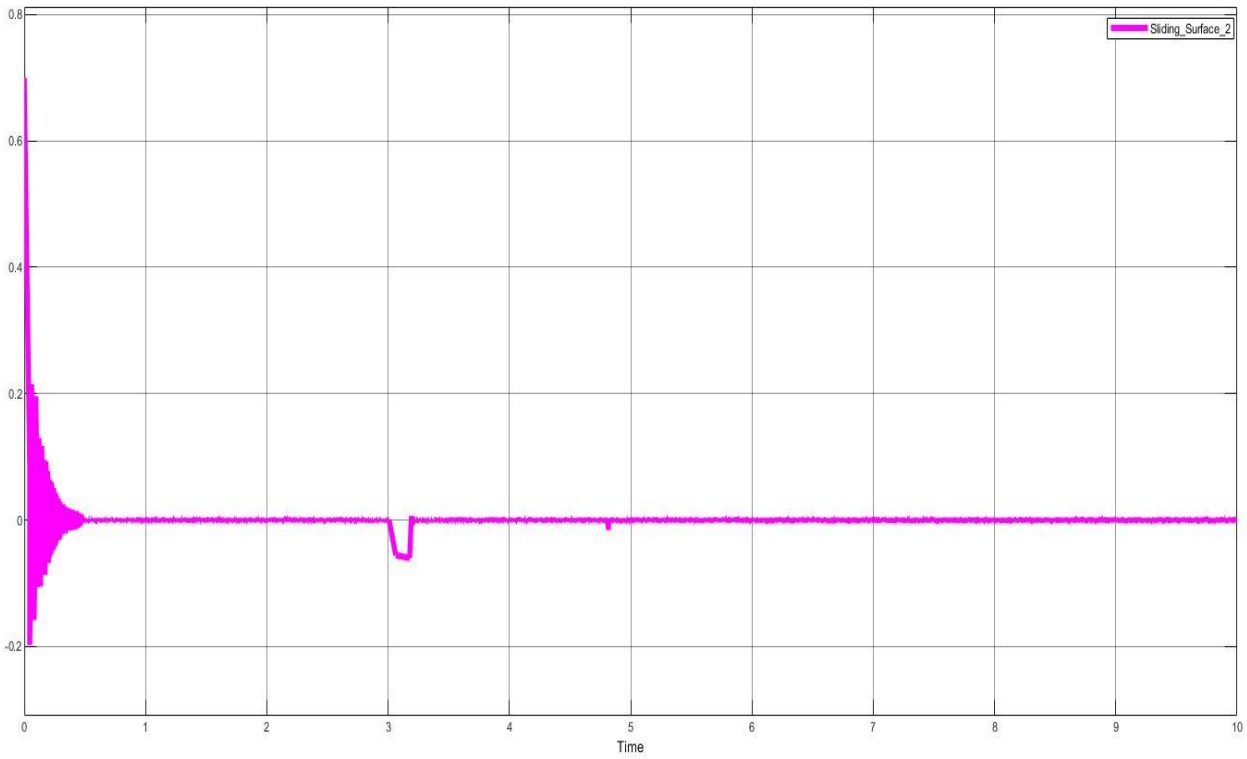

Figure 5.7: Sliding surface for pitch angle regulation

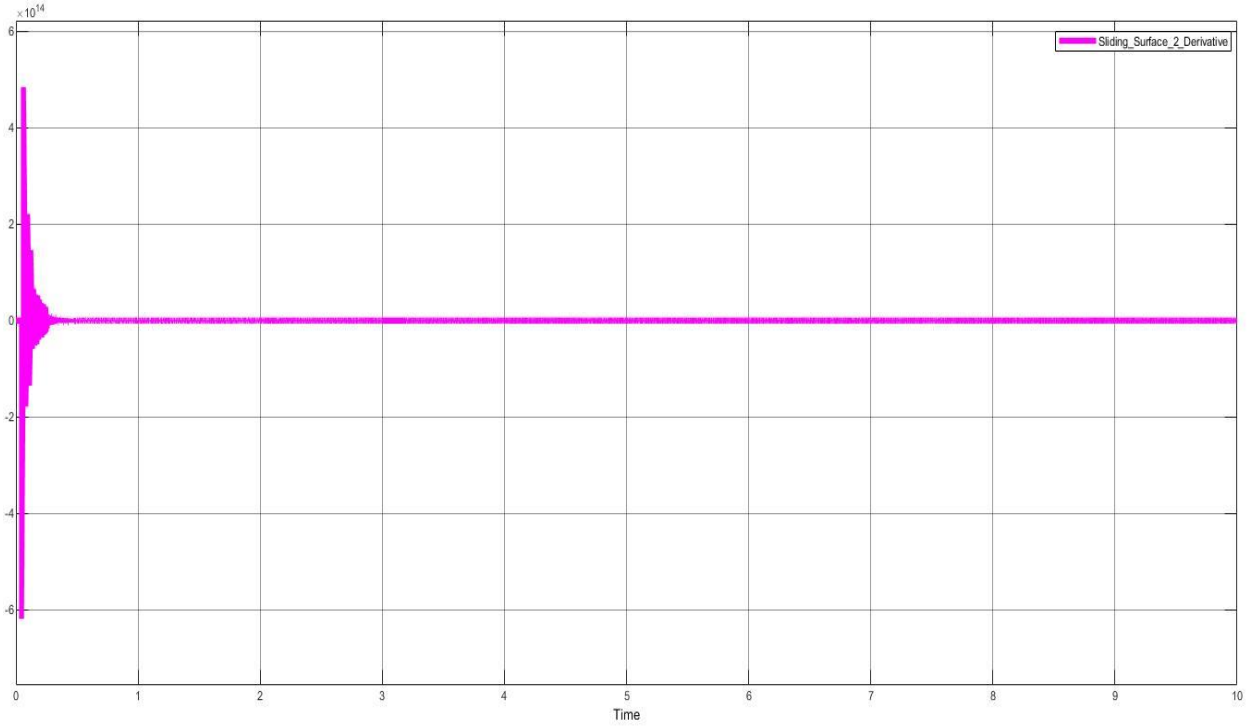

Figure 5.8: Sliding surface derivative for pitch angle regulation

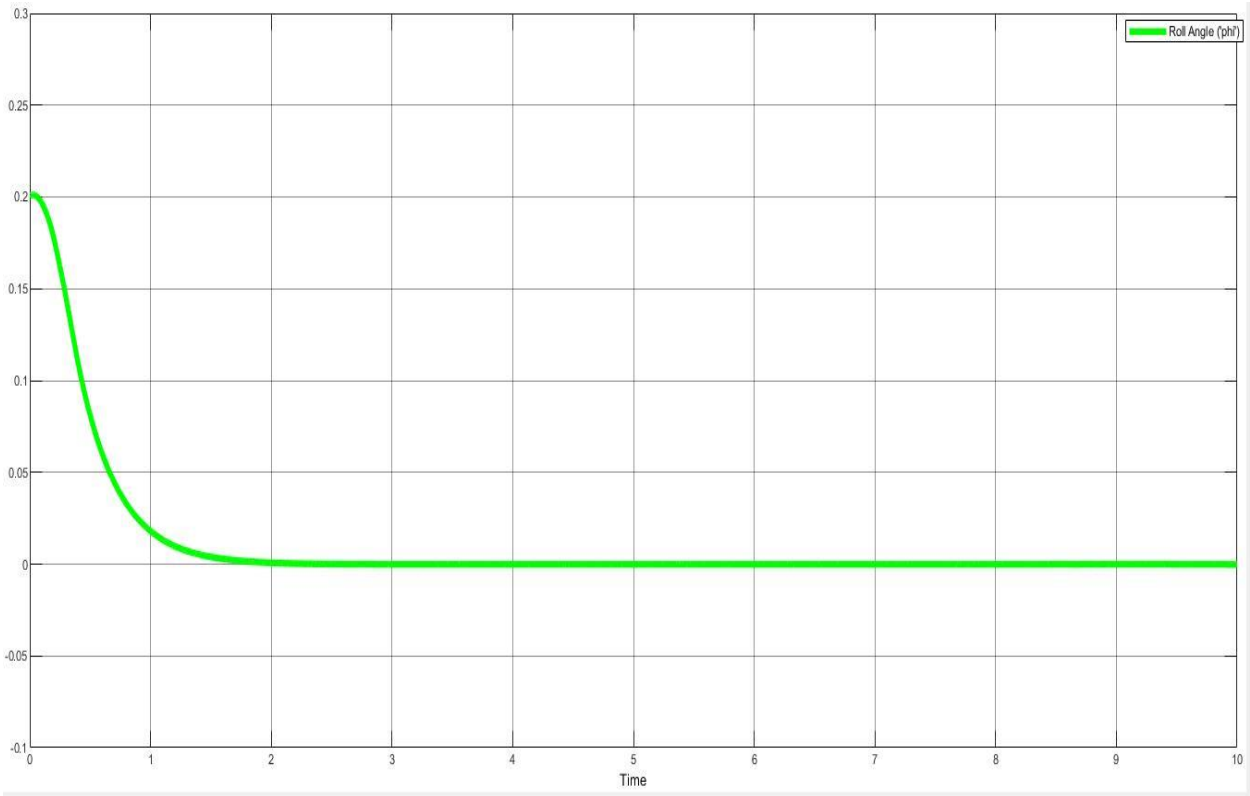

Figure 5.9: Roll angle regulation

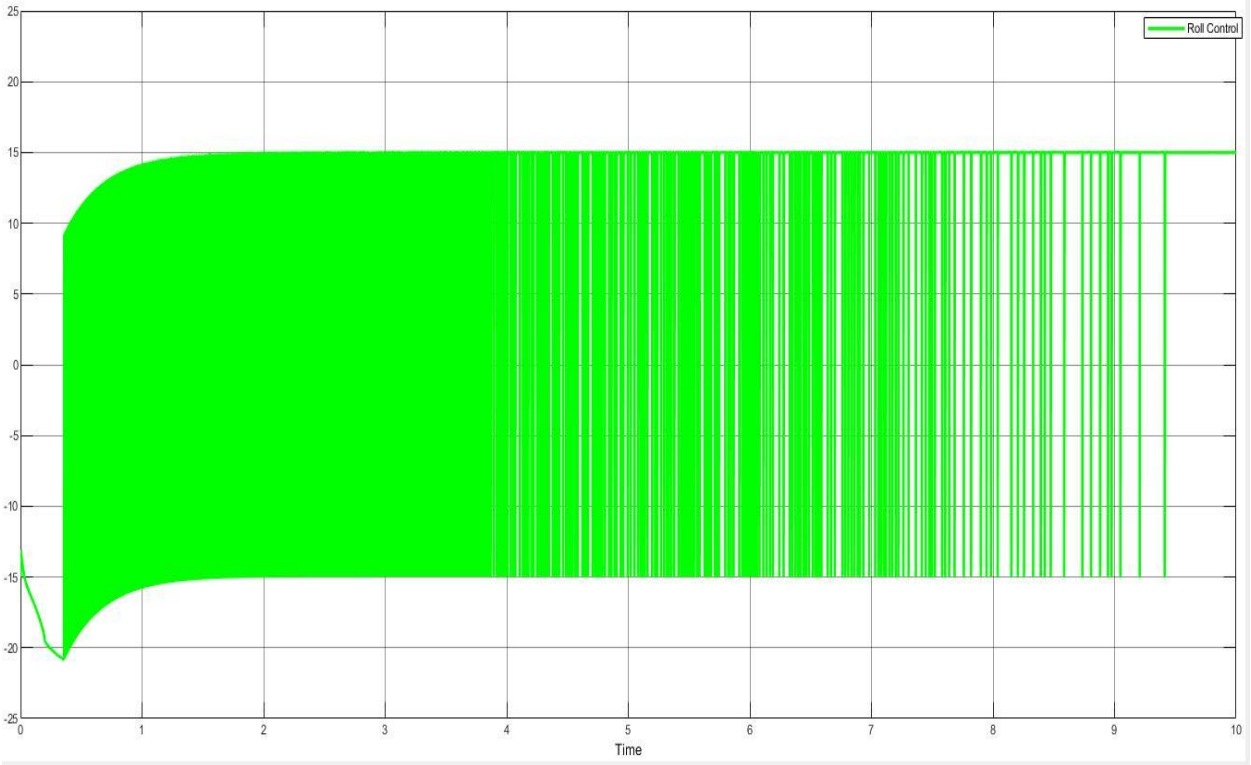

Figure 5.10: Control energy for roll angle regulation

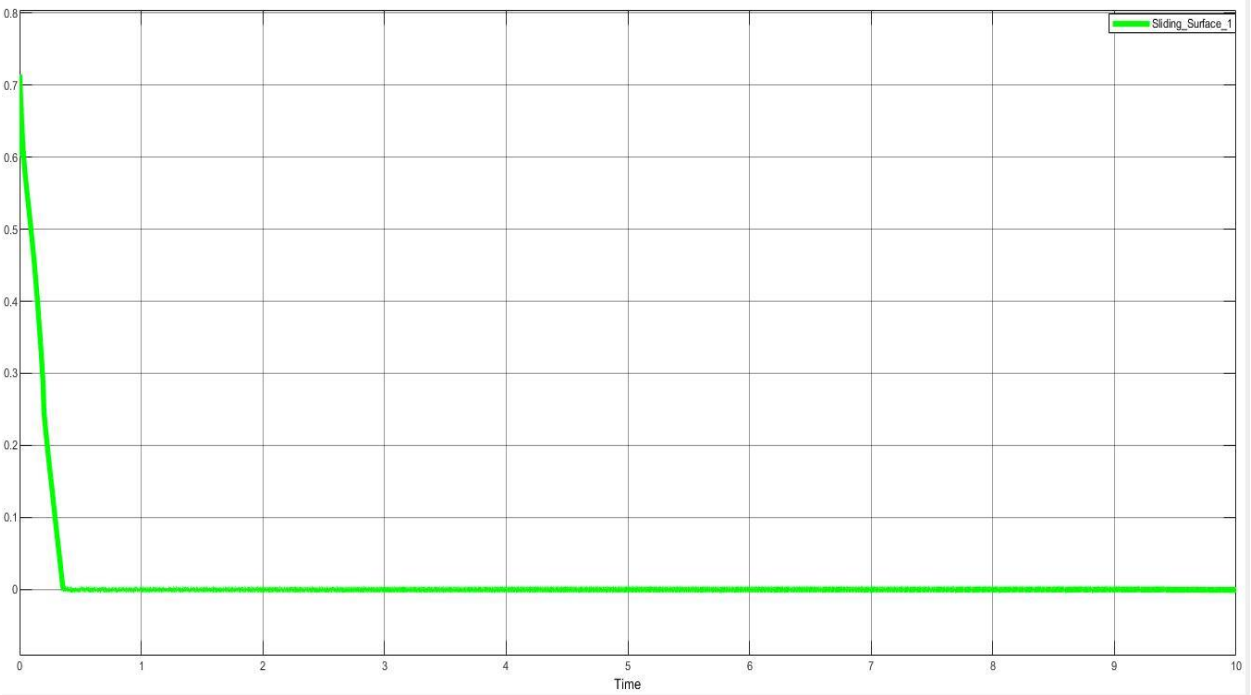

Figure 5.11: Sliding surface for roll angle regulation

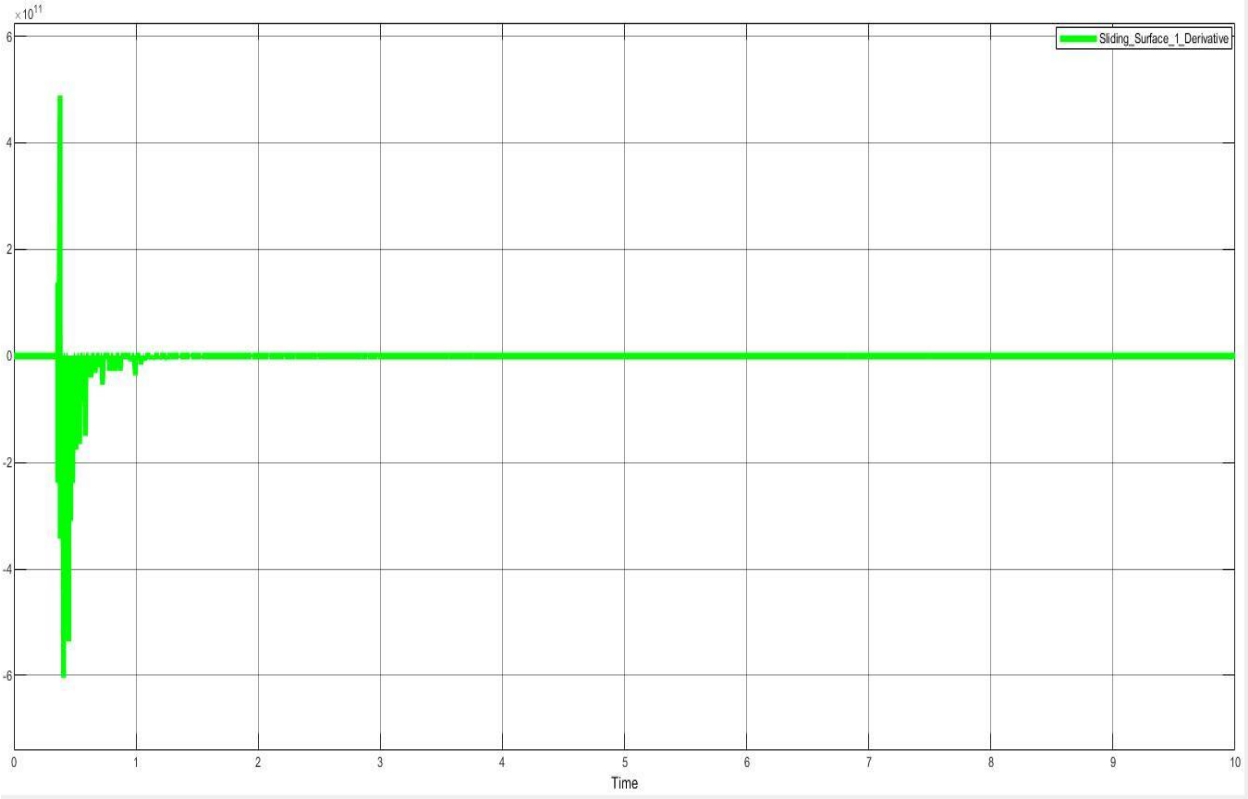

Figure 5.12: Sliding surface derivative for roll angle regulation

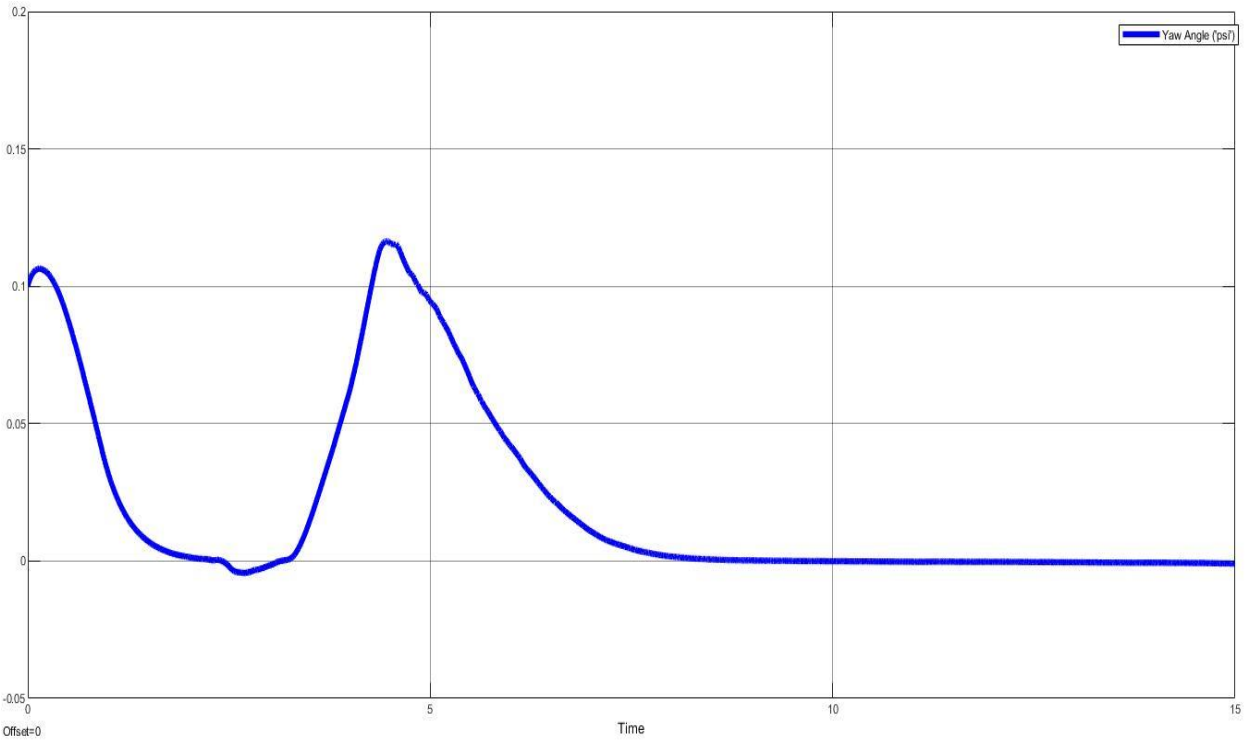

Figure 5.13: Yaw angle regulation

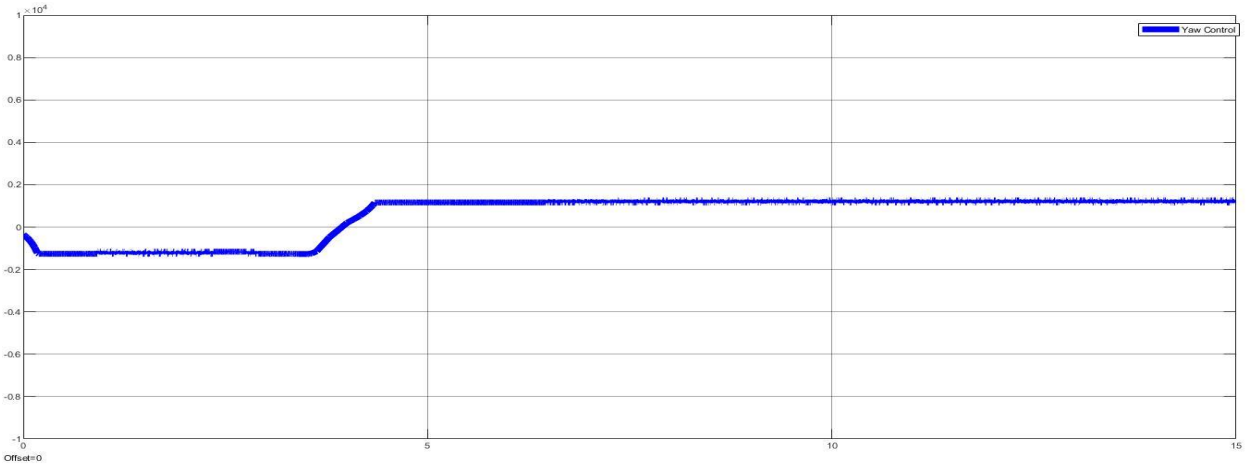

Figure 5.14: Control energy for yaw angle regulation

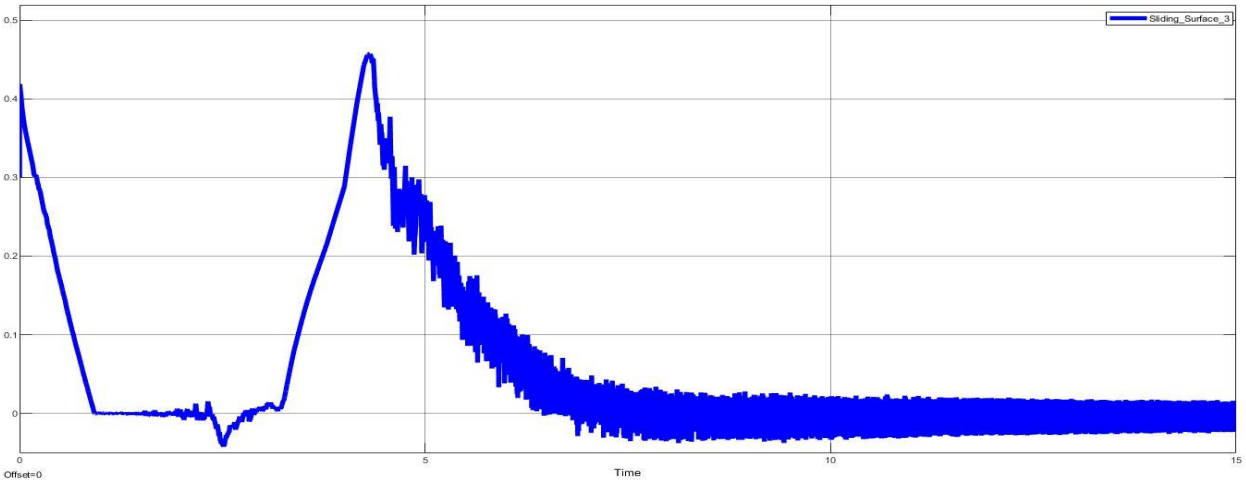

Figure 5.15: sliding surface for yaw angle regulation

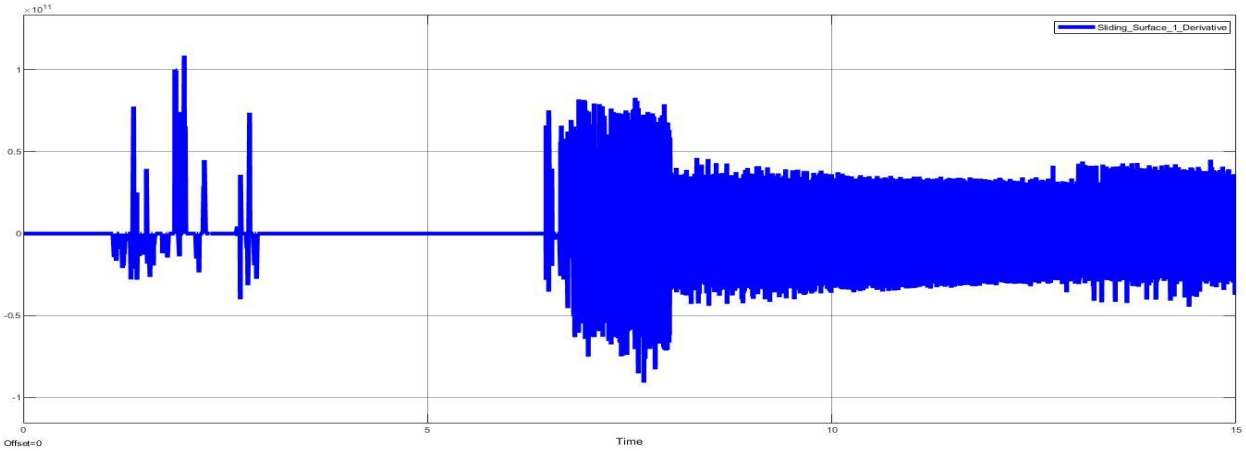

Figure 5.16: sliding surface derivative for yaw angle regulation

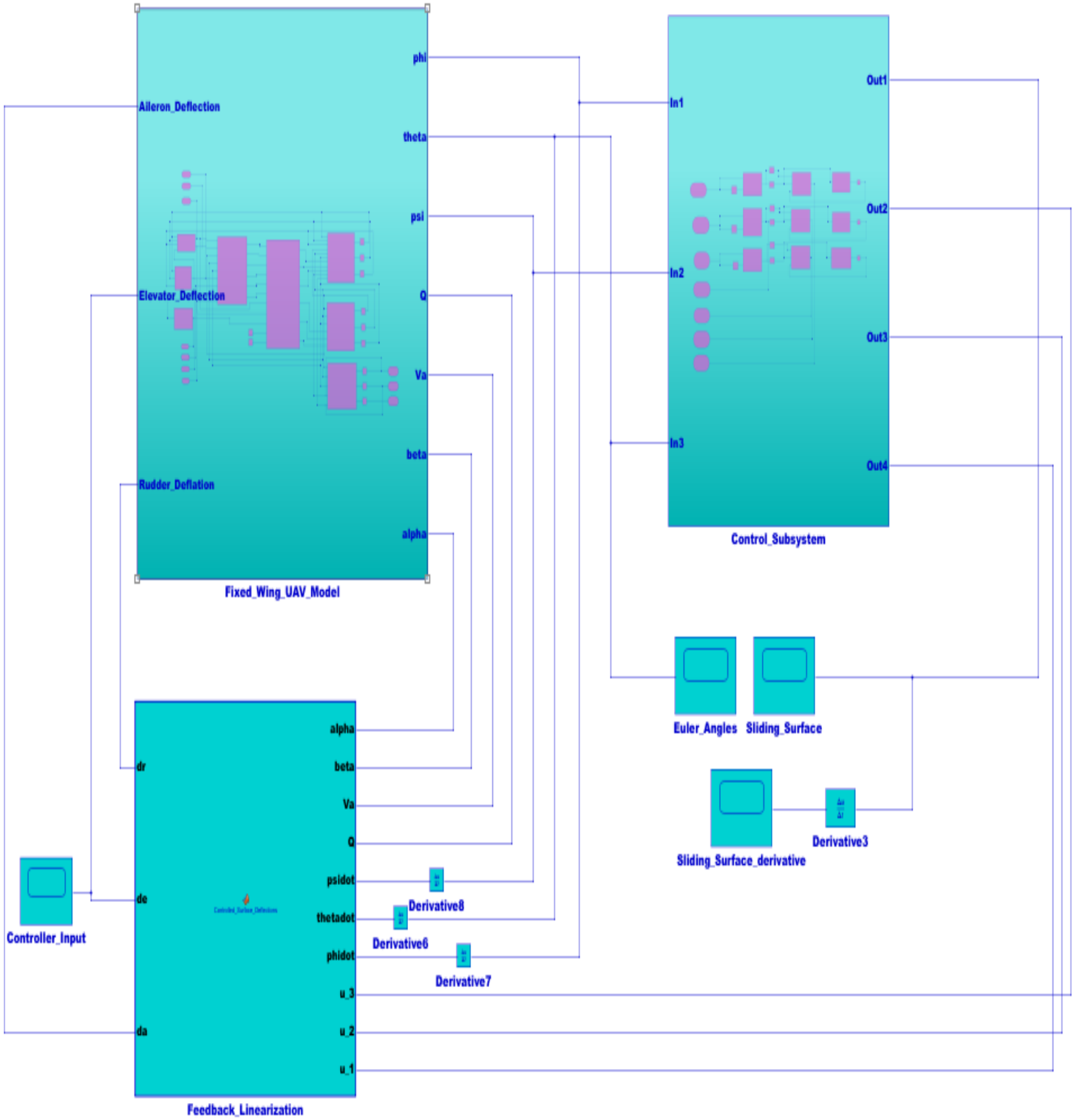

Figure 5.17: Simulink block diagram for regulation control of FWUAV using STW_ SMC

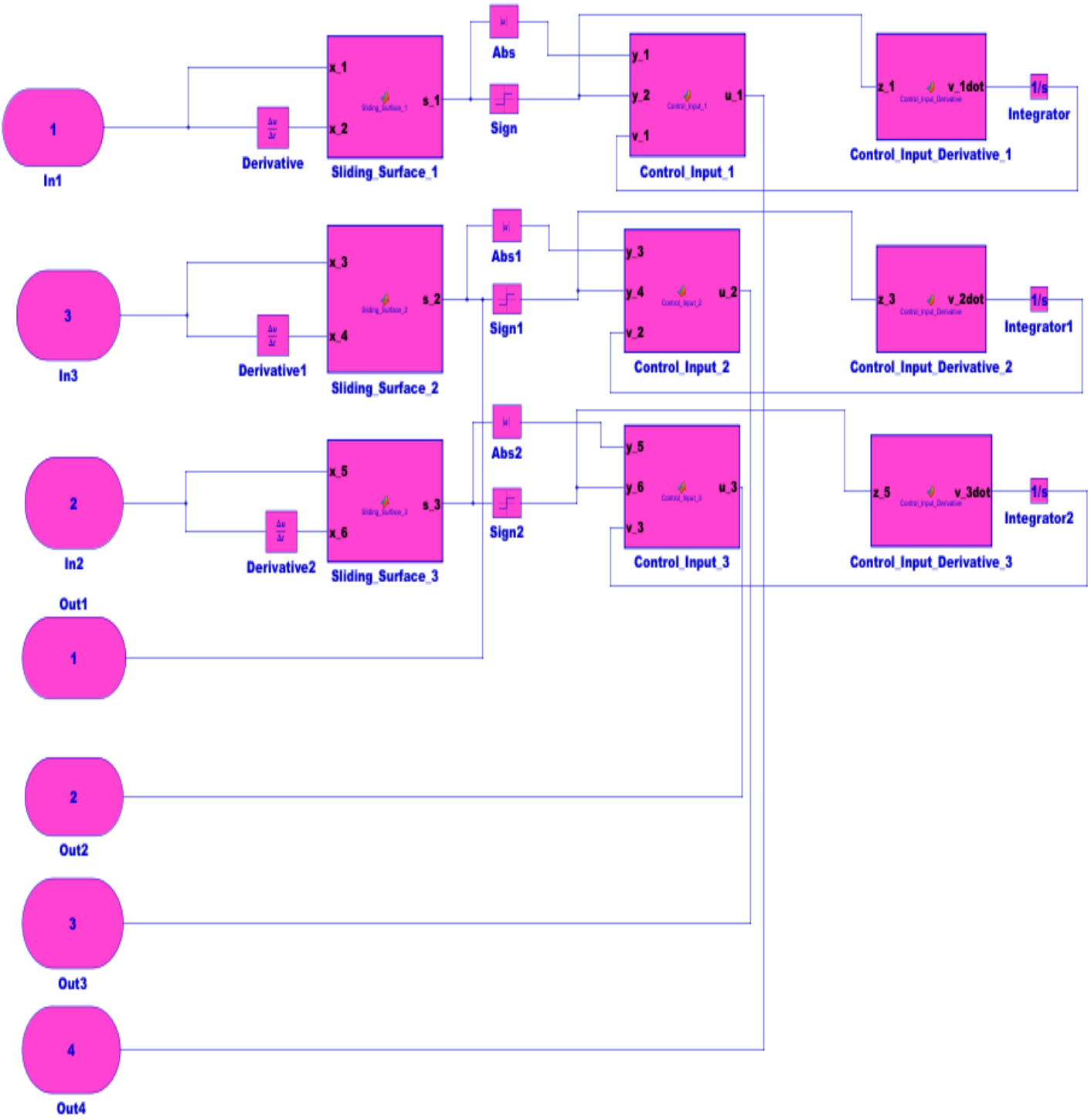

Figure 5.18: The inside of control subsystem of figure 5.17

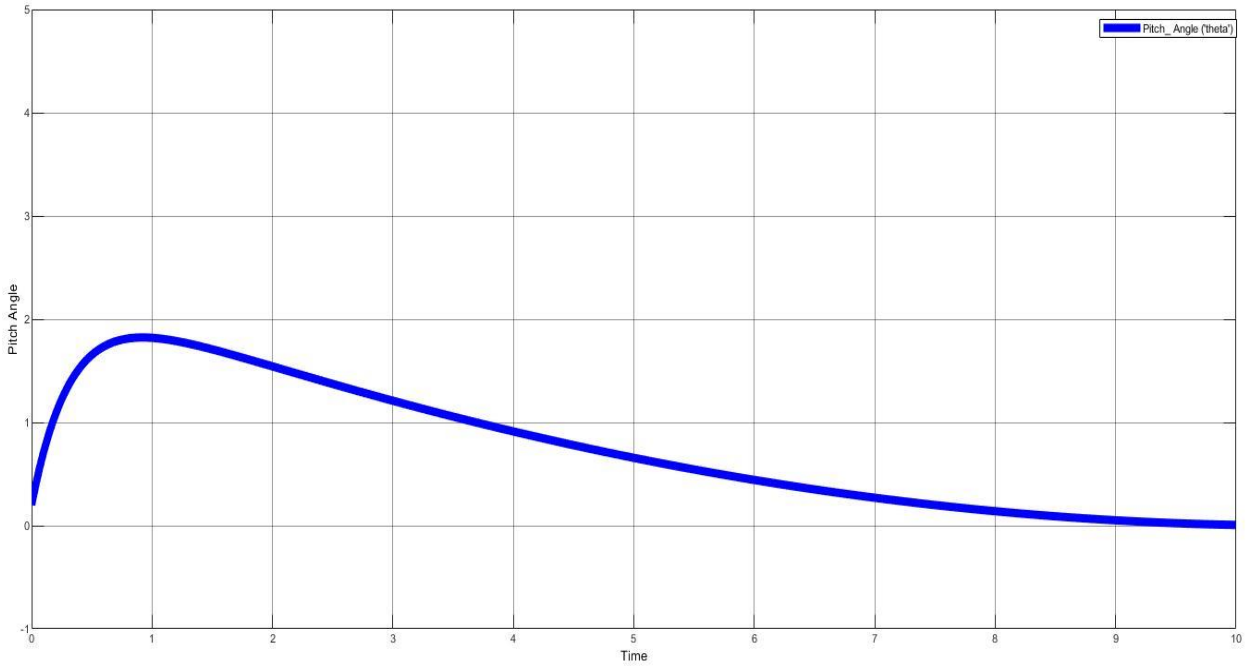

Figure 5.19: Pitch angle regulation

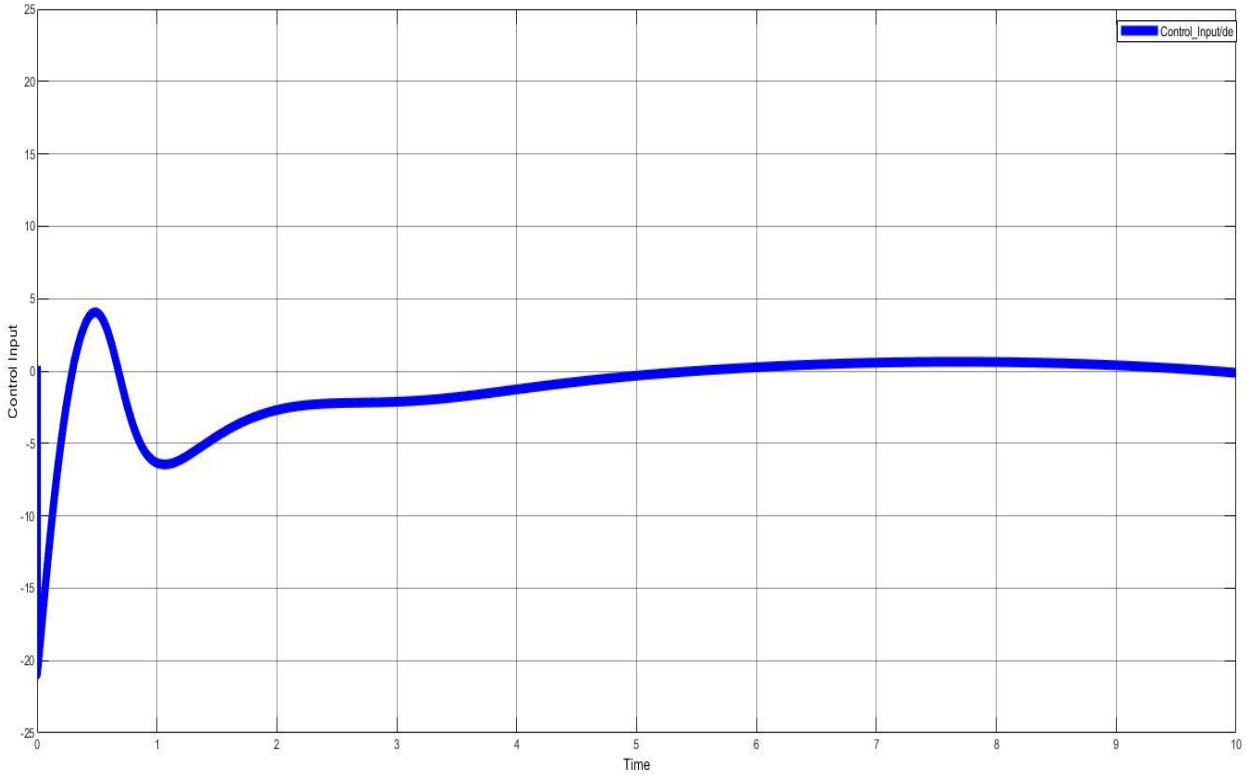

Figure 5.20: Control energy for pitch angle regulation

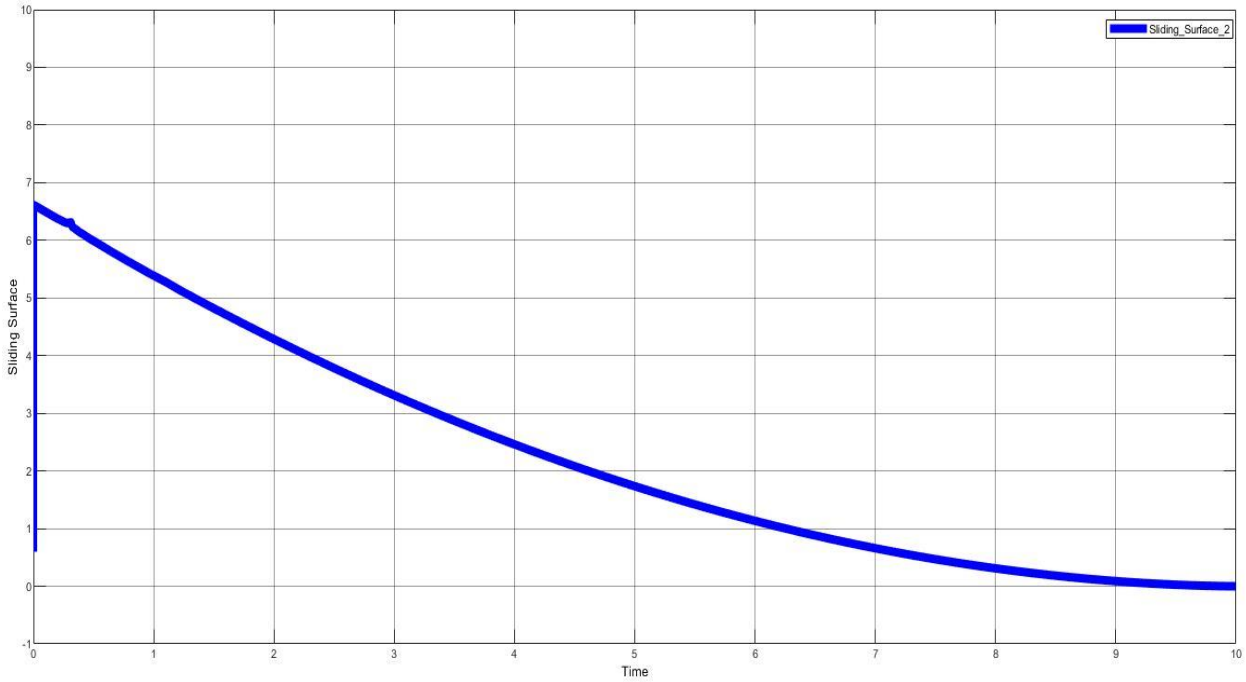

Figure 5.21: Sliding surface for pitch angle regulation

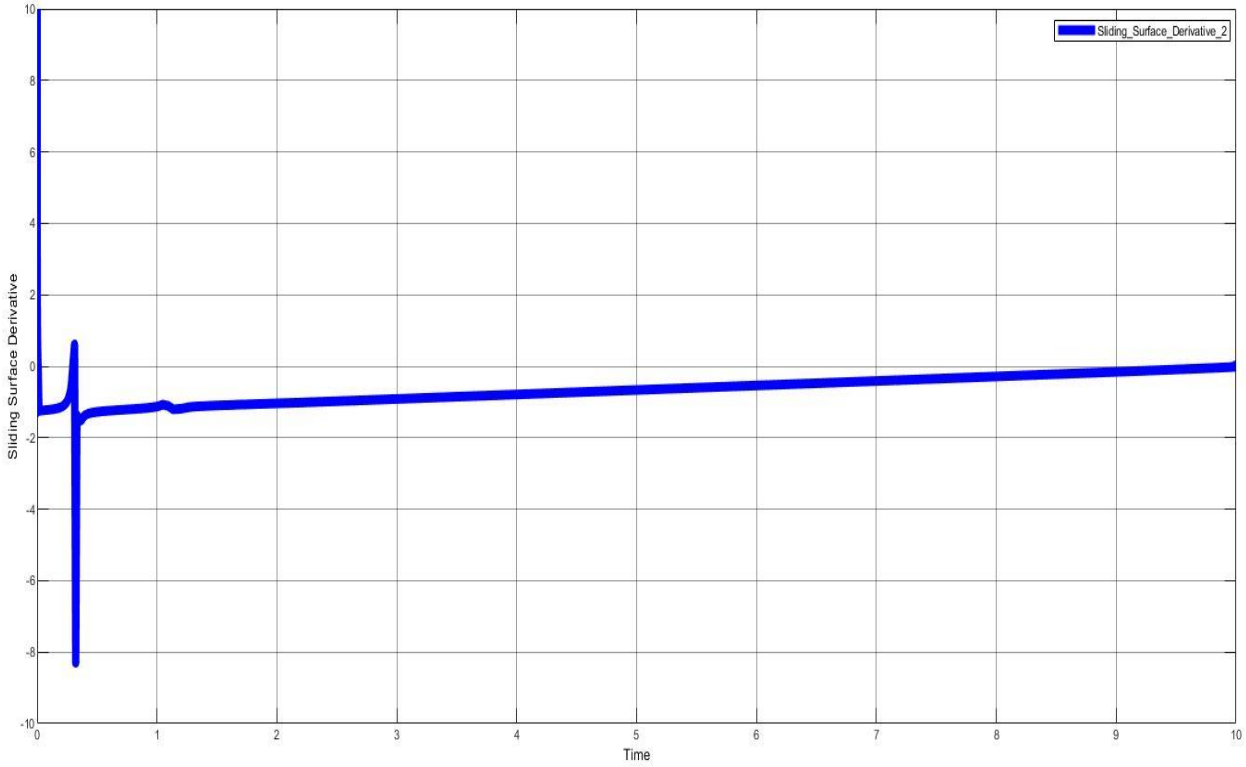

Figure 5.22: Sliding surface derivative for pitch angle regulation

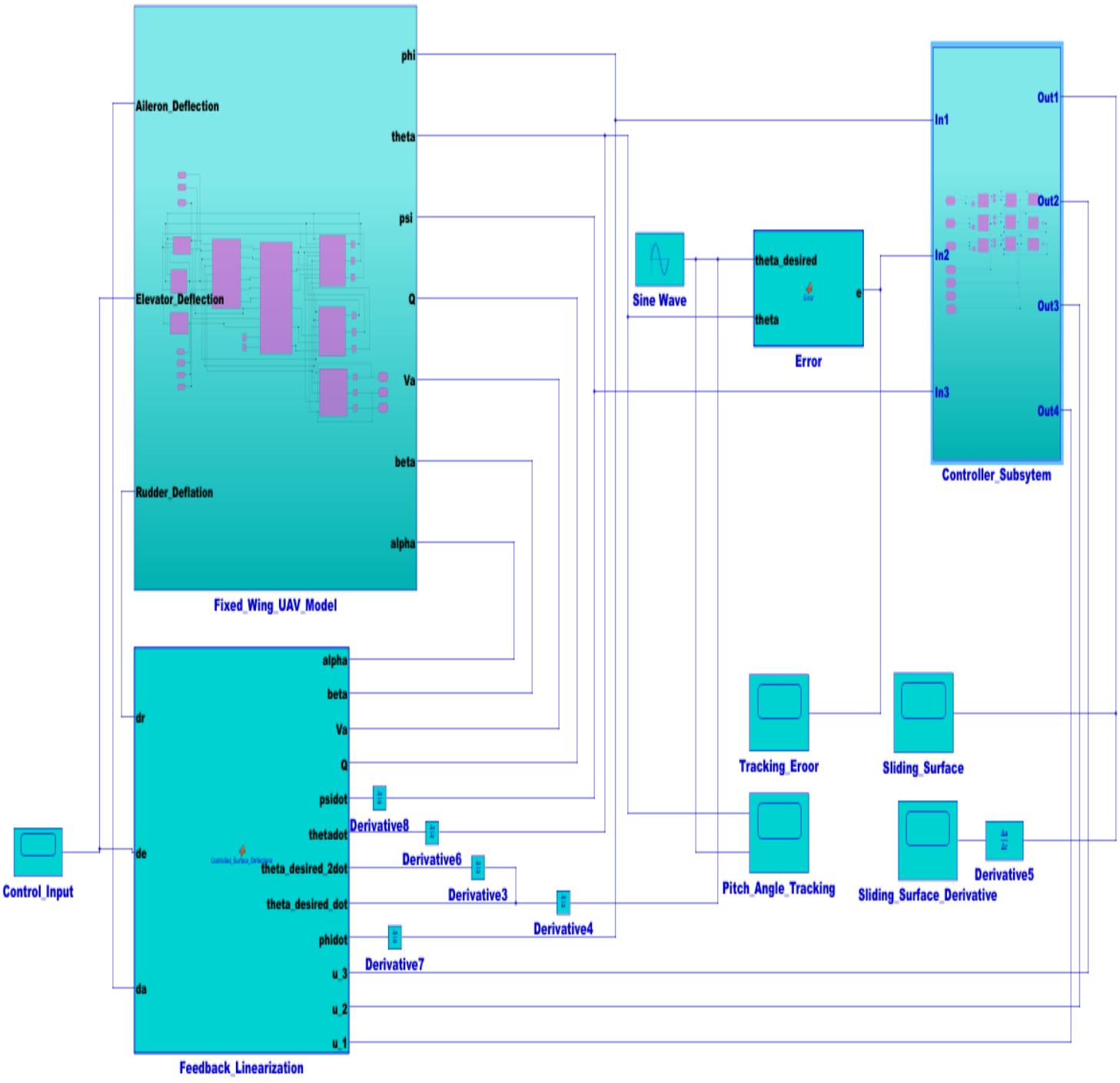

Figure 5.23: Simulink block diagram for tracking control of FWUAV using STW_ SMC

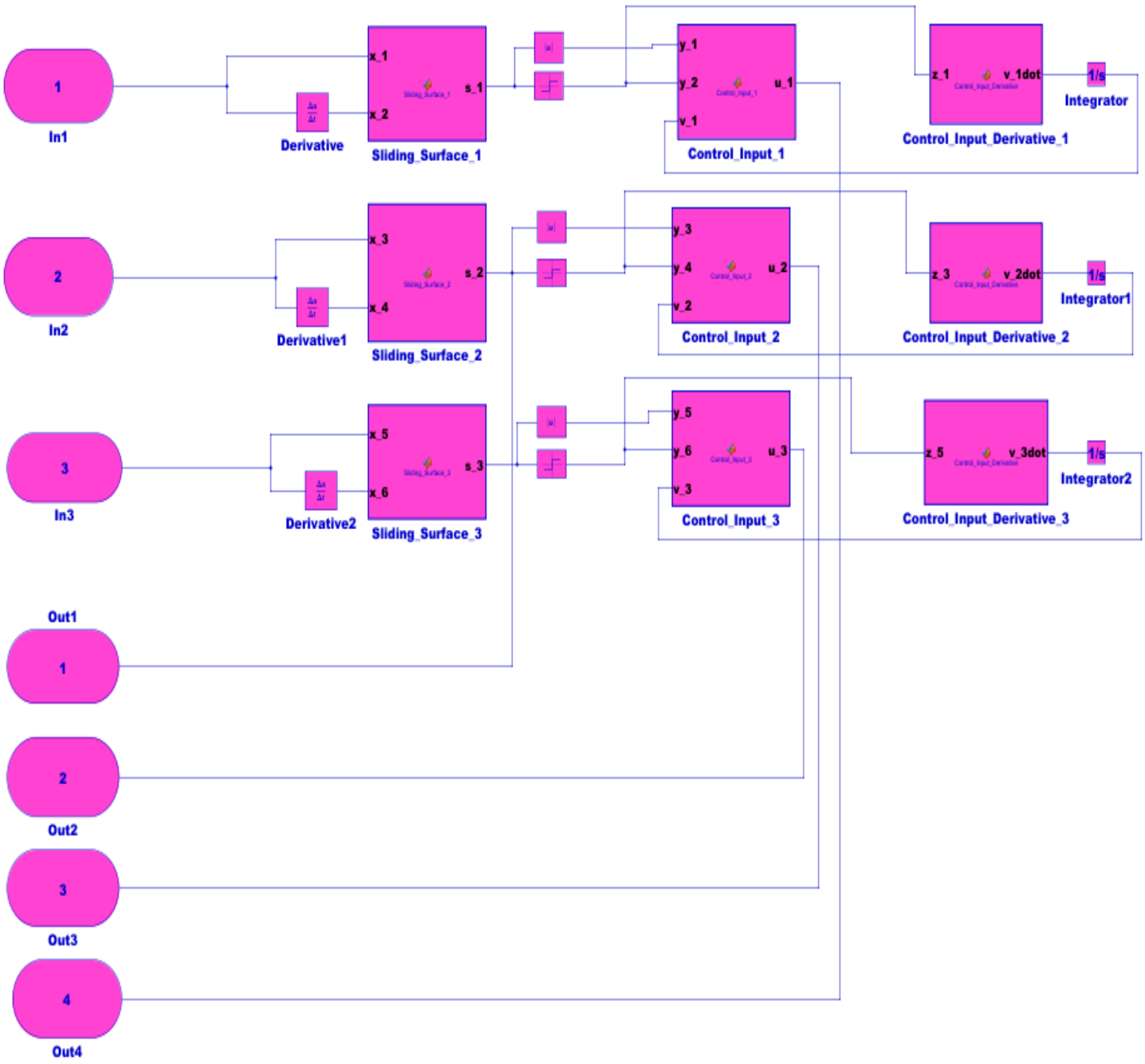

Figure 5.24: The inside of control subsystem of figure 5.23

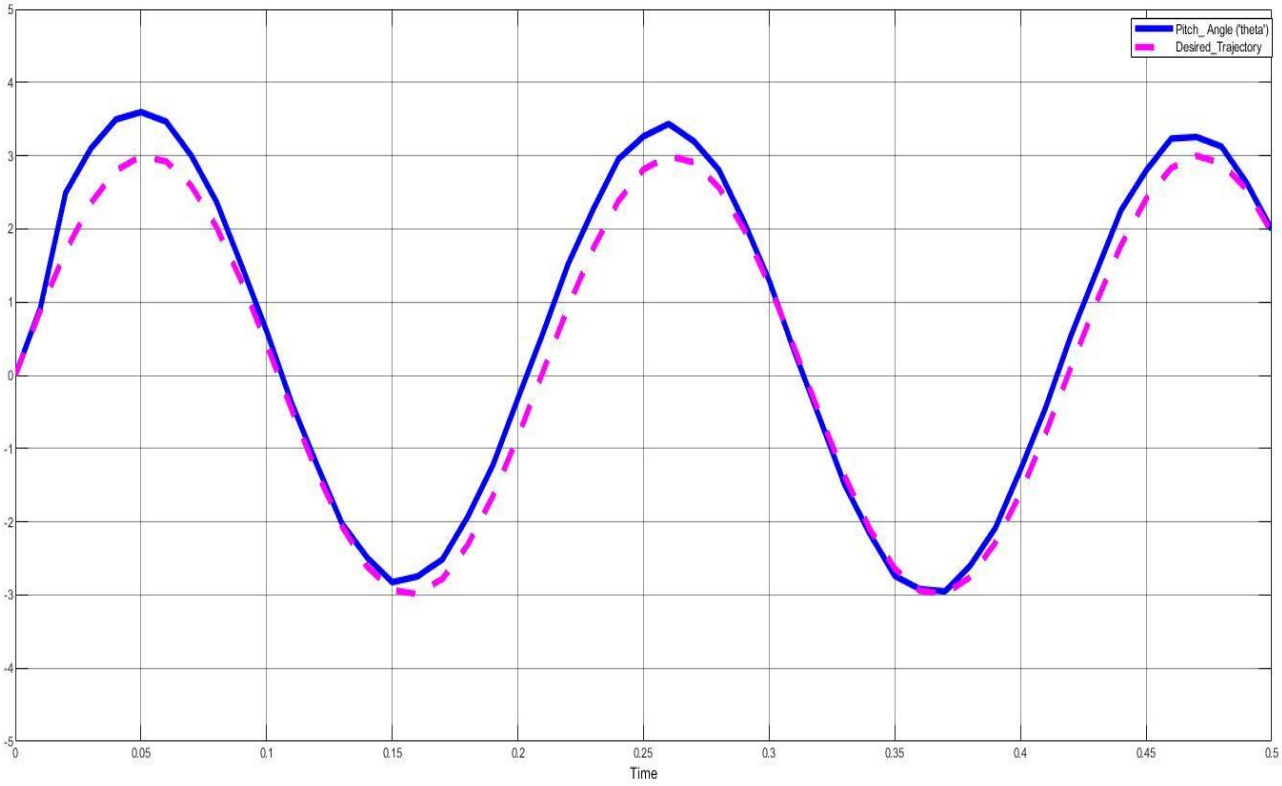

Figure 5.25: Pitch angle tracking a sine wave

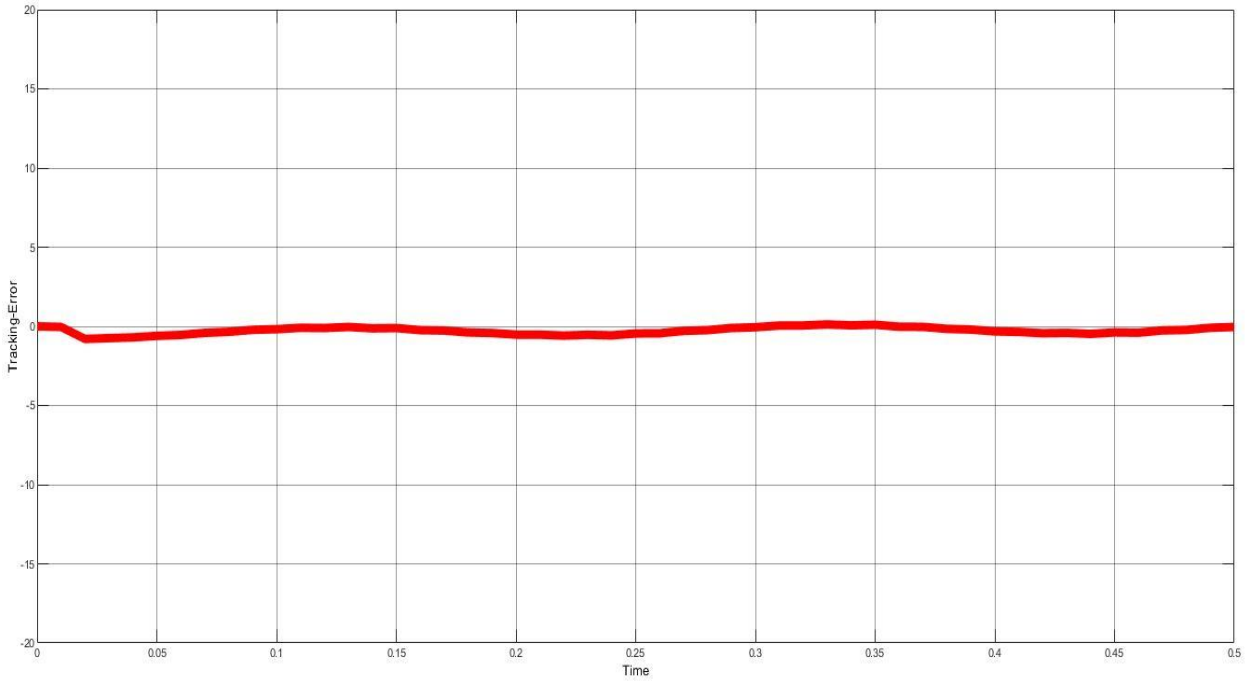

Figure 5.26: Tracking error for pitch angle tracking

5.2. Result Analysis

The strategy used here to show the performance of the controller for regulation problem is to initialize the system with steady state straight & level flight trim point except the state of interest, which would be initialized with error value and then to see how the controller actively reacts to that specific error.

Accordingly, a 0.2 radian (≈10.34 degree) pitch and roll inclination and a 0.1 radian (≈5.17 degree) yaw inclination at angular rate of 0.1rad/sec was introduced as an error. The expected mission of the controller was to reject these errors and bring back FWUAV to its stabilized trim state. Referring to figures 5.5, 5.9 and 5.13 shows that, the controller brings the FWUAV attitude inclination to zero degree within an average of few seconds (1.5 sec. for roll, 2 sec. for pitch and 7 sec. for yaw) as expected. As clearly shown in the figures 5.6, 5.10 and 5.14 the control energy consumption for the overall task and it clearly shows how costly would its implementation be due to the chattering problem. In figures 5.7, 5.8, 5.11, 5.12, 5.15 and 5.16 it has been shown that both the sliding surface and the sliding surface derivatives are all zero to guarantee finite time convergence.

The figures 5.19 to 5.22 the regulation performance of the STW-SMC. The FWUAV had an initially pitch inclination of 0.2 radian (≈10.34 degree) with angular speed of 0.1 radian per second. As expected, the controller brings the pitch inclination to zero degree at around 10 second times (figure 5.19). From figure 5.20 One can easily understand the fact that the chattering problem is eliminated, hence the control energy consumption is greatly reduced at the cost of a relatively longer response time. And in fact, finite time convergence is ensured by the zeroing of the sliding surface and its derivative as illustrated in figure 5.21 and 5.22.

Finally, figure 5.25 shows the reference tracking performance of the STW-SMC.As shown in the figure the actual state of the FWUAV is able to track the reference signal (sine wave) and the frequency for best tracking is found to be 30 Hz.

Chapter Six

6. Conclusion, Recommendation and Future work

6.1. Conclusion

In this paper, modeling and control of a FWUAV is addressed. By assuming the FWUAV as a rigid body & the earth as an inertial frame of reference, the dynamical model the UAV was obtained using the Newton – Euler formulation. Furthermore, longitudinal and lateral-directional motions are addressed separately to minimize the coupled nature of the dynamics. Two scenarios have been considered for model validation purpose and the model meet all the necessary expectations. Due to its simple structure, strong performance in the presence of uncertainties and finite time convergence properties, the sliding mode controller was chosen to address the regulation and reference tracking problem. The longitudinal motion was controlled by both the classical and the super twisting algorithms and a comparison was done in terms of response time & control energy. It was shown in the simulation that the classical SMC's performance for pitch control was better in terms of response time (0.2 seconds for SMC & 0.9 seconds for STW-SMC) but it's implementation would be costly due to the high frequency chattering problem. Whereas the super twisting algorithm takes relatively large response time but it takes minimal effort to do the required task. In addition to the regulation problem reference tracking was done using the super twisting algorithm and the result was satisfactory. Due to the highly coupled nature of the roll and yaw motion, we found controlling the lateral-directional motion using the super twisting algorithm somehow difficult.

Overall, in this research an attempt was done to control one of the most challenging dynamical systems in control engineering i.e., FWUAV. A new and novel approach has been followed by separating the dynamics in to two separate and simpler sub-systems to minimize the complexity issue. All the mathematical work was presented in a way that is simple to understand for any fellow researcher and each and every control equation was presented in its simplest closed form. Every single assumption considered was reasoned out, referenced & clearly justified to increase the credibility of the work. A very immaculate and well-ordered simulation diagrams are provided for anyone who wants to cross-check the results.

Finally, A persistent attempt was done to use a simpler language and a well-organized research presentation to make the thesis attractive for reading.

6.2. Recommendation

The classical SMC produces a faster response time but at the cost of large control energy consumption and the STW-SMC manages the task with minimum control energy but takes a relatively long response time. So, for clients that emphasizes a minimal control energy consumption the STW-SMC is an ideal controller whereas for those who emphasizes fast response time the classical SMC would be a better choice.

6.3. Future work

As a future work, I will try to overcome the challenges in controlling the lateral-directional motion using STW-SMC and I will extend the work of controlling the **FWUAV** to remaining 2-SMC algorithms in order to have a full picture of controlling a **FWUAV** using SMC.

Appendices

Appendix A: Rotation Matrixes

1. Rotation matrix to map the inertial reference frame with the body-fixed reference frame.

$$R(\phi, \theta, \psi) = \begin{bmatrix} C\psi C\theta & C\psi S\theta S\phi - S\psi S\phi & C\psi S\theta C\phi + S\psi S\phi \\ S\psi C\theta & S\psi S\theta S\phi + C\psi C\phi & S\psi S\theta C\phi \\ -S\theta & C\theta S\phi & C\theta C\phi \end{bmatrix}$$

Where ϕ, θ, ψ are the three Euler angles and Cx stands for cos(x), Sx stands for sin(x).

2. Rotation matrix to map the wind-fixed reference frame with the body-fixed reference frame.

$$\hat{C}(\alpha, \beta) = \begin{bmatrix} C\alpha C\beta & S\beta & S\alpha C\beta \\ -C\alpha S\beta & C\beta & -S\alpha S\beta \\ -S\alpha & 0 & C\alpha \end{bmatrix}$$

Where α, β are angle of attack and side slip angles respectively and C stands for cosine and S stands for sine.

3. A matrix that that relates the derivative of the Euler angles with the rotation rates

$$R_r = \begin{bmatrix} 1 & 0 & -\sin(\theta) \\ 0 & \cos(\phi) & \sin(\phi)\cos(\theta) \\ 0 & \sin(\phi) & \cos(\phi)\cos(\theta) \end{bmatrix}$$

Appendix B: Common Trim Points

1. Steady State Straight & Level Flight

$$Xo = \begin{bmatrix} xo \\ yo \\ zo \\ uo \\ vo \\ wo \\ \phi o \\ \theta o \\ \psi o \\ po \\ qo \\ ro \end{bmatrix} = \begin{bmatrix} x \\ 0 \\ 0 \\ u \\ 0 \\ 0 \\ 0 \\ 0 \\ 0 \\ 0 \\ 0 \\ 0 \end{bmatrix} \qquad u = \begin{bmatrix} u1 \\ u2 \\ u3 \\ u4 \end{bmatrix} = \begin{bmatrix} \delta a \\ \delta e \\ \delta r \\ \delta thr \end{bmatrix} = \begin{bmatrix} 0 \\ 0 \\ 0 \\ \delta thr \end{bmatrix}$$

2. Straight Climb

$$Xo = \begin{bmatrix} xo \\ yo \\ zo \\ uo \\ vo \\ wo \\ \phi o \\ \theta o \\ \psi o \\ po \\ qo \\ ro \end{bmatrix} = \begin{bmatrix} x \\ 0 \\ z \\ u \\ 0 \\ 0 \\ 0 \\ \theta \\ 0 \\ 0 \\ 0 \\ 0 \end{bmatrix} \qquad u = \begin{bmatrix} u1 \\ u2 \\ u3 \\ u4 \end{bmatrix} = \begin{bmatrix} \delta a \\ \delta e \\ \delta r \\ \delta thr \end{bmatrix} = \begin{bmatrix} 0 \\ \delta o \\ 0 \\ \delta thr \end{bmatrix}$$

3. Level Circling

$$Xo = \begin{bmatrix} xo \\ yo \\ zo \\ uo \\ vo \\ wo \\ \phi o \\ \theta o \\ \psi o \\ po \\ qo \\ ro \end{bmatrix} = \begin{bmatrix} x \\ y \\ 0 \\ u \\ 0 \\ 0 \\ \phi \\ 0 \\ \psi \\ p \\ 0 \\ r \end{bmatrix} \qquad u = \begin{bmatrix} u1 \\ u2 \\ u3 \\ u4 \end{bmatrix} = \begin{bmatrix} \delta a \\ \delta e \\ \delta r \\ \delta thr \end{bmatrix} = \begin{bmatrix} \delta o \\ 0 \\ \delta o \\ \delta thr \end{bmatrix}$$

4. Circling Climb (Helical Path)

$$Xo = \begin{bmatrix} xo \\ yo \\ zo \\ uo \\ vo \\ wo \\ \phi o \\ \theta o \\ \psi o \\ po \\ qo \\ ro \end{bmatrix} = \begin{bmatrix} x \\ y \\ z \\ u \\ 0 \\ 0 \\ \phi \\ \theta \\ \psi \\ p \\ q \\ r \end{bmatrix} \qquad u = \begin{bmatrix} u1 \\ u2 \\ u3 \\ u4 \end{bmatrix} = \begin{bmatrix} \delta a \\ \delta e \\ \delta r \\ \delta thr \end{bmatrix} = \begin{bmatrix} \delta o \\ \delta o \\ \delta o \\ \delta thr \end{bmatrix}$$

Reference

[1] S. Vaidyanathan and C. H. Lien, *Applications of sliding mode control in science and engineering*, vol. 709. 2017.

[2] C. K. Gilmore, M. Chaykowsky, and B. Thomas, *Autonomous Unmanned Aerial Vehicles for Blood Delivery*. 2019.

[3] X. Yu, J. Yang, and S. Li, "Finite-time path following control for small-scale fixed-wing UAVs under wind disturbances," *J. Franklin Inst.*, vol. 357, no. 12, pp. 7879–7903, 2020, doi: 10.1016/j.jfranklin.2020.06.011.

[4] G. Keifer and F. Effenberger, *济無No Title No Title*, vol. 6, no. 11. 1967.

[5] J. Zhang, Q. Li, N. Cheng, and B. Liang, "Non-linear flight control for unmanned aerial vehicles using adaptive backstepping based on invariant manifolds," *Proc. Inst. Mech. Eng. Part G J. Aerosp. Eng.*, vol. 227, no. 1, pp. 33–44, 2013, doi: 10.1177/0954410011430027.

[6] I. Transactions and O. N. Industrial, "Scheme for Quadrotor UAVs : Experimental Prototyping," 2018.

[7] A. Levant, *Homogeneous High-Order Sliding Modes*, vol. 41, no. 2. IFAC, 2008.

[8] B. M. Albaker and N. A. Rahim, "Flight path PID controller for propeller-driven fixed-wing unmanned aerial vehicles," *Int. J. Phys. Sci.*, vol. 6, no. 8, pp. 1947–1964, 2011, doi: 10.5897/IJPS11.162.

[9] E. Olguín Díaz, *3D Motion of Rigid Bodies*. 2019.

[10] a Noth, S. Bouabdallah, and R. Siegwart, "Dynamic Modeling of Fixed-Wing UAVs," *Master Course Mech. Eng.*, pp. 0–11, 2006.

[11] A. Sarhan and S. Qin, "Adaptive PID Control of UAV Altitude Dynamics Based on Parameter Optimization with Fuzzy Inference," *Int. J. Model. Optim.*, vol. 6, no. 4, pp. 246–251, 2016, doi: 10.7763/ijmo.2016.v6.534.

[12] E. Kayacan, M. A. Khanesar, J. Rubio-Hervas, and M. Reyhanoglu, “Learning Control of Fixed-Wing Unmanned Aerial Vehicles Using Fuzzy Neural Networks,” *Int. J. Aerosp. Eng.*, vol. 2017, 2017, doi: 10.1155/2017/5402809.

[13] H. Castañeda, O. S. Salas-Peña, and J. de León-Morales, “Extended observer based on adaptive second order sliding mode control for a fixed wing UAV,” *ISA Trans.*, vol. 66, pp. 226–232, 2017, doi: 10.1016/j.isatra.2016.09.013.

[14] J. L. Hernandez, I. Gonzalez-Hernandez, and R. Lozano, “Attitude and altitude control for a fixed wing UAV applied to photogrammetry,” *2019 Int. Conf. Unmanned Aircr. Syst. ICUAS 2019*, pp. 498–502, 2019, doi: 10.1109/ICUAS.2019.8798035.

[15] J. A. Guerrero, R. Lozano, G. Romero, D. Lara-Alabazares, and K. C. Wong, “Robust control design based on sliding mode control for hover flight of a mini tail-sitter unmanned aerial vehicle,” *IECON Proc. (Industrial Electron. Conf.*, pp. 2342–2347, 2009, doi: 10.1109/IECON.2009.5415267.

[16] K. P. Valavanis and G. J. Vachtsevanos, *Handbook of unmanned aerial vehicles*. 2015.

[17] Federal Aviation Administration, “Aerodynamics of Flight,” *Pilot. Handb. Aeronaut. Knowl.*, no. Cl, pp. 2–2 to 2–28, 2000.

[18] Wikipedia, “Aerodynamic force.” https://en.wikipedia.org/wiki/Aerodynamic_force (accessed Jul. 29, 2021).

[19] Encyclopedia Britannica, “No Title.” https://www.britannica.com/technology/airfoil (accessed Jul. 29, 2021).

[20] MIT, “AirFoil.” https://www.britannica.com/technology/airfoil (accessed Jul. 29, 2021).

[21] ر. زين الدين, *No Title* 2005 .*طرق وسترتيغى تعليم اللغة العربية*.

[22] A. Forces, “Fluids – Lecture 3 Notes,” *Notes*, vol. 3, pp. 1–5.

[23] H. C. Cuevas, J. De Leon Morales, and E. Olgúín-Díaz, “Path tracking of a fixed-wing autonomous aerial vehicle by high order sliding mode control,” *Proc. ASME Des. Eng. Tech. Conf.*, vol. 3, no. PARTS A AND B, pp. 1037–1046, 2011, doi: 10.1115/DETC2011-48975.

[24] D. T. McRuer, D. Graham, and I. Ashkenas, “Aircraft Dynamics and Automatic Control,” *Aircraft Dynamics and Automatic Control*. 1990, doi: 10.1515/9781400855988.

[25] National Aeronautics and Space Administration, “Axes / Control Surfaces principles of flight,” *Aeronaut. Res. Mission Dir.*, 2010.

[26] S. Mode and C. Principles, “A QUICK INTRODUCTION TO SLIDING MODE.”

[27] I. H. S. Modes, “Integral High-Order Sliding Modes,” vol. 52, no. 7, pp. 1278–1282, 2007.